AD-A104 941 OFFICE OF NAVAL RESEARCH ARLINGTON VA F/G 5/2
NAVAL RESEARCH REVIEWS. VOLUME XXXIII. NUMBER 2.(U)
1981 G A NEECE

UNCLASSIFIED NL

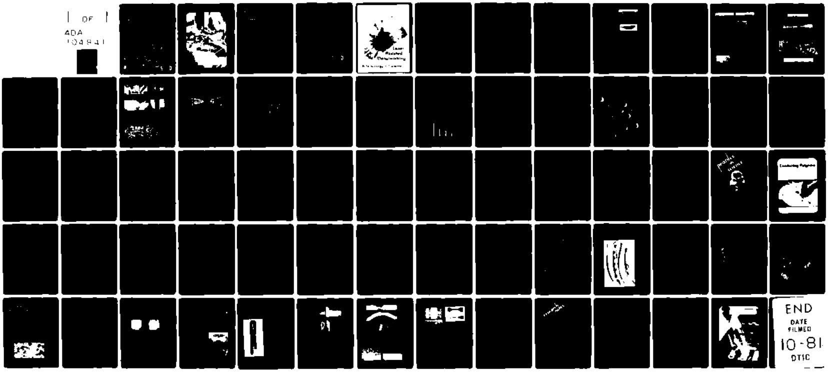

LEVEL

Naval Research Reviews

Office of Naval Research
Spring 1981
Vol XXXIII No. 2

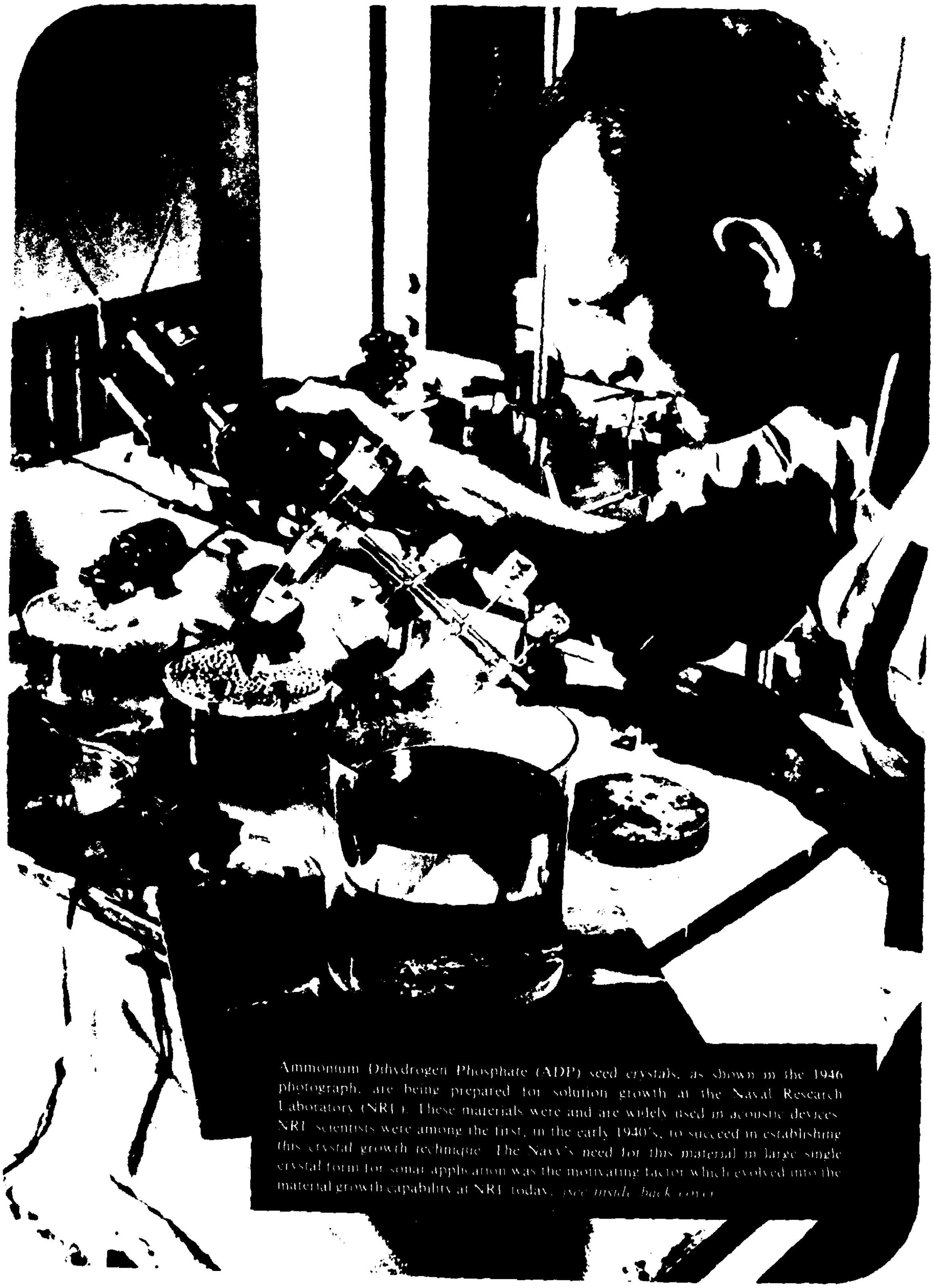

Ammonium Dihydrogen Phosphate (ADP) seed crystals, as shown in the 1946 photograph, are being prepared for solution growth at the Naval Research Laboratory (NRL). These materials were and are widely used in acoustic devices. NRL scientists were among the first, in the early 1940's, to succeed in establishing this crystal growth technique. The Navy's need for this material in large single crystal form for sonar application was the motivating factor which evolved into the material growth capability at NRL today. *(see inside back cover)*

Naval Research Reviews

Office of Naval Research
Spring 1981
Vol XXXIII No. 2

ARTICLES

DEPARTMENTS

Dr. George A. Neece

Dr. George A. Neece, who is the Director of ONR's Chemistry Program is the Scientific Editor for Naval Research Reviews. Dr. Edward I. Salkovitz resigned from the post when he was recently appointed Director of Research Programs for ONR.

Cover Picture

This 16th century woodcut depicts metalworkers pouring hot liquid alloy into moulds.

At furnace A stands a smelter, who pours with a ladle the alloy out of the forehearth into moulds. Another smelter is opening the tap-hole of furnace B, and a workman chips off the accretions from furnace C. The identified items are: D(forehearth), E(ladle), F(moulds), G (wooden hammer), H (tapping-bar), I(steps), K(spatula), and L(hooked bar). At the bottom of the picture, a mine captain is carrying with his pick a cake of alloy to be weighed on the scales.

The woodcut illustration is from "De Re Metallica" by Georgius Agricola. The first latin edition of 1556 was translated by Herbert and Lou Henry Hoover and published by Dover Publication, Inc., New York in 1950.

Naval Research Reviews publishes articles about research conducted by the Laboratories and contractors of the Office of Naval Research and describes important naval experimental activities. Manuscripts submitted for publications, correspondence concerning prospective articles, and changes of address, should be directed to Code 733, Office of Naval Research, Arlington, Va. 22217. Requests for subscription should be directed to the Superintendent of Documents, U.S. Government Printing Office, Washington, D.C. 20402. Yearly subscription prices for this quarterly publication are $6.50 in the United States and Canada and $8.15 elsewhere. The issuance of this periodical is approved in accordance with Department of the Navy publications and printing regulations.

Introductory Note

by

Dr. G.A. Neece, Scientific Editor

Almost all developing technologies are paced by materials capabilities. With increasing demands on technology there are increasing demands on materials performance. The properties of known materials must be thoroughly studied in order to be fully exploited. Since its beginning in 1946, the Office of Naval Research (ONR) has supported the research of many outstanding material scientists. This role gives ONR the distinction of being a pioneering force in many of the important accomplishments in material sciences during the last several decades.

For the timely development of future materials, ONR seeks an improved understanding of chemical, physical, and mechanical behavior of metals, alloys, ceramics, composites, and polymers. Research is aimed toward determining the limiting factors underlying the mechanical behavior and physical properties as materials are subjected to complex loading and extreme environment conditions. A further aim is to develop desirable structures through stringent control of important processing steps. This requires research efforts on processing and fabrication techniques, on strengthening mechanisms, deformation and fracture, and on such physical characteristics as magnetic and electrical properties.

Special needs exist for definition of predictable behavior of inorganic nonmetallic engineering materials in the presence of mechanical stress. Included here are ceramics, glasses, graphites, cements, composites, inorganic films, and coatings. Limitations imposed by severe environments need to be studied (including not only high temperatures but particle impingement, corrosive media, and electrical stressing). Mechanisms for protection against these need to be investigated, also.

Composite materials represent a future potential for lightweight, high-strength applications and for improvements of electronic and magnetic materials. Research is necessary to advance knowledge in a variety of fields. We can include adhesive polymers, organic filament precursors, high-strength filaments, flake and film reinforcement, nondestructive testing of composites, metal laminates, and organic-matrix and metal-matrix composites.

In this issue of *Naval Research Reviews*, devoted to material sciences, are four articles representing the diverse nature of ONR's Material Sciences Program. ONR strives to obtain the best scientific research possible for the tax payer's dollar. Through its contract research program, ONR was able from its beginning to attract distinguished members of the civilian scientific community to a program of basic research aimed at providing the base for future technology. In this way ONR will continue to blend the talents of the civilian scientific community with the needs of the Navy for rapid technological advances in order to create the new Navy capable of meeting the needs of tomorrow.

By

L. R. Hettche, E. A. Metzbower, J. D. Ayers, and P. G. Moore
Material Science and Technology Division
Naval Research Laboratory

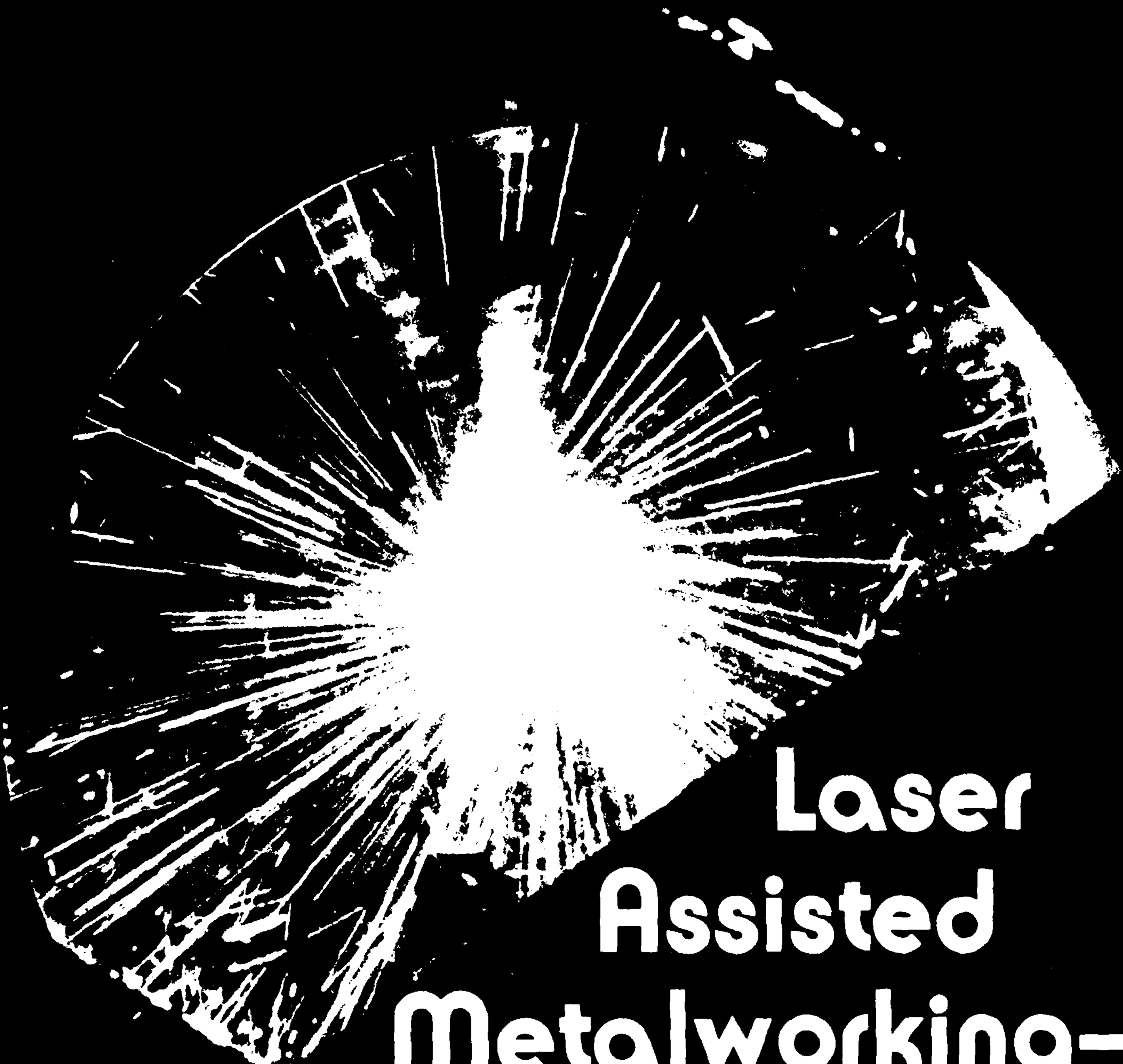

Laser Assisted Metalworking—

A Technology in Transition

Introduction

Early in the development of the laser it was recognized that coherent radiation, as a readily controllable source of intense energy, offered significant potential, if not an altogether new capability, for materials processing and fabrication. Initial industrial applications utilized high-intensity pulsed-laser radiation for precision operation, such as hole-drilling, trimming, and welding of thin-gage materials in electronic assemblies[1]. As the availability of high energy continuous wave (CW) lasers increased, particularly with the advent of the multi-kilowatt CO_2 laser, the range of so-called laser-assisted metalworking (LAM) operations expanded and now includes thick-section welding[2] and cutting[3], machining[4], and a wide variety of surface modification procedures. It is in the area of surface processing that the laser has demonstrated the capacity to perform conventional tasks, such as transformation hardening[5] and cladding[6], and has provided new capabilities as well. These include microstructural refinement via rapid melting and solidification[7], alloying[8], in-situ composite formation[9], and bulk structural build-up by laser deposition of sequential layers of metal alloy.[10]

Although various LAM operations have undergone differing degrees of research and advanced development, and while some applications have transitioned to production status, it is a fair assessment that the anticipated widespread utilization of LAM has not yet been achieved. For example, the Department of Defense (DoD) has sponsored research and development of LAM for the specialized requirements of defense systems. A chronology of DoD-sponsored R&D programs in this area is tabulated in Table I. Although these programs have advanced our understanding and proficiency in various LAM operations, the only production line transition which has resulted to date is laser-beam cutting of aerospace alloys[11]. It is important to note however that the total DoD investment in completed LAM programs is estimated to be less than 3 million dollars. This sum is judged to be a modest level of support in view of the costs usually required for development of sophisticated technology as well as the yet-to-be-described pay-back potential of LAM technology. Ongoing DoD efforts listed in Table I, however, represent a more aggressive support of LAM for the near term and are directed more towards industrial transition than previous programs.

Laser-assisted metalworking has also been under investigation by private industry for the past decade. Noteworthy applications which evolved from these efforts include a 3kW CO_2 laser/workstation system for welding industrial-type lead batteries[12] and a 0.5kW unit for case-hardening the walls of power-steering gear housings[13]. These, as well as other, LAM applications not only proved to be more economical than conventional methods but also demonstrated that high-energy lasers can operate safely and reliably in a production line environment. Because of proprietary considerations, it is difficult to estimate the level of LAM development in the private sector. However, based on the export of high energy lasers, it is apparent that there is considerable foreign interest in LAM technology, particularly in Japan and Italy. In fact, the steadily growing interest in LAM technology, both domestic and foreign, has provided incentive for laser manufacturers to develop competitive lines of multi-kilowatt lasers and ancillary equipment.

In contrast to the past evolutionary development of laser assisted metalworking, it is a premise of this paper that this technology is poised for accelerated growth and accelerated transition over the next decade. This forecast is based on the demonstrated and rapidly emerging capabilities of LAM to alleviate, if not obviate, many of today's pressing economic problems, such as critical materials shortages, declining productivity, and soaring energy and maintenance costs. These economic factors are all responsible for the increase in acquisition and ownership costs of defense systems; therefore, it is not surprising that DoD applications are leading candidates for large-scale LAM production impact.

This thesis is developed and supported in this paper by the presentation of technical highlights on emergent LAM research opportunities which promise to impact naval requirements and applications. A convenient road-map to these discussions is provided in Figure 1. Here regimes of power density versus interaction time are indicated for various LAM opera-

tions. Opportunities for naval applications are associated with thick-section welding of naval structure and surface modification for improved corrosion and wear-resisting alloys, all pervasive naval materials requirements. Insofar as these applications are a subset of metalworking technology, these discussions are representative of LAM opportunities in other sectors of defense and industrial production.

Following the technical highlights, economic considerations of LAM are addressed. Central to this discussion is the concept of a multi-workstation, time-sharing LAM facility. Again, while the data supporting these discussions are for naval applications, it is believed that this concept has much broader applicability.

Laser Surface Modifications

The high power-densities attainable with laser beams have made possible the development of a wide range of surface modification techniques. Table II lists those processes known to us. Some of these techniques are adaptations of ones long popular in industry, while others were made possible by the rapid heating and cooling rates attainable with high-power lasers. Transformation hardening is typical of those techniques which are adapted from earlier practice. It utilizes the laser beam to briefly heat the surface of a steel sample to austenitizing temperatures, permitting conduction cooling by the unheated base metal to quench the heated zone and produce a hard, marten-

Table I
Chronology of DOD Programs in Laser Assisted Metalworking

• Laser Beam of Thin Sections HY-Steels, Titanium and Aluminum	NAVSEA/DTNSRDC	1972-73
• Establishment of a Continuous Wave Laser-Welding Process	USAF/SCIAKY	1973-75
• Laser-Beam Welding in Ship Construction	NAVSEA/DTNSRDC/ROHR	1975
• Laser Beam Welding of 5456 Aluminum Panel	NAVSEA/DTNSRDC/ROHR/UTRC	1975
• Laser Cutting of Aerospace Alloys	USAF/AIA	1975-76
• Basic Laser Welding Capabilities	ONR/NRL/UTRC	1976-79
• Laser Welding at Very High Power Levels	NAVSEA/NRL	1976
• DoD MTAG Metal Subcommittee, Laser Processing Workshop	DTNSRDC	1977
• Laser Beam Welding of Armor Steels	US ARMY/IITRI	1978
• Laser Beam Welding of SSBN HY-80 Tees	NAVSEA/DTNSRDC/Electric Boat/UTRC	1978-79
• Laser Glazing and Laser Layering of Alloys	ONR/ARPA/UTRC	1978-80
• Laser Hardening of Jet Engine Bearings	USAF/SKF	1979
• Applications of Lasers in Materials Processing Conference	ASM/NRL	1979
• Laser Assisted Metalworking of Naval Alloys	ONR/NRL	On-going
• Laser Machining	ARPA/USAF/GE	On-going
• Laser Welding of Ordnance Structures	NAVSEA/NRL/FMC (MANTECH)	On-going
• Laser Hardening of CAMS	NAVSEA/NSWC	On-going

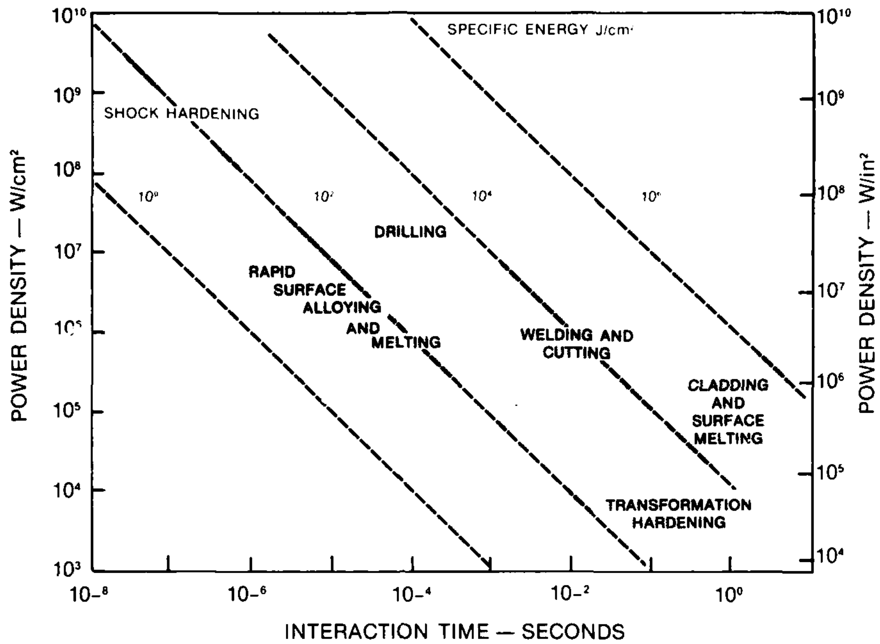

Figure 1. Power density, interaction time spectrum for Laser Beam Processing of Metals and Alloys.

sitic structure on the surface. The advantages which accrue from using laser (or electron-beam) heating rather than induction or flame heating are that minimal heating of the bulk material can prevent thermal degradation of bulk metal and can limit distortion of the part during quenching[5].

Laser glazing[7] differs from transformation hardening in that the surface layer is melted, not simply cycled through a set of solid-state phase transformations. The melting and rapid resolidification makes possible surface hardening, through the refinement of microstructure, of a wide range of alloy types. It can, in some alloys, improve the corrosion resistance[14] by eliminating or minimizing phase separation. Surface alloying, to be discussed in detail subsequently, can improve both the corrosion and wear-resistance of a wide range of alloy types. It does so by introducing alloying elements which improve the corrosion resistance or which stabilize hard, wear-resisting phases.

Laser cladding, a patented process[6], is similar to traditional weld-cladding processes in that it uses the energy of the laser beam to fuse a metallic overlayer and weld it to the surface of the base metal. The material to be clad to the surface can be in the form of a loosely adhering powder or it can be wire-fed directly into the weld pool. The consolidation of coatings with lasers differs from laser cladding only in the means of applying the cladding material prior to laser melting. That is, a coating previously applied by a process such as flame spraying or plasma spraying is laser-remelted to remove residual porosity or to improve its adherence to the base metal[15,16]. These two processes are both suited for producing corrosion and wear-resisting surfaces and the preferred technique for any particular application is dependent upon numerous factors. In principle, the ease of applying diverse coatings by the thermal-spray processes should recommend the consolidating route, but problems related to the presence of trapped gases in flame- and plasma-sprayed coatings may limit the widespread adoption of this approach[16].

Research at NRL has led to the laser melt/particle injection process, which can be used to modify surfaces in several distinct ways.[9,17] This process will be discussed after consideration of surface alloying with lasers. These two processes, will be considered in greater detail than the others because the authors believe that of the six types listed in Table II they are of the greatest current interest from both a scientific and a naval technology point of view.

Laser Surface Alloying: This process consists of melting the surface of a metal workpiece, adding known amounts of other metals, mixing these com-

Table II
Techniques for Modifying metal Surface by Laser Processing

• Transformation hardening
• Laser glazing
• Surface alloying
• Laser cladding
• Consolidation of coatings
• Laser melt/particle injection

ponents, and allowing them to resolidify. This process produces a surface layer with a chemical composition and properties which are different from the substrate material. This technique allows the surface properties of a structure to be tailored to the surface requirements without sacrificing the bulk characteristics. The surface layer is also metallurgically bonded to the substrate and provides a high degree of adhesion. Other reasons for laser surface alloying are that rapidly solidified structures are produced and that surface coverage rates of up to 1 cm^2/sec are often obtained.

There are three classes of processing conditions used to produce laser surface alloys: (1) low power density, (2) high power density, and (3) high power density but with the beam rastered at a high speed[18]. With the first approach, specially designed optics are used to obtain a beam spot with a power density of 10^5 to 10^6 W/cm^2 which is slowly swept across the specimen. The surface layer is held molten long enough for convection currents to establish themselves within the molten pool and to provide for the mixing of the components. The second class of processing conditions makes use of the plasma produced by the interaction of the laser with the melt pool to stir the pool and to mix the components. The third class is a hybrid of the first two where a high power-density beam is very rapidly rastered to produce a low average power density.

Figure 2(a) shows the cross section of a low carbon steel specimen from which a chromium steel surface alloy was made. In this case, the AISI 1018 steel was first coated with an 8 μm-thick layer of chromium. A focused, 5kW, CO_2 laser beam was swept across the surface at 50 cm/sec to melt the coating along with a portion of the substrate. The degree to which the components are mixed is illustrated in the chromium x-ray display of Figure 2(b) which shows that chromium was dispersed throughout the depth of the melt.

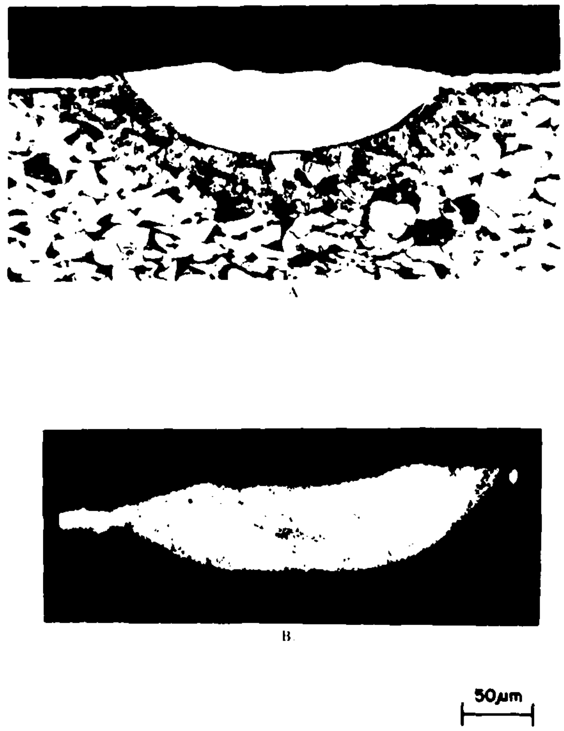

Figure 2. (a) Polished and etched cross section of an AISI 1018 steel coupon which was coated with an 8 m thick layer of chromium and laser surface alloyed using a focused 5 kW laser swept at 50 cm sec. (b) A chromium x-ray display of the cross section in (a).

A larger surface may be processed by using successive passes, each one of which overlaps with the previous pass. This process is illustrated in Figure 3 where a Ti-6Al-4V surface was alloyed with molybdenum. After this single set of passes, there remains some variation in composition within the melts as indicated by the large dark arcs that result from the etching. By reprocessing the surface alloy of Figure 2 using identical conditions, a substantially uniform composition is obtained. The result is shown in Figure 4 where the molybdenum addition has produced a single-phase surface alloy.

There are several possible disadvantages to laser surface alloying. There is a certain amount of roughness introduced by the melting process and, although conditions can be chosen to minimize the roughness, either the application must be tolerant of the roughness or the surface must be refinished after laser processing[19]. A very strong crystallographic texture can be introduced by the solidification process as a result of the faster growth of grains with particular

crystallographic planes orientations in the direction of the temperature gradient[29]. The change in texture is most pronounced with fine-grained materials where favorably oriented grains will be closer together and so will more quickly squeeze out less favorably oriented grains. The most significant drawback of laser surface-processing is the residual stress introduced by the rapid, localized heating of the surface. These residual stresses limit the number of materials that can be processed since many will crack as a result of the processing. Short of this the residual stresses can cause warpage of a workpiece, require a stress-relieving heat treatment, or other stress-modifying treatment, such as peening. In any application these drawbacks will have to be weighed against the advantages described previously.

Two major technical issues remain to be addressed. The first is determining the best method of introducing the alloying elements. This can be accomplished either by the addition of a powder mixture, an alloy powder, or wire, directly to the melt, or by coating the specimen using traditional techniques before the laser processing. The second issue is the development of techniques for quality assurance which will insure the batch-to-batch reproducibility of the product.

The Laser Melt/Particle Injection Process: This process, shown schematically in Figure 5, consists of melting a shallow pool on the surface of a sample which is translated under a focused laser beam, and of blowing powder particles into the melt pool from a fine nozzle positioned about 1 cm away. The powder consists of either, hard, wear-resisting particles which dissolve to only a limited extent in the melt, or metallic particles which are deliberately dissolved in the melt to accomplish surface alloying. Alternatively, the processing conditions can be adjusted so that the beam melts just enough of the sample surface to weld down a coating which is built up from powder blown into the melt pool. For purposes of discussion, these three variations of the process will be called; (1) particle injection (when minimal dissolution occurs), (2) injection alloying (when full dissolution occurs), and (3) injection cladding (when substrate melting is minimized). Of these three variations, particle injection has been most fully explored, and most of our discussion will refer to it.

Wear-resisting layers have been produced on iron, nickel, titanium, aluminum, and copper based alloys by injecting titanium carbide or tungsten carbide into their surfaces. The processing can be done as isolated melt passes of the type shown in Figure 6, or as extended area coverage like that shown in Figure 7. The single melt pass shown in Figure 6 was produced by injection TiC particles into a melt pool produced in Ti-6Al-4V. This pass employed a laser power of 6kW and a sample translation speed of 5 cm/sec. This scanning electron photomicrograph shows both the top surface of the sample and a sectional view through the melt pass. Examination of this photo will reveal a significant difference between carbide-injected surfaces and wear-resisting surfaces produced by coating techniques such as plasma spraying. That is, the wear-resisting particles are incorporated into the bulk metal, and are not simply stuck onto the surface. The advantage of this feature is that the wear-resisting surface is an integral part of the material and cannot be flaked off by thermal or mechanical stress.

Extended area coverage of the sort shown in Figure 7 is produced by overlapping single passes of the sort shown in Figure 6. The 5052 Al sample shown in Figure 7 was made by injecting −170 + 220 mesh TiC into a 3-mm-wide melt pass, and by advancing the sample 1 mm after each pass under the beam. This processing produced a sample with a uniform carbide distribution, but with a relatively rough surface, as can be seen in the profile view shown in Figure 7. For most applications smoother surfaces are required, but this presents no great difficulty because the surface can be ground and polished as shown in the two-surface view of Figure 8. This sample has a particularly uniform distribution of carbide particles in its surface as a result of the wide overlapping of melt passes. In some other carbide/metal pairs experimented with, it has not been possible to get carbide distributions as uniform as that in Figure 8 because interactions between the carbide and the metal limit the amount of overlapping which can be employed. This point will be illustrated by a discussion of the interactions which occur when TiC is injected into Ti-6Al-4V.

In Figure 6 the metal matrix between the injected carbide particles looks substantially darker than does the unmelted base metal. This dark appearance derives from the presence of fine carbides in the metal matrix. These carbides can be seen in Figures 9a and 9b, which show higher resolution views of a sectioned surface similar to that in Figure 6. The large, injected carbide particles in these photos were partially dissolved in the molten Ti-6Al-4V during processing, but upon solidification the dissolved carbide partitioned out as fine TiC dendrites between the injected particles. The dendritic carbides are evident in these photos because the metal matrix originally surrounding them was etched away. The metal matrix, still evident between the dendrites, is believed to be very similar in composition to the base Ti-6Al-

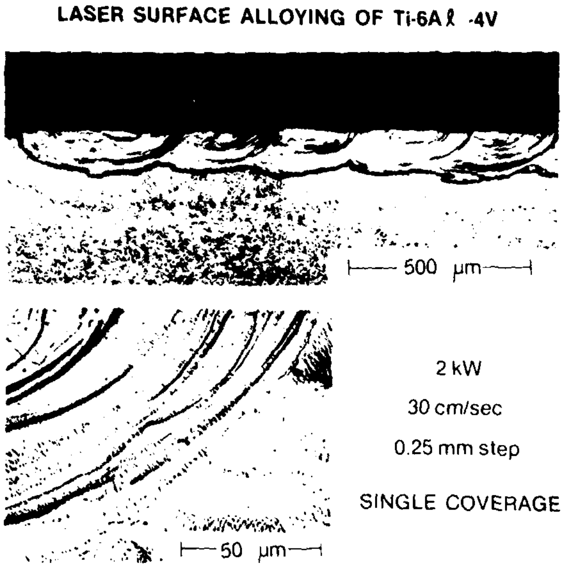

Figure 3. Polished and etched cross section of a molybdenum rich surface alloy produced by successive overlapping melts of a molybdenum coated Ti-6Al-4V specimen. The laser processing conditions are shown.

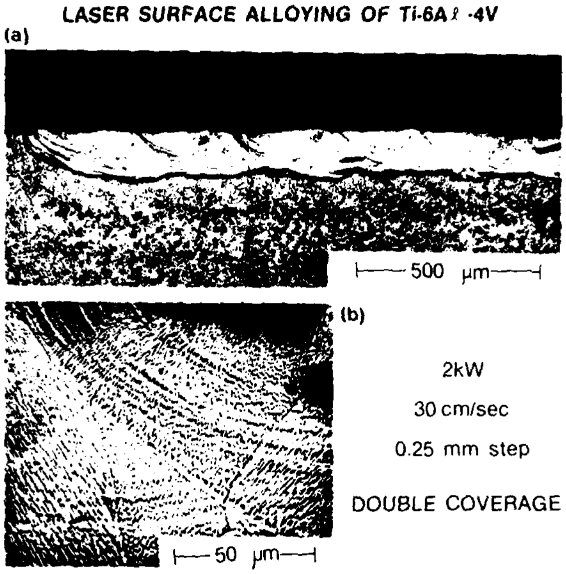

Figure 4. (a) Polished and etched cross section of a molybdenum rich alloy first processed as the specimen in Figure 2, and then reprocessed to provide additional mixing. (b) High magnification photograph showing the columnar dendritic structure of the surface alloy in the vicinity of a melt overlap.

4V. This partial dissolution and repartitioning of carbides in Ti-6Al-4V and in other transition metal alloys experimented with is of importance because it tends to embrittle the metal matrix. When this occurs, thermal stresses produced during processing can cause cracks to form in the hardened surface layer.

The major technical issue to be resolved with regard to application of the process is determination of the best way to limit this crack formation. One approach is to limit the opportunity for dissolution by minimizing the amount of overlap between melt passes. Figure 10 demonstrates the results of such an approach for TiC injected into Ti-6Al-4V. The photo reveals that this approach leads to a less uniform distribution of carbide particles in the surface,

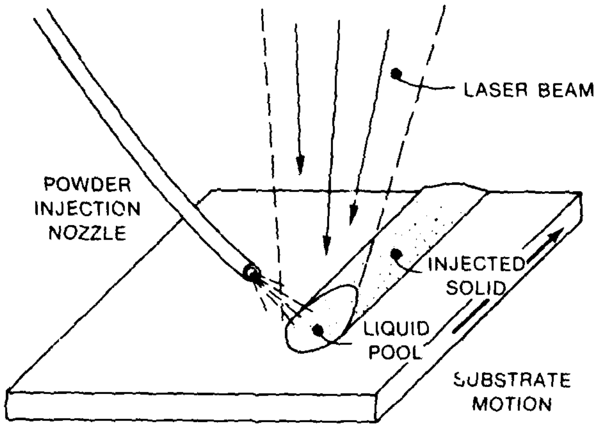

Figure 5. Injection of particles into a melt zone established by a high power laser beam.

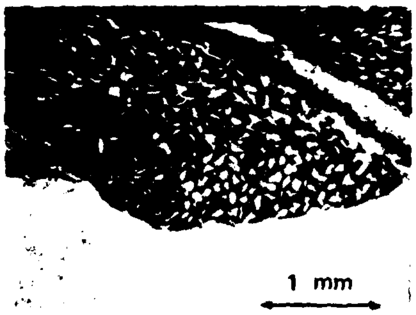

Figure 6. Sectional view of Ti-6Al-4V sample injected with TiC particles.

Figure 7. Sectional view of 5052 aluminum injected with TiC in a series of overlapping melt passes.

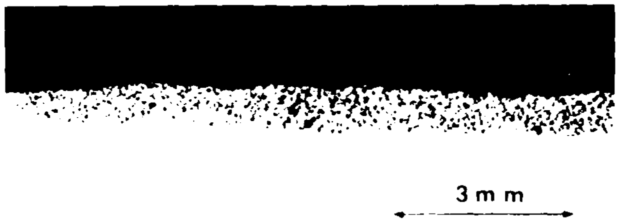

Figure 8. Sample shown in Figure 7, after surface was ground and polished.

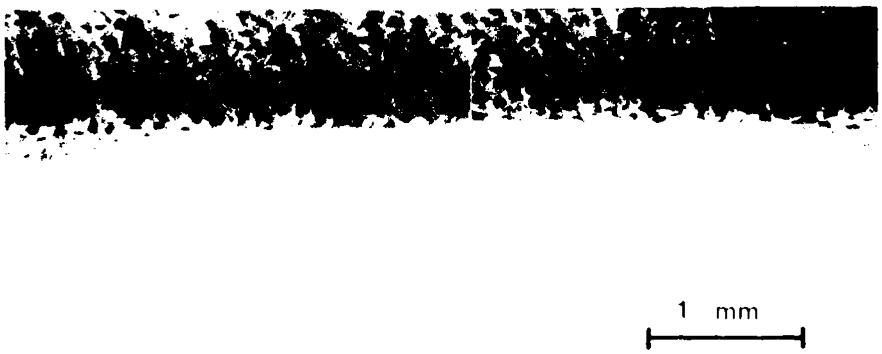

Figure 9. Fine dendritic TiC within Ti-6Al-4V matrix injected with coarse TiC.

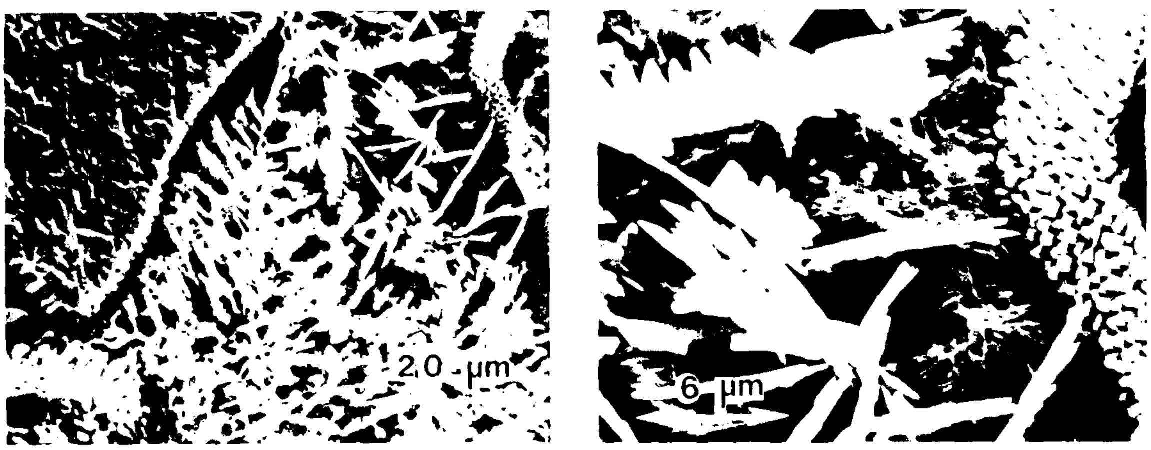

Figure 10. Sectional view of Ti-6Al-4V sample injected with TiC. Surface was ground flat after injection processing.

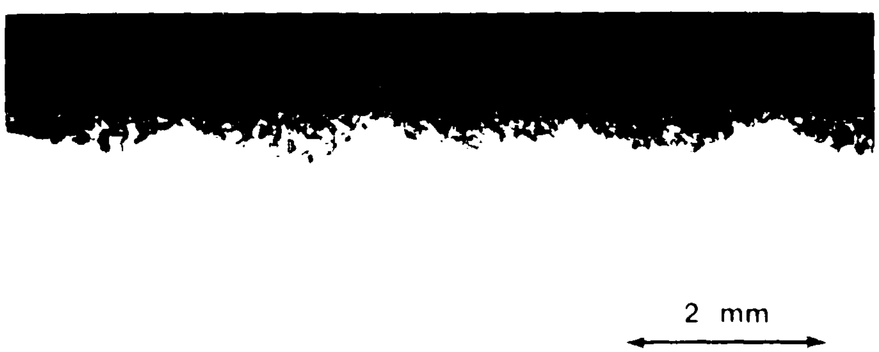

for some applications this may not be critical. Other possible approaches to limit particle dissolution are to employ spheriodized carbides, thereby minimizing surface area and reducing the number of crack initiation sites[21], or to precoat the injected particles with a film of a material with limited solubility in the melt.

As mentioned earlier, the laser melt/particle injection process can also be used to accomplish injection alloying and injection cladding. Neither of these variations has yet been explored in detail, but results to date indicate that both approaches offer potential advantages over established techniques. The principle advantage in both variations is that the surface modification can be accomplished in one processing step. That is, no precoating or elaborate surface preparation is required. Further research may well show additional advantages.

Laser Beam Welding

Today, laser beam (LB) welding is no longer a research curiosity; it is an emerging, innovative fabrication process which has just begun to be exploited. Single-pass LB welds have been made in a wide variety of metals and alloys, ranging in thickness from a few thousandths to one inch. This capability has been illustrated in numerous studies, including a fundamental research study sponsored by the Office of Naval Research.[22] These welds have a simple square-butt geometry and are autogeneous, although filler metal additions can be made. Because of power limitations of industrial-type lasers (15-20kW), LB welds in thickness greater than one-inch require multi-passes and filler metal addition.

The most distinctive feature of LB welding, however, is the increase in speed over conventional arc processes. Table III lists typical parameters associated with single-pass LB welding of a number of common structural alloys. In the case of the quench and temper steel entry of Table III, the conventional arc process requires eight to nine passes at six inches-per-minute for a through thickness welding speed of only 0.8 inches per minute. The 30 fold increase in speed in LB over conventional arc welding translates into approximately, an equivalent percentage manpower saving for the fabrication of this typical weld joint thickness.

Both pulsed and continuous wave (CW) lasers can be used to weld although the process is different in each case. If in the interaction between the laser pulse and the workpiece the power density is low and the pulse length is long, a conduction weld can be made since the absorbed energy will be conducted radially away from the interaction point. Conduction welds are either a series of spot welds or, by overlapping the series of spots, a seam weld. At higher power densities the absorbed energy is so great that evaporation of the surface occurs before a significant quantity of heat can be removed by conduction. In this case a cavity or keyhole is formed through the thickness of the workpiece. The cavity (Figure 11) is maintained against the fluid-dynamic forces of the liquid metal surrounding it by the pressure of the vaporized metal. Metal is progressively melted at the leading edge of the moving pool and flows around the deep penetration cavity to the rear of the pool where it solidifies. Thus the laser-beam welding process requires a balance of forces between the power density and the welding speed. A high depth-to-width ratio weld is a characteristic of a keyhole-produced weld.

Table III
Laser Welding Speed

	Power (kW)	Thickness (in)	Speed (ipm)
Al Alloys	8	0.5	70
Quench and Temper Steels	14	0.75	25
Low Carbon Sheet	5	0.035	200
Ti Alloys	12	0.5	35
Grade B Ship Steel	12	1.0	30

The metal vapor that is generated by the interaction of laser beam and material produces free electrons which absorb energy from the laser beam directly. By absorbing this incoming laser energy and reradiating the energy at a lower power density, plasma formation serves to limit weld penetration. Therefore, an effective means of plasma suppression must be provided in laser-beam welding. This requirement of LB welding is handled readily by flooding the beam-workpiece interaction site with an inert gas and presents no serious limitations to the process.

Except for the plasma suppression requirements, the keyhole phenomenon of deep-penetration LB welding is similar to the electron beam (EB) welding process. Both of these high-energy beam processes produce high depth-to-width ratio welds with narrow fusion zones, narrow heat-affected zones, and have low heat inputs with corresponding low distortion. A comparison of weldment cross-sections in 0.5-inch thick HY steel weldments are shown in Figure 12 for LB, EB, and convention shielded metal arc (SMA) and gas metal arc (GMA) processes. Both LB and EB welding are high-speed joining processes and, as such, demand automation. Additional requirements for EB beam welding are vacuum environment and the shielding of x-rays produced by the interaction of the E-beam with the metallic workpiece. The atmospheric propagation and interaction characteristic of LB provide a decided advantage over EB in many applications. These include the welding of large structural components and the time-sharing of the beam between two or more work stations.

In accordance with the unique capabilities of LB welding for fabricating large structural components, the remainder of the discussion in this section will focus on LB welding of the following naval structural alloys: aluminum alloys, high-strength HY steels, and readily weldable mild steel. In general, it can be anticipated that the relative weldability of an alloy by LB welding will be shared by the EB process. Moreover, the weldability of an alloy by conventional processes will be indicative of the process development and parameter optimization required for high-energy beam welding.

Aluminum Alloys: The corrosion-resisting 5000-series aluminum alloys are often selected for naval structures where weight is an important if not a critical consideration. The major alloying element in these alloys is magnesium and the properties of these alloys result from a strain-hardening mechanism. The alloying elements also contribute to the strengthening mechanism by creating dispersed phases as well as a hardened solid solution. Any heat treating process will destroy the degree of strain hardening in these alloys, either partially or completely, depending upon the time-temperature history of the heat application.

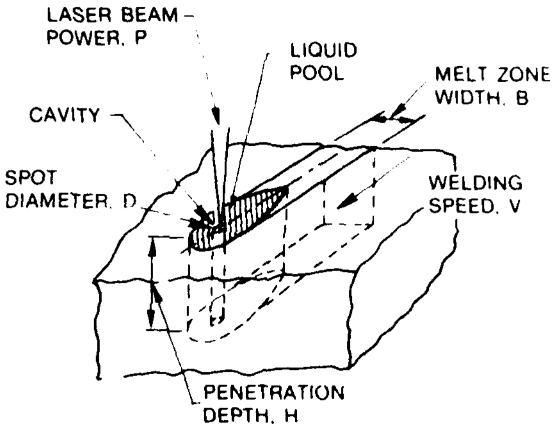

Figure 11. Pictorial of the laser beam welding process illustrating the keyhole.

LB welding of Al 5456 H116 alloy destroys the strain hardening in the fusion zone as well as in part of the heat-affected zone. This is seen in Figure 13, which compares the microstructure of the base plate and the fusion zone. The process of fusion-zone purification[23,24] is prevalent in the LB welds of these alloys. In this process inclusions, second phases, etc. are evaporated away by means of the high temperature they experience during the welding process. Counting the inclusions in the fusion zone and counting the inclusions in an equal area of the base plate indicates that only four percent of the inclusions remain in the fusion zone after laser beam welding. Another result of fusion-zone purification is a decrease of about ten percent of magnesium in the fusion zone as compared to the base plate. This is a result of the lower evaporation temperature of Mg as compared to Al.

Hardness traverses across the base plate, heat-affected zone, and the fusion zone show a considerable decrease in hardness values in both the fusion and heat-affected zones. The mechanical properties of the weldments demonstrate a slight increase in yield strength as well as a decrease in ultimate strength and ductility. The fracture toughness of the weldment is equivalent to that of other welding processes despite the large concentration of pores that are seen on the fracture surfaces.

Porosity is a very common problem in aluminum alloys welding and is a result of a dramatic change in the equilibrium concentration of hydrogen at the liquidus temperature. The equilibrium concentration

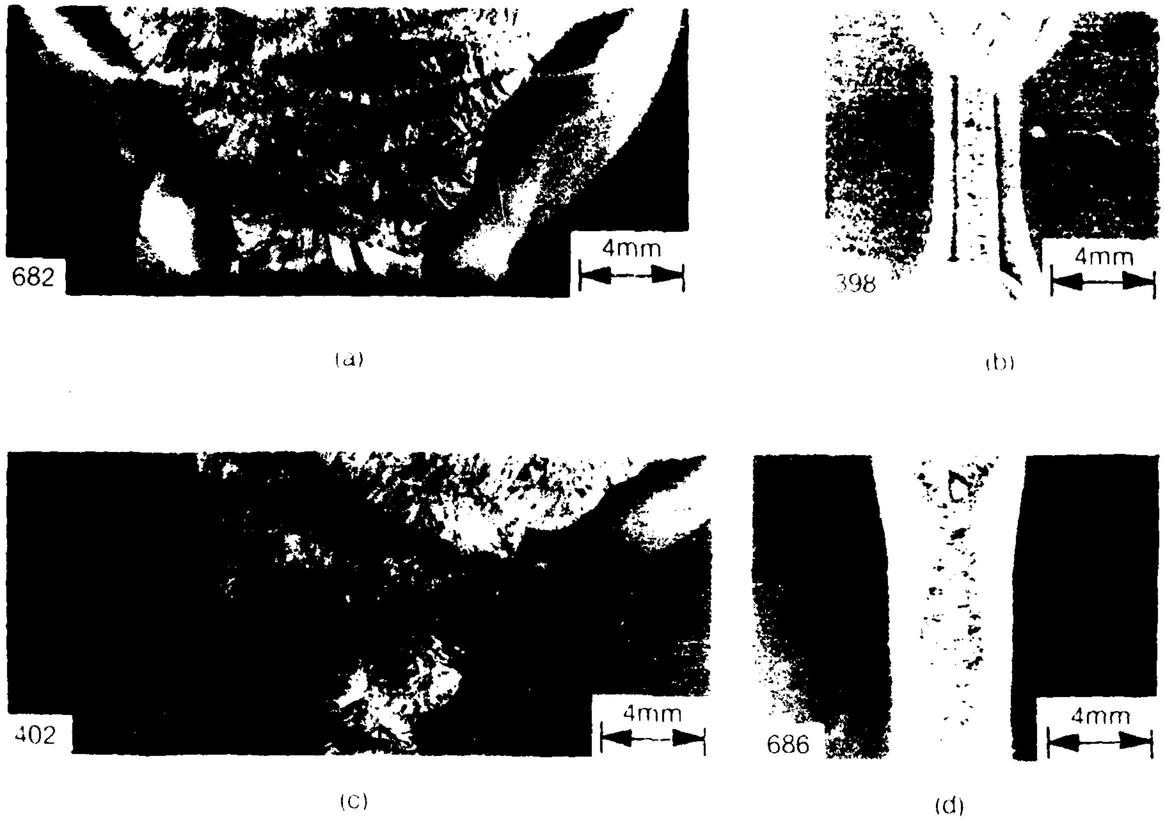

Figure 12. Cross sectional views of 0.5 in thick weldments (a) SMA weld; (b) EB weld, (c) GMA weld, and (d) LB weld.

uidus temperature. The equilibrium concentration of hydrogen in the liquid is almost twenty times greater than that of the solid. In conventional welding processes porosity can be minimized. A basic study of these problems was recently completed under ONR sponsorship.[25]

The technical issues concerning LB welding of marine aluminum alloys are: keyhole stability, which

Figure 13. Microstructures from LB weldments of Al 5456 (a) base plate and (b) fusion zone.

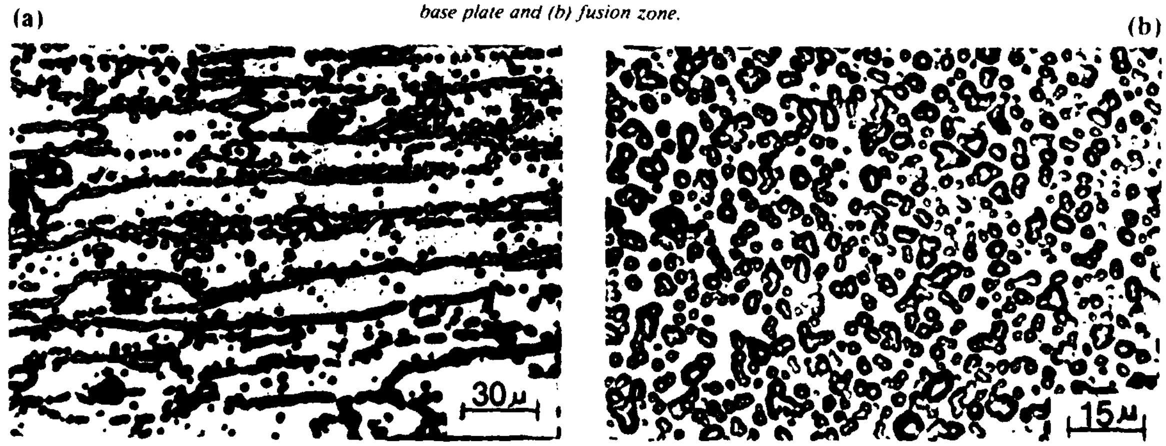

is a problem resulting from the oxidation of Al, and the minimization of porosity in the fusion zone which most likely can be achieved by proper process parameters, including filler metal additions, and which should result in better properties.

HY Steels: These premium naval alloys are weldable, quenched and tempered, martensitic steels which have yield-strengths from 80,000 psi (HY-80) to 130,000 psi (HY-130). HY-80 is used extensively by the navy for high-valued platforms, such as pressure hulls, and HY-130 is a candidate higher strength replacement. The initial investigation into laser-beam welding by NRL compared the properties and structures of HY-130 weldments fabricated by shielded metal arc (SMA), gas metal arc (GMA), electron beam (EB), and laser-beam (LB) techniques. Cross-sections of weldments from each of these processes were previously presented in Figure 12. All of the weldments were 0.5 in thick. The SMA and GMA weldments were made with filler metal, whereas the EB and LB weldments were autogeneous. The EB weldments had a cosmetic pass in order to remove slight undercut. Considerable differences can be seen in the width and the grain size of both of the fusion and heat-affected zones.

A detailed analysis of the microstructures of the different weldments as well as their hardnesses, mechanical properties and fracture toughnesses was completed on these weldments[26]. Hardness traverses were made in the mid-thickness regions of each weldment. The measurements were begun at the center of the weld and extended across the weld and (HAZ) into the unaffected base plate. Fusion zone hardnesses were found to be at a perceptibly higher level for the EB and LB welds than for the SMA and GMA welds. The EB and LB weldments revealed noticeably steeper hardness gradients than the SMA and GMA weldments.

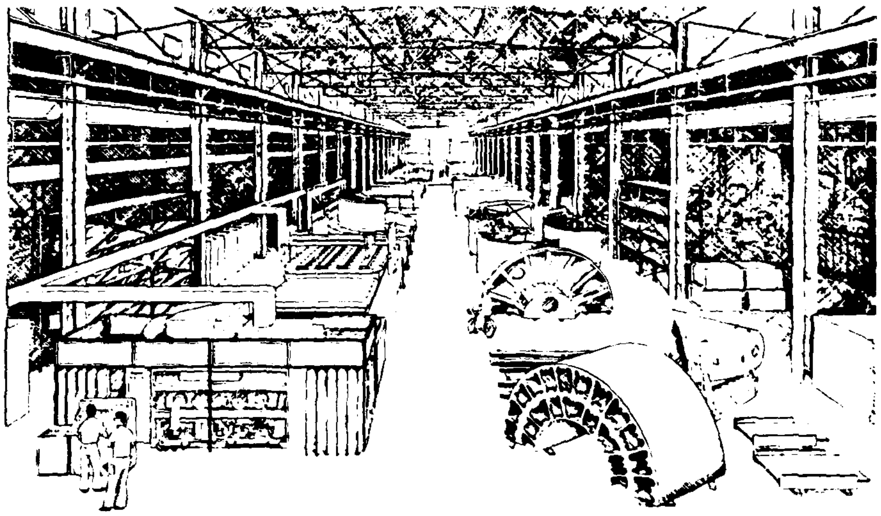

Artist's concept of the laser-beam welding system to be installed at the Naval Industrial Ordnance Plant (NIROP), Minneapolis.

Transverse-weld tension specimens were machined from the weldments for testing at room temperature. Base metal specimens of the same configuration also were prepared in order to have a basis for comparison. These specimens were machined with the longitudinal axes of the specimens aligned normal to the principal rolling direction of the plate. The SMA weld joints were the only ones which fractured in the weld metal. This was due to porosity in the SMA weld which resulted in a lower tensile strength compared to the base plate, and which also contributed to low values of ductility. The other weldments fractured in the base plate indicating that the weld joint was stronger than the base metal itself. Consequently all of the mechanical properties (yield strength, ultimate strength, ductility, reduction-in-area) required of the weldment were satisfied.

The fracture toughness of these weldments was measured using a subsized 12 mm (0.5 in) thick, dynamic tear (DT) specimen. The room temperature fracture toughness of the base metal was over 800 ft-lb. The fracture toughness of both the SMA and GMA weldments was slightly over 500 ft-lb, whereas the EB weldment was about 600 ft-lb and LB weldments were over 700 ft-lb. The Navy's fracture toughness requirement for HY weldments is 500 ft-lb. Thus all of the weld processes produced satisfactory fracture toughness.

Several HY-130 LB welds were later tested for fracture toughness at lower temperatures. A transition was found at 10°F (-12°C). The addition of filler metal to the weld zone and post-weld heat treatment both with the laser and in a furnace have moved this transition temperature to at least 0°F (-18°C). Many different techniques are being tried at present to improve further this toughness/temperature relationship.

LB weldments of HY-80 have been fabricated and tested. The weldments were shown to possess satisfactory mechanical properties, i.e., they possessed adequate strengths and ductilities as measured by the standard tension and bend test. Because of solidification cracking, however, the fracture toughness was unsatisfactory in these weldments. The solidification cracking is a result of the low heat input/fast welding speed of the laser beam welding process as well as the high sulfur and phosphorous content of the alloy.

Through the commonality of interest in high strength quench and tempered steels, a cooperative research program on LB welding of these alloys has evolved between the United Kingdom, Australia and the United States. The objective of the program is to develop sound LB weldments which satisfy the stringent requirements of marine structures. Pedigree materials with different amounts of deoxizers have been exchanged for LB welding between the U.S. and the U.K. The Admirality Marine Technology Establishment in the U.K. is testing the weldments for corrosion fatigue and stress corrosion cracking. The Welding Institute in the U.K. is fabricating LB weldments on their 7 kilowatt laser. The Materials Research Laboratory in Australia is characterizing the LB weldments especially their defect structure. The roll of NRL is to fabricate laser beam weldments, characterize their structures, and measure their mechanical properties and fracture toughness.

In high-strength steels LB welding offers the advantage of eliminating the preheat necessary in the conventional welding processes. With increasing energy costs, the savings due to elimination of preheat can be appreciable. Because most LB welds can be made as autogeneous welds (that is without filler metal), considerable savings can be accrued in large and complex structures.

The technical issues for these steels concerns the low temperature fracture toughness of the alloys and a welding methodology that would eliminate solidification cracking.

Weldable Structural Steel: The most prevalent steel used in naval structures is a weldable structural steel. This mild steel is a carbon-manganese alloy and has been called by various names: mild steel, AISI 1020, ASTM A-36. The alloy has a minimum yield strength of 36,000 psi, a tensile strength of 58,000-80,000 psi and a minimum elongation of 23 percent in 2 inches. Figure 14 compares the microstructure of the steel base plate and the fusion zone. The base plate microstructure is ferrite with some pearlite. Where as the fusion zone is bainite. Mechanical properties of these weldments were determined by standard tension specimens as well as by transverse side-, face, and root-bend test. Transverse tension specimens failed in the base plate, indicating that the weld properties exceeded that of the base plate. The bend specimens did not crack when subjected to a 180-degree bend around the correct size mandrel. Normally no toughness requirements exist for standard weldments. Hardness traverses across the base plate, heat-affected and fusion zones showed a moderate increase in hardness in the areas affected

Figure 14. Microstructure of Mild Steel Laser Beam Weldment (a) base plate and (b) fusion zone.

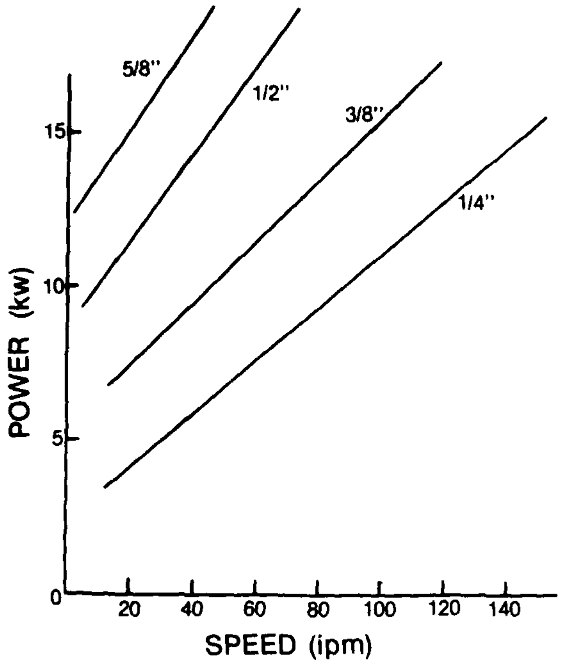

Figure 15. Laser beam power needed to butt-weld different thicknesses of plate of mild steel as a function of welding speed.

by the heat from the laser beam. This increase is a result of the phase transformation from pearlite to martensite.

Recent experimental studies at NRL have demonstrated the relationship between laser power and welding speed for a series of slates of different thickness. These results are shown in Figure 15. The weld parameters were developed for single-pass, autogeneous butt welds. This weld joint is the type that is expected to be utilized most frequently in a manufacturing facility. The simple butt weld configuration offers the greatest economic return in that edge preparation is minimized and filler metal is not needed.

The technical issues for LB welding of A-36 steel involve plasma dispersion techniques for production welding, weld joint design and edge preparation, the use of filler metals, the degree of fit-up required, and the development of multi-pass techniques for weldment thicknesses in excess of one inch.

In terms of weldability and gross tonnage use, mild steel fabrication is a leading naval candidate application for LB welding. It is not surprising, therefore, that LB welding of thick section, mild steel structural components is being pursued presently at the Naval Industrial Reserve Ordnance Plant (NIROP), Minneapolis. This facility manufactures guided missile launching systems and gun mounts for

Figure 16. Laser price and dollar-per-watt versus output (kW) for commercially available CO_2 lasers (Ref. 22).

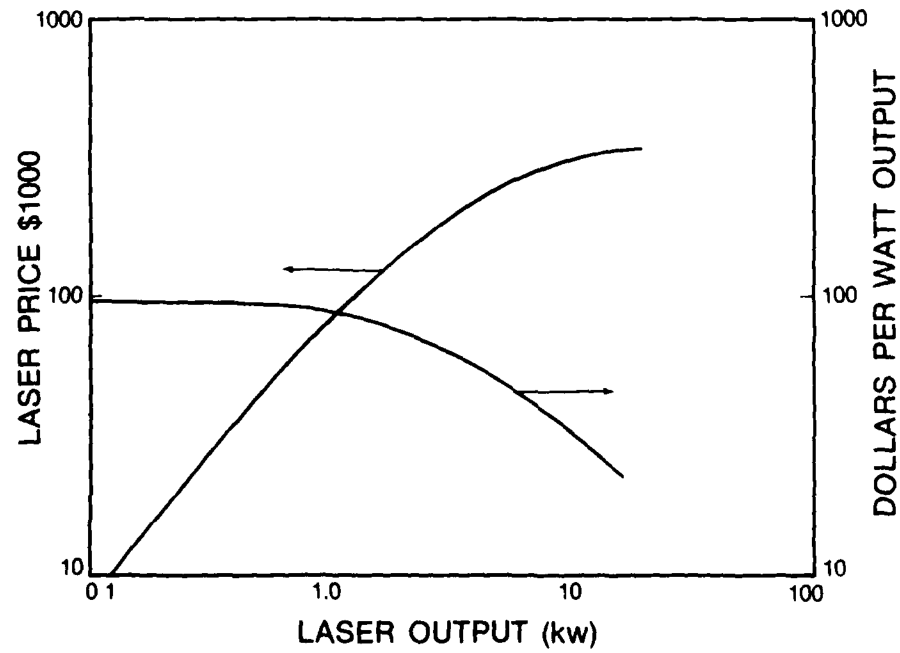

surface combatants. An inventory of the length, thickness and joint configuration of various components of these structures has shown that LB welding offers a faster and more economical than present techniques. Large-scale introduction of fully automated LB welding and other LAM operations are leading manufacture technology candidates to significantly reduce costs and improve reliability of Navy and Marine Corps weapon systems. As the title of this article states, it is anticipated that laser-assisted metalworking will be, truly, a technology in transition over the next decade.

LAM Economics

Notwithstanding the demonstrated and emerging capabilities of laser-assisted metalworking described herein, economic rather than technical considerations will determine whether LAM will be adopted or rejected for industrial applications. Usually, the selection of LAM over conventional metalworking methods is based on straight-forward cost-benefit analysis for the depreciation lifetime of the equipment. In this type of one-on-one comparison, LAM is often found to be cost-effective but requires a higher initial investment. As shown in Figure 16, the cost-per-kilowatt as well as the efficiency of CW lasers improve as the power level is increased. This trend[27] favors LAM for applications requiring high-energy outputs, such as multiple work stations with time-sharing facilities. In stand-alone operations, however, initial costs, lack of industrial experience, and conservative attitudes have been impediments to the introduction of LAM into U.S. industry.

LB welding of large naval ordnance structures was previously cited as a LAM application which offers significant cost savings over conventional welding fabrication. This forecast was based on a comprehensive feasibility study[28, 29] sponsored by the Naval Sea System Command at its Naval Industrial Reserve Ordnance Plant (NIROP) in Minneapolis. The weld-shop operation at this Navy-owned, contract operation facility requires approximately three hundred thousand manhours annually, and there exists a three hundred and sixty million dollar fabrication backlog at NIROP. Hence, this facility not only represents a challenging prospect for LAM but also offers an opportunity for a Navy test bed demonstration of this technology.

As part of the LB welding study at NIROP, a model was constructed of the weld-shop procedures. This model identified both on-station and off-station operations associated with various weld-joint configurations. Actual production-time standards were then utilized to estimate the time savings incurred by LB welding for various generic weld joints. As anticipated, the major time saving was derived from a reduction in burn-time, i.e., the time during which the arc is stuck in conventional welding or beam-on time in laser-welding. The production-time standards also showed that 50% of the total welding jointing time is associated with burn-time. Significant time saving also occurred from reduced straight cost associated with adoption of laser-beam welding.

Having determined the time (manpower) saving per each generic LB welding operation, it than became necessary to quantify the amount of potential LB weldments at NIROP and to define the corresponding tooling and fixturing requirements. Unlike the high volume, repetitious character of previous LAM industrial applications, LB welding at NIROP is for small-lot labor-intense components of large naval ordnance structures, such as the guided-missile launch structures shown in Figure 17. Accordingly, the engineering drawings of several guided missile launch structures and gun mounts were analyzed, and candidate LB welds were cataloged according to thickness, length, joint configuration, and alloy type. In addition, the tooling requirements for each weldment was classified into one of the following categories: linear, girth, planar, or 3-D-plunging. These four categories of tooling are illustrated in Figure 18. Ranges of weldment parameters in this inventory were 0.25 to 1.0 inch in thickness, 5 to 15 feet in length, and either mild or HY steels.

These data coupled with NIROP's production schedules and labor costs allow the calculation of cost savings which would be derived from the installation of a laser beam welding

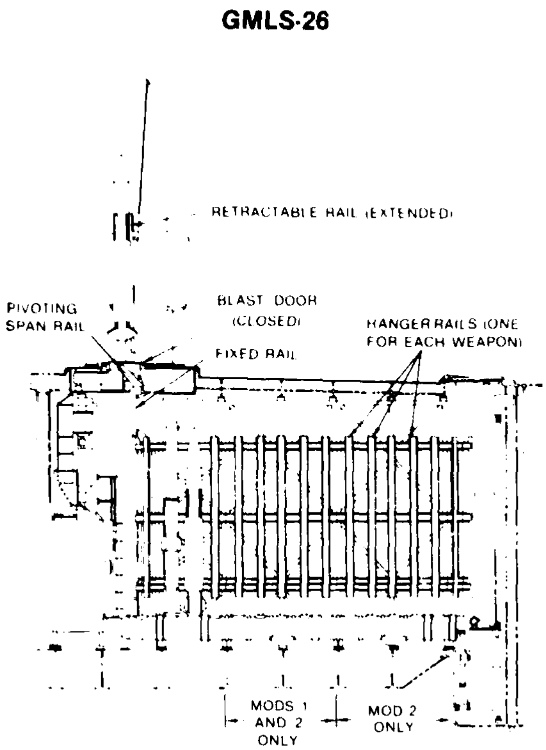

Figure 17. Mark-26 guided missile launch structure produced at NIROP Navy surface combatants.

facility. These results are graphically illustrated in Figure 19 for various combinations of tooling categories and alloys. Simple linear welds of mild steel are seen to offer the highest saving (approximately 7000 hours or 375K dollars per year) of all cases investigated. However, significant savings are realized for other tooling categories as well as alloy (HY) steel components.

Other important parameters in this analysis are the workstation utilization and laser burn-time, i.e., the number of hours per year that the workstation is occupied and the number of hours per year that the laser operates. These figures are displayed in an accumulative plot, Figure 20. For example, linear welding of both mild and alloy steel component requires 2000 hours per year of workstation utilization (approximately one shift) and only 50 hours of laser burn-time. The corresponding figures for linear and girth welding of both mild and alloy steel components are 3000 hours for the workstation and 80 hours of laser burn-time. This level of LB welding would require two workstations operating one shift per year or one workstation operating two shifts per year.

Based on the above results as well as other analyses, the Naval Sea Systems Command has

Figure 18. Man hour and dollar saving for various LB weld tooling categories and alloy types.

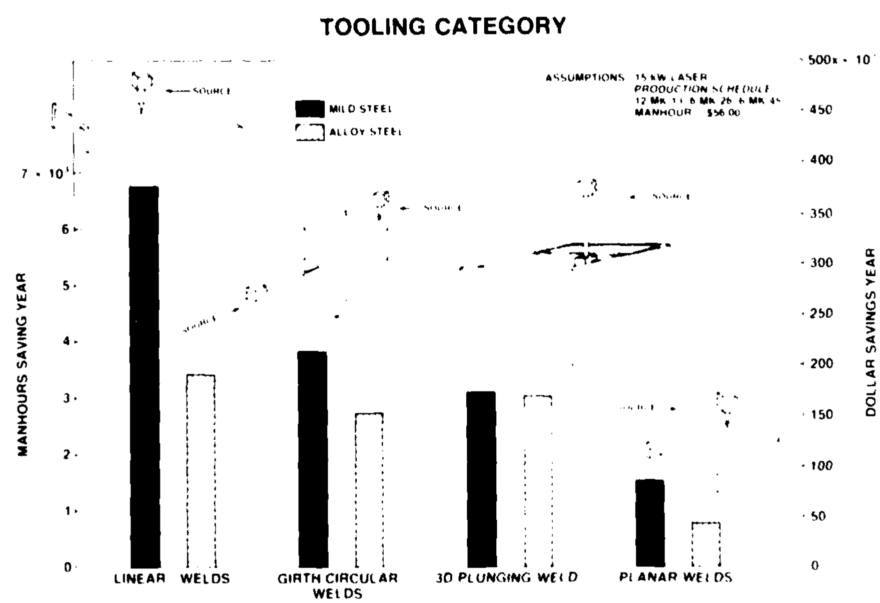

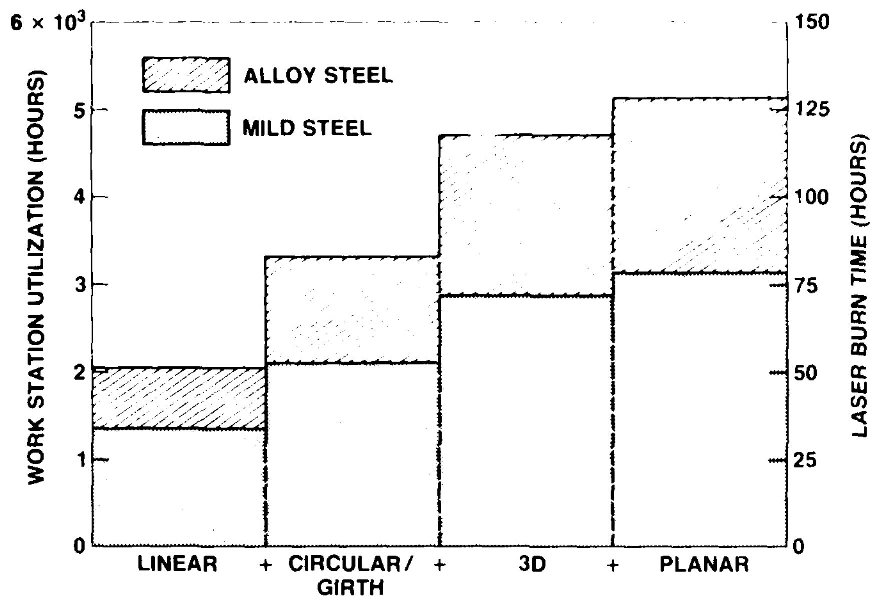

Figure 19. Accumulative plot of workstation occupancy and laser beam burn-time for various tooling categories and alloy types.

sponsored a Manufacturing Technological Program at NIROP to develop a laser-beam welding capability. This facility will contain a 15kW CO_2 laser and two workstations. Initial production-line LB welding at NIROP will focus on linear and girth welds of mild steel components. It is anticipated that this facility will payback within the first 3 years of full operation. As defined in Figure 20, the laser will be used only approximately 50 hours per year for the initial production schedule. Hence, there will exist significant opportunity to accommodate other workstations. Such an expanded capability could include other tooling—alloy combinations defined in Figure 19, as well as other LAM operations, including surface heat-treatment, cladding, alloying, particle injection, cutting, drilling and machining. Indeed, as a Navy test-bed prototype for LAM, this facility will serve as a springboard for establishing similar capabilities in other Navy fabrication plants, shipyards, and private industrial contractors. Indeed, it is anticipated, as the title of this paper states, that laser-assisted metal-working will be, truly, a technology in transition over the next decade. ■

References

1. "Laser Applications in Micromachining, Electronic Fabrication and Hardening" Session 3 of *Industrial Applications of High Power Laser Technology*, Ed. John F. Ready, Proceeding of the Society of Photo-Optical Instrumentation Engineers, San Diego, California (1976).

2. Conrad M. Banas, "High Power Laser Welding—1978" *Optical Engineering*, Vol. 17, (1978), and in *Laser in Modern Industry*, Ed. John F. Ready, Society of Manufacturing Engineers, Dearborn, Michigan (1979).

3. Simon L. Engel, "Laser Cutting of Thin Materials" in *Lasers in Modern Industry*, Ed. John F. Ready, Society of Manufacturing Engineers, Dearborn, Michigan (1979).

4. Stephen M. Copley and Michael Bass, "Shaping Materials with a Continuous Carbon Dioxide Laser" in *Applications of Lasers in Materials Processing*, Ed. E. A. Metzbower, American Society of Metals, Metal Park, Ohio (1979).

5. F. D. Seaman and D. S. Gnanamuthu, "Using the Industrial Laser to Surface Harden and Alloy", *Metal Progress, Vol. 108,* No. 3, p. 67 (1975).

6. D. S. Gnanamuthu, "Cladding", United States Patent No. Re. 29815, 24 (October 1978).

7. E. M. Breinan, B. H. Kear, and C. M. Banas, "Processing Materials with Lasers," *Physics Today, Vol. 29,* No. 11, p. 44 (1976).

8. L. S. Weinman, J. N. DeVault, and P. Moore in *Application of Lasers in Materials Processing,* Ed. E. A. Metzbower, American Society of Metals, Metal Park, Ohio (1979).

9. R. J. Schaefer, T. R. Tucker, and J. D. Ayers, "Laser Surface Melting with Carbide Particle Injection," *Laser and Electron Beam Processing of Materials,* Academic Press, N.Y., New York, p. 749 (1980).

10. E. M. Breinan, C. O. Brown and D. B. Snow, "Program to Investigate Advanced Laser Processing of Materials", ONR Technical Report, Contract N00014-78-C-0387, August 1979.

11. John R. Williams, "Summary of Air Force Program in Laser Cutting", in *Industrial Applications of High Power Laser Technology,* Ed. John F. Ready, Proceeding of the Society of Photo-Optical Instrumentation Engineers, San Diego, California, (1976).

12. F. P. Gagliano, "Application of Lasers in Battery Welding", in *Lasers in Modern Industry,* Ed. John F. Ready, Society of Manufacturing Engineers, Dearborn, Michigan (1979).

13. Michael Yessik, R. P. Scherer, "Practical Guidelines for Laser Surface Hardening" in *Laser in Modern Industry,* Ed. John F. Ready, Society of Manufacturing Engineers, Dearborn, Michigan (1979).

14. T. R. Anthony and H. E. Klein, "Laser Surface Melting of Stainless Steel for Corrosion Protection", Proceedings of the Society of Photo-Optical Instrumentation Engineers, Vol. 198, p. 82 (1980).

15. G. C. Irons, "Laser Fusing of Flame Sprayed Coatings", *Welding Journal, Vol. 57.* No. 12, p. 29 (1978).

16. J. D. Ayers and R. J. Schaefer, "Consolidation of Plasma-Sprayed Coatings by Laser Remelting", Proceedings of the Society of Photo-Optical Instrumentation Engineers, Vol. 198, p. 57 (1980).

17. J. D. Ayers, T. R. Tucker, and R. J. Schaefer, Rapid Solidification Processing, Principles and Technologies, II, Ed. R. Mehrabian, B. H. Kear, and M. Cohen, Claitor's Publishing Division, Baton Rouge, Louisiana (1980).

18. Peter G. Moore, and Leslie S. Weinman, in *Laser Application in Materials Processing,* Ed. John F. Ready, Proceedings of the Society of Photo-Optical Instrumentation Engineers, Bellingham, Washington (1979).

19. P. Moore, C. Kim, and L. S. Weinman, in *Laser-Solid Interactions and Laser Processing—1978,* Ed. S. D. Ferris, H. J. Leamy, and J. M. Poate, American Institute of Physics, New York (1979).

20. S. M. Copley, D. Beck, O. Esquivel, and M. Bass, in *Laser-Solid Interactions and Laser Processing—1978,* Ed. S. D. Ferris, H. J. Leamy, and J. M. Poate, American Institute of Physics, New York (1979).

21. J. D. Ayers and T. R. Tucker, *Thin Solid Films, 73,* 1, 201 (1980).

22. E. M. Breinan and C. M. Banas, "Evaluation of Basic Laser Welding Capabilities", ONR Technical Report, Contract N00014-74-C-0423, November 1975.

23. E. M. Breinan and C. M. Banas, "Fusion Purification During Welding with High Power CO_2 Lasers", Proceedings of the Second International Symposium of the Japan Welding Society, Osaka, Japan, (Aug. 24-25, 1975).

24. E. M. Breinan, etal., "Evaluation of Basic Laser Welding Capabilities", ONR Technical Report, Contract N00014-74-C-0423, March 1977.

25. D. B. Snow, etal., "Evaluation of Basic Laser Welding Capabilities", ONR Technical Report, Contract N00014-74-C-0423, July 1979.

Continued on page 47

Energetic Prepolymers for Advanced Navy Cast Cured Propellants and Explosives

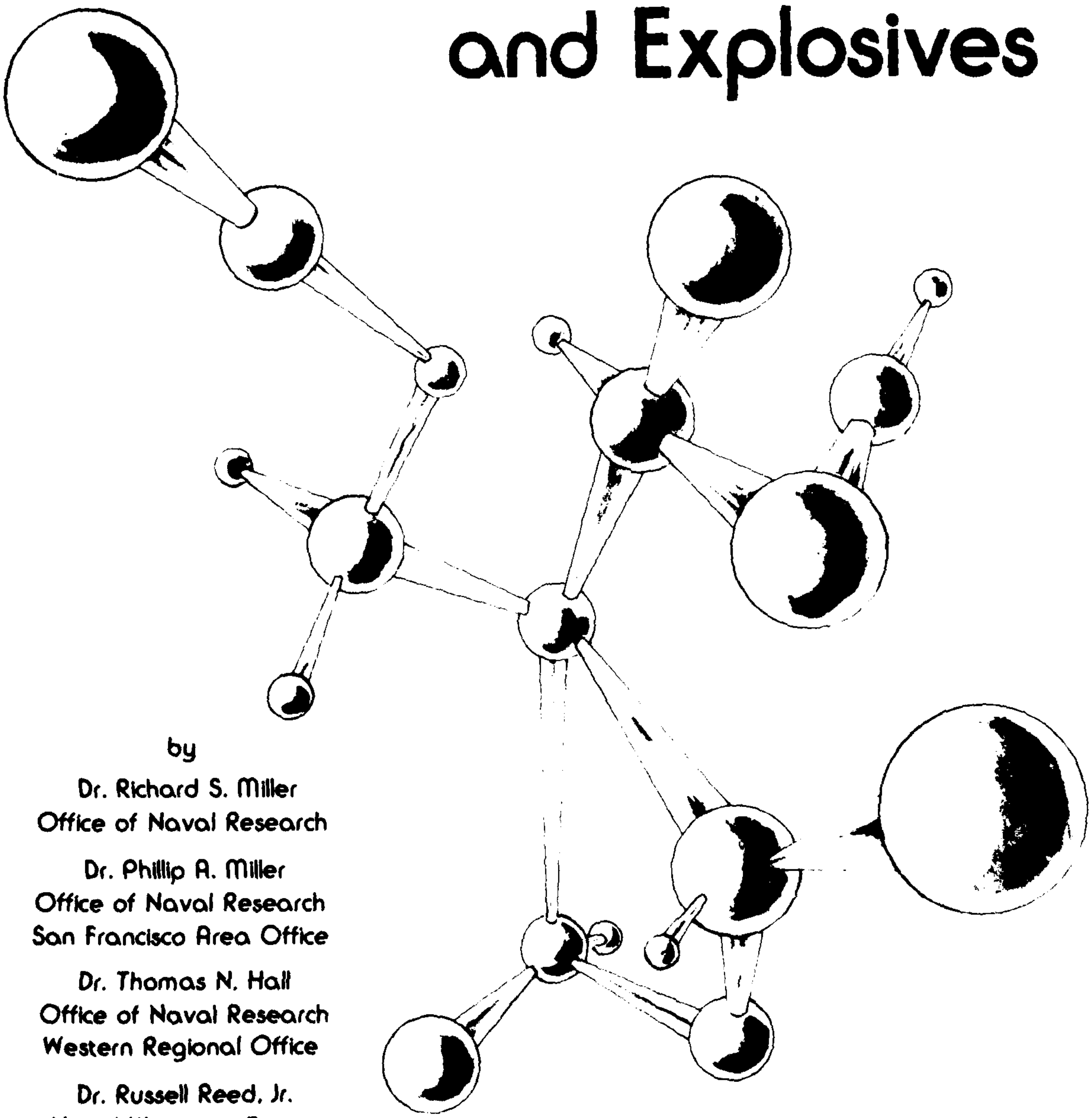

by

Dr. Richard S. Miller
Office of Naval Research

Dr. Phillip A. Miller
Office of Naval Research
San Francisco Area Office

Dr. Thomas N. Hall
Office of Naval Research
Western Regional Office

Dr. Russell Reed, Jr.
Naval Weapons Center

Introduction

The energetic prepolymers with which this article is concerned are intended for use in the manufacture of cast cured explosives and propellants for Navy weapons systems. The cast curing process involves mixing the following ingredients in a device very similar to that used in the baking industry for bread dough: (1) high explosive crystals; (2) aluminum powder (usually); (3) an oxidizer such as ammonium perchlorate; and (4) a liquid, relatively low molecular weight prepolymer which functions as a binder. The thoroughly mixed, viscous slurry of solid ingredients in the prepolymer is poured into a warhead or missile casing and heated to accelerate the polymerization (curing) process of the binder. The polymerization process ties the ends of the linear prepolymer molecules to one another. A rubbery, explosive-particle-filled solid is the result. The advantages of the cast cure process include: (1) the ability to formulate complex mixtures of solids into a rubbery material with moduli and strain capabilities acceptable for most applications, (2) the incorporation of a high solids loading to increase the performance figure of merit of the propellant or explosive, and (3) the manufacture of very large propellant or explosive charges with complex geometries. Very large charges often require the pouring of the several mixes into the same casing before the entire charge is heated to initiate the polymerization process. Since the polymerization process occurs with little change in volume, the structural integrity of the propellant or explosive in its casing is maintained. The disadvantages include the very careful control required of mixing conditions and a limit on the useful pot life of the mix before it is poured.

The curing or crosslinking process occurs at the ends of prepolymer chains. The prepolymer chains are difunctional; that is, they are terminated at both ends by a chemically reactive group which is often the hydroxyl(– OH) group. The mix also contains small molecules that have two or three reactive isocyanate (-NCO) groups that react with the hydroxyl groups (-OH) at the ends of the prepolymer molecules to form urethane

$$(-\overset{\displaystyle \mathrm{H}}{\overset{|}{\mathrm{N}}}-\overset{\displaystyle \mathrm{O}}{\overset{\|}{\mathrm{C}}}-\mathrm{O}-)$$

crosslinks. The prepolymer chain ends are linked to one another in the process to create a seemingly endless crosslinked polymer network.

The mechanical properties, fracture characteristics, and hazards of use of cast cured propellants and explosives are dependent on the volume and regularity of the crosslinked network. If too little prepolymer is incorporated in the explosive or propellant formulation as a result of increasing the volume fraction of solids loading, the cured material is mechanically weak and generally hazardous and unacceptable for use. In addition, the small-strain rubbery modulus and strain capability of the material are dependent upon the regularity of the crosslinked network. The modulus for any given polymer backbone is dependent on the density of crosslinks whereas the strain capability is dependent upon the number of atoms in the backbone that exist between crosslinks.

The cast cure method of making high performance, insensitive propellants and explosives based on the chemical crosslinking process is a relatively new development. The first process that was used to make large propellant grains was the cast double base process in which a mixture of a double base (nitroglycerin dissolved in nitrocellulose) solid propellant and a liquid plasticizer, usually nitroglycerin based, is poured into a mold and heated. The nitroglycerin-based plasticizer is absorbed into the nitrocellulose and makes it swell. Ultimately the swollen nitrocellulose particles become tightly packed together and coalesce to form a nonporous cast solid mass. The cast double base process and its modifications have been used to produce many Navy, Army, and Air Force missiles. The applications include Terrier, Talos, second stage Polaris, third stage Minuteman missiles and the Polaris and Poseidon gas generator missile launchers. The cast double base process was initially discovered by Dr. John Kincaid in 1942 and patented by himself and Dr. Henry Shuey.[1] Currently they are deeply involved in the technology development of cast cured propellants for Navy use in tactical strategic missiles. The need to increase the

energy density of propellants by increasing the solids loading and the size of the propellant grains above that feasible for the cast modified double base process has led to the development of high energy propellants based on the cast cure method.

Non-Energetic Prepolymers Currently Used in Cast Cured Propellants and Explosives

The non-energetic, hydroxyl-terminated prepolymers used in cast cured propellants and explosives can be classified into three types: (1) hydroxyl-terminated poly(butadiene), (2) polyesters based on reactions of adipic acid and difunctional alcohols such as diethylene glycol, and (3) polyethers polymerized from the oxides of propylene or ethylene. The thermodynamic properties of these types of nonenergetic prepolymers are presented in Table 1. The goal of the ONR program is to create energetic analogues of both hydroxyl-terminated poly(butadiene) and polyethers. The table also contains the thermodynamic properties of RDX and HMX as well

Table 1: Properties of Nonenergetic Prepolymers, Energetic Prepolymers, and Nitramine Explosives

Nonenergetic Prepolymers	Density grams/cc	Heat of Formation joules/gram
Hydroxyl-terminated poly(butadiene) (HTPB)	0.90	0
Poly(diethylene glycol adipate) (PGA)	1.19	−4740
Poly(ethylene glycol) (PEG)	1.18	−4427
Energetic Prepolymers		
Poly(2-fluoro-2,2-dinitroethyl glycidyl ether) (Poly(FNGE))	1.50	−2452
Poly(3,3-bis(azidomethyl) oxetane) (Poly(BAMO))	1.30	+2489
Poly(glycidyl azide) (GAP)	1.30	+1180
Nitramine Explosives		
HMX	1.90	+251
RDX	1.80	+276

as those of representative energetic prepolymers. The energetic prepolymers have both increased density and a more positive heat of formation than their nonenergetic analogues and contribute to an explosive's or propellant's figure of merit. Polymers with densities greater than 1.2 grams per cubic centimeter (g/cc) and with more positive heats of formation are sought. Additional property goals include chemical stability between −54 and 74 °C, terminal hydroxyl groups on all polymer chains, a low liquid viscosity or a low melting point coupled with a high solubility in and compatibility with plasticizers, and glass transition temperatures of the crosslinked plasticized binders below −65 °C.

Advantages of substituting energetic binders for nonenergetic binders are: (1) improved density and performance figure of merit at equal polymer volume fraction or increased polymer content and (2) improved mechanical properties at equal performance. An additional advantage is an increased flexibility in the formulation of the materials for other needs, such as burning rate, to meet system requirements. The potential advantages of the use of energetic polymers in high energy propellants and metal fragmenting explosives are best illustrated by numerical examples of theoretical performance.

Theoretical performance figures of merit for a hypothetical high energy propellant are shown in Figure 1. The figure of merit is plotted as a function of the volume fraction of polymer in the nitroglycerin plasticized propellant. The baseline propellant (Point A) with a poly(ethylene oxide) (PEG) polymer has a normalized figure of merit of 1.0. The normalized figure of merit (that is the figure of merit for energetic prepolymer propellant divided by the baseline figure of merit for PEG propellant) for the propellant incorporating high energy polymer is 1.02 (Point B) at the same 10.4% volume fraction of polymer. The increase in the figure of merit for the propellant containing energetic polymer would result in a significant performance increase for the missile. The effect of the energetic polymer on the volume fraction of polymer at the baseline performance level is dramatic. At the same baseline performance, the volume of polymer could be increased to 27% (Point

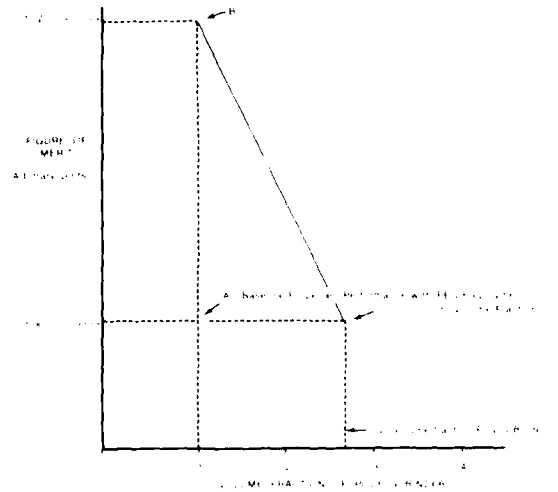

Figure 1: Figure of Merit for a High Energy Missile Propellant as a Function of the Volume Fraction of Poly G Prepolymer in the Hypothetical Formulation

C). The increase in polymer content is 170% and would likely result in a propellant with superior mechanical properties. Any combination of improved performance and polymer volume fraction above the baseline is described by the curve between Points B and C for the propellant formulated with the energetic polymer. The incorporation of energetic polymer also increases formulating flexibility.

The figure of merit (detonation pressure) for a hypothetical armor piercing explosive charge is plotted as a function of the polymer volume fraction in Figure 2. The base line (Point D) is 291 kilobars for an explosive with 21% volume fraction poly-(ethylene glycol) binder. The theoretical figure of merit (detonation pressure) for the explosive containing the energetic polymer (Poly G) as a function of its volume fraction is shown between Points E and F. Inspection of the plot (Point E) indicates that an additional 23 kilobars of metal fragmenting capability (detonation pressure) would result from the formulation containing an equal volume fraction of the energetic polymer. The same baseline performance (Point F) could be achieved in a formulation that contains 38% by volume of the energetic polymer. In this example, the volume of polymer is increased 81% at the

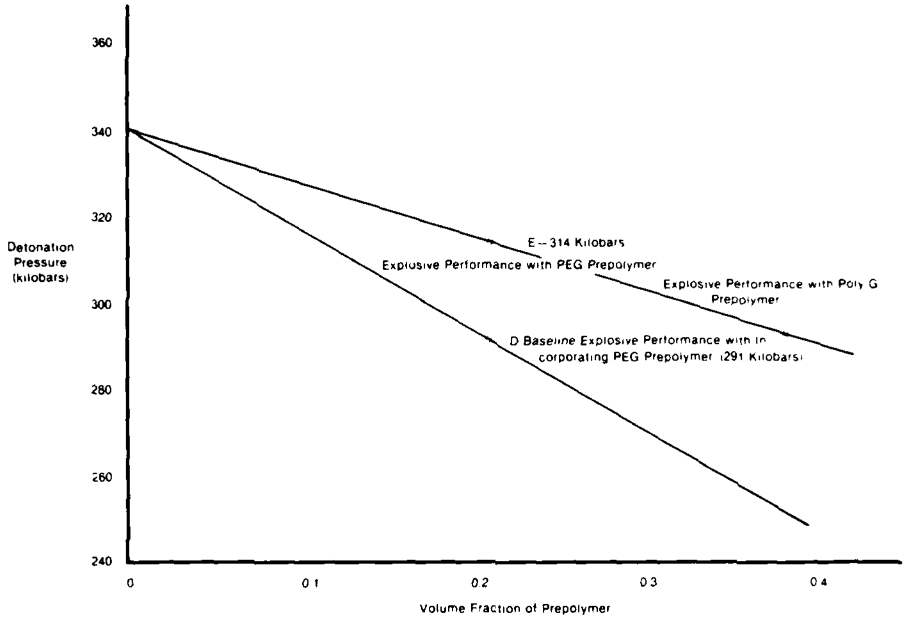

Figure 2: Detonation Pressure-Figure of Merit for a Metal Fragmenting RDX Containing Explosive as a Function of the Volume Fraction of Poly G and PEG Polyether Prepolymers in the Hypothetical Formulations.

baseline level of performance; formulating flexibility is also evident.

Synthesis Strategies to Energetic Prepolymers

Modification of Preformed Polymers

The most direct strategy is to modify the structure of commercially available prepolymers. This has the advantage of simplicity and the general availability of low cost polymeric substrates with acceptable molecular weight and functionality for crosslinking. Disadvantages include: (1) the limited chemical modification techniques available to modify the structures of the polymeric substrates, (2) the possible destruction of the vital functional groups of the prepolymer, and (3) the difficulty of separating the polymeric products of undesirable side reactions from the properly substituted useful polymer product. In addition, the possibility of engineering the molecular structure of the polymer to meet specific chemical and physical property goals is limited. Two variations of approach are currently being pursued under Air Force Rocket Propulsion Laboratory and ONR sponsorship. Dr. Milton Frankel at Rocketdyne Division of Rockwell International, under Air Force contract, is pursuing the development of

glycidyl azide polymer (GAP). The Rockwell approach is to polymerize epichlorohydrin and subsequently to substitute an azido group for each chloro substituent appended to the poly(epichlorohydrin) polymer backbone using sodium azide.

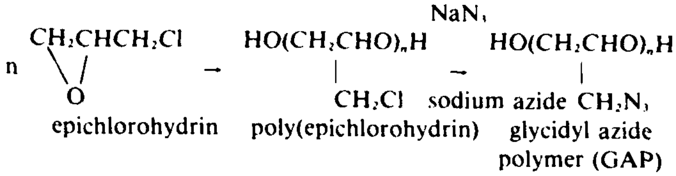

At the University of Massachusetts at Amherst, Professors James C. W. Chien and C. Peter Lillya under ONR support are applying a variant of a new nitro substitution technique published by Corey and Estreicher in 1978 which shows the substitution of a nitro group across the double bonds of small unsaturated olefinic molecules.[2] The nitro group is introduced by a two step reaction. The first reaction utilizes the attack of a mercurinium positive ion ($HgCl^+$) on an olefinic double bond and the subsequent rapid addition of nitrite ion to the adjacent olefinic carbon as a result of carbon-nitrogen bond formation to create a nitro-mercuri adduct. In the second step, reaction of this adduct with base yields the desired nitro olefin.

The research at the University of Massachusetts has successfully demonstrated the addition of nitrite ion across a fraction of the double bonds of hydroxyl-terminated poly(butadiene) that is used in the production of many cast cured propellants and explosives. The details of the nitromercuration reaction may be found in reference (3).

Energetic Monomer Synthesis and Polymerization

ONR support of research to synthesize energetic polymers was initiated in August 1947 at Aerojet-General Corporation and continued until July 1959.[4] From a historical point of view this early work had a very important impact on the development of high performance explosives and propellants although the impact was not a result of the use of energetic

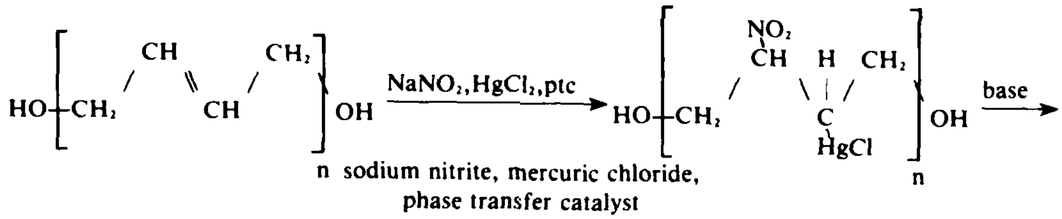

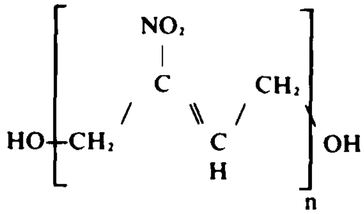

Nitro substituted hydroxyl-terminated poly(butadiene)

polymers. The synthesis of energetic polymers was attempted using vinyl, addition, and condensation polymerization approaches. Vinyl polymerization techniques, similar to those used to make today's commercially available vinyl polymers such as poly(ethylene), were attempted with monomers that were synthesized in the program. Some of the vinyl polymers such as poly(2,2-dinitropropyl acrylate), a distant relative of well known polymers such as

poly(methyl methacrylate) (Plexiglas), were evaluated in propellant compositions. However, large scale use of the materials did not materialize.

Condensation polymerizations of energetically substituted diols and acid chlorides of energetically substituted dicarboxylic acids were attempted. These materials are analogous to the polyester nonenergetic polymers such as poly(diethylene glycol adipate) (PGA) used in today's high energy Navy propellants. Unfortunately, the polymerizations of energetically substituted diols and acid chlorides of dicarboxylic acids were unsuccessful. Later work on high energy polyesters at the Naval Ordnance Laboratory, now the Naval Surface Weapons Center, was more successful, but even those materials developed shortcomings that made their large scale use impractical. At the present time, a new approach to energetic condensation polymers is being pursued at that laboratory.

The early ONR energetic polymers program made important contributions. The first contribution suggested earlier was to develop the initial technical base of polyurethane binders. The early ONR energetic polymers program synthesized nitro substituted low molecular weight nitro diols and low molecular weight nitro isocyanates and reacted them to form highly nitro substituted, high molecular weight, hydroxyl-terminated polyurethanes. The first step in the polymerization of high molecular weight polyurethanes is shown below. Polymer chain extension occurs as a result of subsequent sequential diisocyanate and diol addition.

$$\underset{\text{difunctional diol}}{2\,\mathrm{HO{-}A{-}OH}} + \underset{\text{difunctional isocyanate}}{\mathrm{O{=}C{=}N{-}B{-}N{=}C{=}O}} \rightarrow$$

$$\mathrm{HO{-}A{-}O{-}\overset{\overset{O}{\|}}{C}{-}\overset{\overset{H}{|}}{N}{-}B{-}\overset{\overset{H}{|}}{N}{-}\overset{\overset{O}{\|}}{C}{-}O{-}A{-}OH}$$

(Initial hydroxyl-terminated polyurethane prior to chain extension)

Unfortunately, the materials because of their structure were brittle solids unless they were plasticized; these polymers were not very useful. However, the production of these materials required urethane polymerization technology to be perfected. Noteworthy in this development were the use of: (1) metal chelates to catalyze the urethane polymerization reaction, (2) trifunctional curing agents to obtain three-dimensional crosslinked networks, and (3) techniques such as vacuum degassing and the elimination of acidic impurities to prevent gas-producing side reactions. As a result of the technical base for polyurethane binder crosslinking developed under this early program, the successful development of polyurethane binders used in today's Navy weapons was accelerated. Specifically, the rapid development of nonenergetic, hydroxyl-terminated poly(butadiene) (HTPB) binders benefited from this early research. HTPB binders were announced in 1962 by Sinclair Petrochemicals and, after full production capability was established in 1970 by Atlantic Richfield, the Navy successfully exploited these materials in cast cured propellant and explosive development programs. Advantages of the use of hydroxyl-terminated poly(butadienes) over other polymers such as carboxy-terminated butadiene-acrylonitrile copolymers were the higher solids loadings, superior performance, better low temperature mechanical properties, and lower cure temperatures.

The second contribution was an early attempt to synthesize energetically substituted polyethers. It was from this initial work that the success of the ongoing program can be traced. Early attempts to synthesize nitropolyethers from systems such as 2,2-dinitro-1,3-propanediol and formaldehyde failed; however, subsequent attempts to polymerize nitro substituted epoxides such as glycidyl nitrate met with more success and looked promising as the program ended. Current research is concentrating on the synthesis and polymerization of energetically substituted cyclic ethers.

The cyclic ether types under investigation are derivatives of epoxides (formula I, 3-membered ring), oxetanes (formula II, 4-membered ring) and tetrahydrofurans (formula III, 5-membered ring):

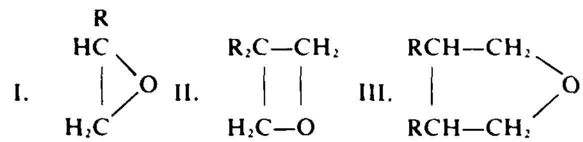

(a substituted ethylene oxide) (a 3,3-disubstituted oxetane (a 3,4- disubstituted tetrahydrofuran)

R is a substituent; numerical substituent location on the cyclic ring starts at the 1-position of the oxygen (O) atom

Dr. Milton Frankel synthesized the first energetically fluoro substituted cyclic ether monomer, 2-fluoro-2,2-dinitroethyl glycidyl ether (FNGE) in 1967 at Rocketdyne Division of Rockwell International under Air Force Armament Test Laboratory sponsorship. Dr. Vic Grakauskas in 1970 also reported the synthesis in an account of research supported by ONR and other agencies.[5] The monomer was synthesized by reacting an energetic alcohol, 2-fluoro-2, 2-dinitro-ethanol (FDNE), with epichlorohydrin and promoting the reepoxidation of the monomer with a basic reaction reaction medium.

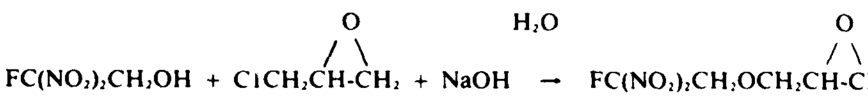

FDNE epichlorohydrin 2-fluoro-2,2-dinitroethyl glycidyl ether (FNGE)

The landmark synthesis of the thermally stable energetic FDNE alcohol was reported by Dr. Mortimer Kamlet and Horst Adolph in 1968 at the Naval Ordnance Laboratory and substantially improved by Drs. Grakauskas and Baum in the same year; the fluoronitroalcohol and its precursors are extremely versatile reagents.[6] The polymerization of fluorodinitroethyl glycidyl ether (FNGE) was later attempted under sponsorship of the Air Force Rocket Propulsion Laboratory at the Rocketdyne Division of Rockwell International. Unfortunately, adequate molecular weight and difunctionality of this polymer were not obtained. The lack of control of the difunctionality and molecular weight of the polymer resulted in unacceptably poor mechanical properties when the polymer was used to formulate cast cured propellant samples. The high density ($1.5 g/cm^3$) of the polymer of fluorodinitroethyl glycidyl ether (Poly G), its liquid state, and favorable explosive skid test results from Lawrence Livermore Laboratory were sufficiently enticing that the polymerization was again initiated in October 1978 under ONR sponsorship using new techniques that were successful in the polymerization of energetically substituted oxetanes.

Energetically Substituted Oxetanes and their Polymers:

The success of the ONR energetic polyether prepolymer program as of this writing is a result of the polymerization of energetically substituted oxetanes. Work on energetically substituted oxetane synthesis to obtain precursor monomers for energetically substituted polyether prepolymers was first proposed to ONR by Dr. Kurt Baum of Fluorochem, Inc. in November 1976.[7] Dr. Baum proposed to investigate the synthesis of nitro and fluoro substituted propane diols and their oxetane derivatives which could be converted into polyether prepolymers. However, the chemistry of fluoronitropropanediols had not been extensively explored and several years of work were anticipated before a fluoronitrooxetane

could possibly be made. The potential of fluoronitroalcohols was great because the presence of fluorine was known to inhibit deformylation in basic media. Basic reaction conditions are necessary to synthesize closed ring cyclic ethers such as oxetanes. The destructive non-fluoro dinitroalcohol deformylation (formaldehyde elimination) reaction can be illustrated as follows:

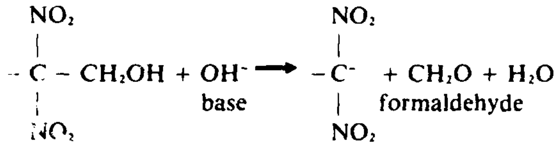

Reactions leading to fluoronitro prepolymers such as poly(3-fluoro-3-nitrooxetane) (poly(FNOX)) were postulated by Dr. Baum to be possible because of the stabilizing effect of fluorine substitution.

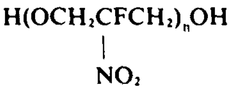

poly (3-fluoro-3-nitrooxetane) or poly(FNOX)

A Russian synthetic procedure to make the 2-fluoro-2-nitro-1,3-propanediol (FNPD) had been reported but it proceeded in poor yield and was not practical to pursue. Dr. Baum suggested an ingenious route that started from a commercially available methanol ester of malonic acid. In November 1976, 65 grams of the desired fluoronitromalonate had been readily prepared for conversion to the desired fluoronitrodiol. In February of 1977, the conversion of the fluoronitromalonate to the desired fluoronitrodiol was demonstrated. The fluoronitromalonate, when reacted with formaldehyde and sodium hydroxide, forms the 2-fluoro-2-nitro-1,3-propanediol (FNPD).

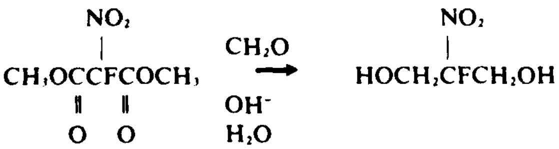

dimethyl 2-fluoro-2-nitromalonate

2-fluoro-2-nitro-1,3-propanediol (FNPD)

By May of 1977, Dr. Baum and Dr. Phillip Berkowitz had improved the synthesis to a yield of 89%.

In July of 1977, the mono and ditriflate esters of 2-fluoro-2-nitro-1,3-propanediol (FNPD) with triflic anhydride (trifluoromethanesulfonic anhydride) were made. In September 1977, the reaction of the monotriflate ester with base yielded the desired 3-fluoro-3-nitrooxetane (FNOX).

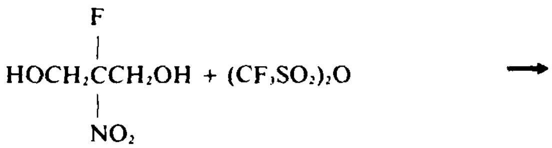

(FNPD) triflic anhydride
2-fluoro-2-nitro-1,3-propane diol

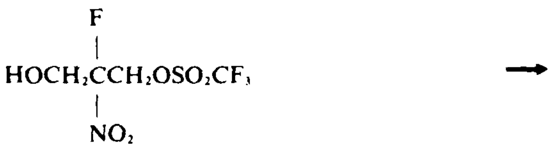

monotriflate ester

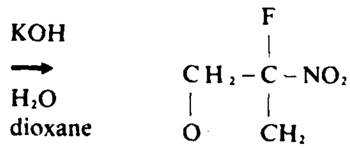

(FNOX)
3-fluoro-3-nitrooxetane

In December 1977, Dr. Baum successfully polymerized 3-fluoro-3-nitrooxetane (FNOX) using phosphorus pentafluoride as a catalyst. The polymer had a density of 1.59 g/cc and a molecular weight of 2500. The crystalline nature of the polymer was responsible for its high melting point of 234° C and an onset of decomposition of 290 °C

This successful synthesis of the energetic oxetane, 3-fluoro-3-nitrooxetane (FNOX), and its polymerization were very significant for two important reasons. Firstly, the polymerization of the 4-atom oxetane ring appeared to be more susceptible to control of molecular weight and functionality than the 3-atom epoxide ring. Secondly, the synthesis of oxetanes with different energetic substituents was possible, thereby greatly increasing the number of hydroxyl-terminated homopolymers available to the formulator of cast cured energetic propellants and explosives. In addition, the copolymerization of oxetanes would probably be possible. Copolymerization would theoretically further improve physical properties by providing prepolymers with lower glass transition temperatures.

Because of the promise that cyclic ether (and in particular oxetane) polymerizations appeared to offer, the ONR research program was expanded to accomplish three objectives. The first objective was to increase the number of available energetically substituted oxetane and other cyclic ether monomers. The second objective was to increase our understanding of the mechanisms of cyclic ether polymerizations from both theoretical and experimental points of view. The third objective was to reinvestigate the polymerization potential of fluorodinitroethyl glycidyl ether (FNGE) in the light of the success of phosphorus pentafluoride in polymerizing the fluoronitrooxetane (FNOX).

In November 1978, a new research program under the research direction of Dr. Milton Frankel was initiated at the Rocketdyne Division of Rockwell International to explore the relationship between the structure of energetic azido ($-N_3$) containing molecules and their sensitivity to explosion when impacted. The long term objective was to identify impact insensitive azido molecular structures, to incorporate them into cyclic ethers (with the emphasis on oxetanes), and subsequently to attempt their polymerization. In the first two months of the research, a series of hydrocarbon molecules containing a single energetic azido group was synthesized. The identities and properties of the monoazidoalkanes may be found in Table 2. All the monoazidoalkanes exhibited very good resistance to explosion when impacted; it was concluded that the impact sensitivities of polymers made from monomers containing one azido group should be acceptably low. Subsequently, the range of molecular structures was increased to include the incorporation of two azido groups into the same molecule. The identities and properties of the diazido compounds are also listed in Table 2. Examination of the results in this series of experiments indicates a strong dependence of impact sensitivity on molecular structure. Only 2,2-bis(azidomethyl) propane had a low impact sensitivity similar to the monoazidoalkanes. In March 1979, Dr. Frankel synthesized an oxetane monomer, 3-3-bis(azidomethyl) oxetane (BAMO). The monomer is made simply by reacting sodium azide with 3,3-bis(chloromethyl)-oxetane (BCMO) in solution. The azido group easily displaces the chloro substituent. The BAMO is obtained in high yield, and of great immediate practical importance are both the commercial availability of sodium azide and the relatively easy synthesis of 3,3-bis(chloromethyl)oxetane (BCMO) from inexpensive chemicals.[7]

$CH_2—C(CH_2Cl)_2$ | | $O—CH_2$	NaN_3 $\longrightarrow$	$CH_2—C(CH_2N_3)_2$ | | $O—CH_2$
3,3-bis(chloromethyl) oxetane (BCMO)	sodium azide	3,3-bis(azidomethyl) oxetane (BAMO)

Table 2: Properties of Mono and Diazidoalkanes

Monoazidoalkanes

Compound	Structure	Density g/cc (24 C)	Impact Sensitivity* in.-lb., 50% fire
1-Azidopropane	$CH_3CH_2CH_2N_3$	0.87	>250
2-Azidopropane	$CH_3CH(N_3)CH_3$	0.85	>250
1-Azidobutane	$CH_3CH_2CH_2CH_2N_3$	0.87	>250
2-Azidobutane	$CH_3CH_2CH(N_3)CH_3$	0.86	>250
1-Azidopentane	$CH_3(CH_2)_3CH_2N_3$	0.87	>250
1-Azidohexane	$CH_3(CH_2)_4CH_2N_3$	0.86	>250
Azidocyclohexane	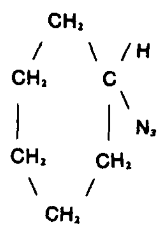	0.97	>250
TMETN (Control)	—	—	30

Diazidoalkanes

Compound	Structure	Density g/cc (25 C)	Impact Sensitivity* in.-lb., 50% fire
1,2-Diazidopropane	$N_3CH_2CHN_3CH_3$	1.09	<5
1,3-Diazidopropane	$N_3CH_2CH_2CH_2N_3$	1.11	<5
1,4-Diazidobutane	$N_3CH_2CH_2CH_2CH_2N_3$	1.07	57
2,3-Diazido-1-propanol	$N_3CH_2CH(N_3)CH_2OH$	1.26	7.5
2,2-bis(Azidomethyl)-propane	$CH_3C(CH_2N_3)_2CH_3$	1.03	>250
TMETN (Control)	—	—	30

*A high numerical Impact Sensitivity determination indicates the compound has *little* sensitivity to explosion when impacted.

The polymerization of 3,3-bis(azidomethyl)oxetane (BAMO) at Rocketdyne was initiated in July 1979. The initial research concentrated on the control of molecular weight using water as a chain terminator and boron trifluoride as the chain initiator. In current experiments, glycerol is used as the chain terminator to insure that the number of hydroxyl groups in each polymer chain is two or greater. However, the insolubility of glycerol in the reaction solvent seems to limit the role the glycerol plays in controlling the polymerization process and the resulting molecular weight and functionality of the polymer.

In July of 1979, Dr. Donald Ross, Mr. John Guimont and Mr. Gerry Manser of SRI International initiated research to synthesize a new energetic oxetane monomer and to extend the control of oxetane polymerizations. The first year of the research project was devoted to the successful synthesis of a new fluoronitroethoxyoxetane monomer and a nitro-substituted tetrahydrofuran. In September of 1980, Mr. Manser made a breakthrough in the methodology of polymerizing energetically substituted oxetanes. Prior to the breakthrough, Mr. Manser utilized the methodology used by Dr. Frankel in his polymerization studies of 3,3-bis(azidomethyl)-oxetane (BAMO). In this scheme, the ratio of catalyst to monomer is varied to control the molecular weight, and a small quantity of water or glycerol (which are almost insoluble in the reaction mixture) is added to terminate the growing polymer chains; the results of this type of polymerization are generally not predictable before experimentation is begun. Mr. Manser's technique substitutes a higher concentration of a soluble diol such as 1,4-butanediol for the inherently low concentration of the almost insoluble water or glycerol in the reaction mixture. As a consequence of these changes, the molecular weights of the prepolymer can be predicted before the polymerization experiments have begun. He has found that the molecular weight of the resultant hydroxyl-terminated polyether prepolymer can be predicted by a simple calculation. For example, if the ratio of the number of oxetane to diol molecules is 16 to 1 in the reaction mixture, then the molecular weight of the polymer equals the sum of the molecular weights of 16 oxetane units and one butanediol unit. Although not proven, the number of initiated polymer chains is probably equal to the number of diol molecules. The diols presumably enter the polymerization sequence by quickly reacting with the boron trifluoride catalyst to form an adduct which in turn initiates polymerization. Propagation then proceeds through oxetane chain extension. The polymerization process is terminated by the addition of water or alcohol. This ca[illegible]ity to predict and control molecular weight has been demonstrated for the newly synthesized 3-methyl-3-(2-fluoro-2,2-dinitroethoxymethyl)-oxetane (FOE) with an energetic nitrodiol, 3-hydroxymethyl-5,5-dinitrohexanol, and for 3,3-bis(azidomethyl)oxetane (BAMO) with 1,4-butanediol.

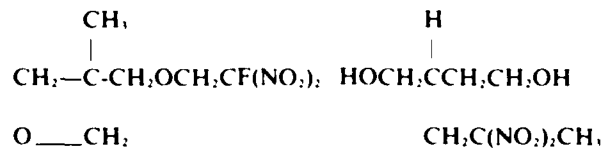

3-methyl 3-(2-fluoro-2,2-dinitroethoxymethyl)-oxetane (FOE)

3-hydroxymethyl-5,5-dinitrohexanol

The discovery of this polymerization scheme by Mr. Manser makes feasible the controlled synthesis of other energetic homo- and copolymers based on other diols and oxetanes.

Dr. Baum's research after the successful synthesis of the 3-fluoro-3-nitrooxetane (FNOX) was directed at the synthesis of the 3,3-dinitrooxetane (DNOX). In June 1980 the successful synthesis of 3,3-dinitrooxetane (DNOX) was reported. Earlier an intermediate, 3-hydroxyoxetane (HYOX), was synthesized which makes possible the preparation of other energetically substituted oxetanes. The hydroxyl group of this oxetane may be replaced by a number of energetic substituents. For example, the triflate ester of 3-hydroxyoxetane (HYOX) may be displaced by fluorodinitroethanol (FDNE) as shown below.

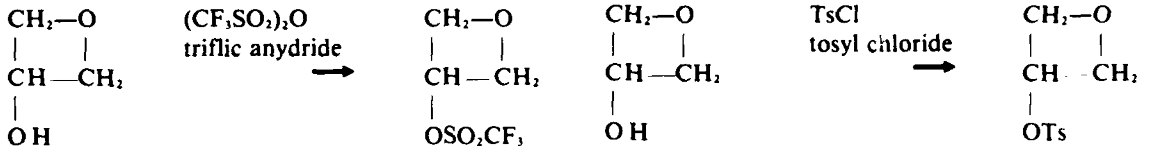

(HYOX) 3-hydroxyoxetane — triflate ester — (HYOX) 3-hydroxyoxetane — tosylate ester

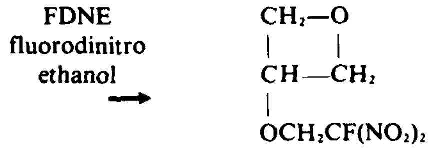

3-(2-fluoro-2,2-dinitroethoxy)
oxetane (FNEO)
($C_5H_7N_2O_6F$)

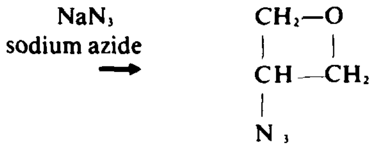

3-azidooxetane (AZOX)

The resulting energetically substituted oxetane ether (FNEO) is isomeric with fluorodinitroethyl glycidyl ether (FNGE); that is, it contains the same number and types of atoms and will probably be easily polymerized by the Manser technique.

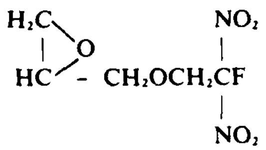

Isomeric fluorodinitroethyl glycidyl ether (FNGE)
($C_5H_7N_2O_6F$)

The net effect will be a polymer isomeric with Poly G (poly(FNGE)) but with controlled molecular weight and difunctionality. The synthesis of this new monomer and its polymerization will be attempted in 1981. As an accomplished fact, the reaction of sodium azide with the tosylate ester of 3-hydroxyoxetane (HYOX) produced 3-azidooxetane (AZOX).

This energetic 3-azidooxetane (AZOX) monomer was polymerized successfully by Dr. Baum using phosphorus pentafluoride. The liquid 3-azidooxetane (AZOX) polymer is isomeric with glycidyl azide polymer (GAP) being developed at Rocketdyne under Air Force Rocket Propulsion Laboratory sponsorship. In addition, it is predicted that the additional carbon atom in the backbone of the 3-azidooxetane (AZOX) polymer will, for a given molecular weight of polymer, provide a crosslinked poly(AZOX) elastomer with higher elongation than that of glycidyl azide polymer (GAP). The structures of glycidyl azide polymer (GAP) and 3-azidooxetane (AZOX) polymer are shown below. Both polymers have been shown to be thermally stable to 120 °C by Dr. Milton Farber at Space Sciences Incorporated under ONR sponsorship using mass spectrometric techniques.

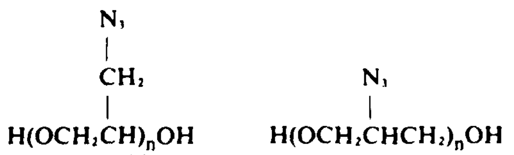

Glycidyl azide polymer (GAP) — 3-azidooxetane (AZOX) polymer

The polymerization of 3-azidooxetane (AZOX) will be reinvestigated using the technique of Mr. Manser. The copolymerization of 3,3-bis(azidomethyl)oxetane (BAMO) and 3-azidooxetane (AZOX) will also be possible and will provide an azido copolymer with a less regular structure which will lower its glass transition temperature and improve its flow properties.

The propensity for energetic oxetane monomers synthesized by Power Program supported investigators to homo-and copolymerize is being investigated using theoretical quantum chemical techniques at The Johns Hopkins University under the direction of Professor Joyce Kaufman in a research program that was initiated in Oct of 1979. Dr. Kaufman is calculating electrostatic molecular potential energy contour maps for monomers of interest to the ONR research program. Currently useful bond-distance and bond-angle data are now being supplied for selected monomers by Dr. Jerome Karle, Director of the Laboratory for the Structure of Matter at the Naval Research Laboratory. Dr. Karle and his colleagues, Drs. Richard Gilardi and Clifford George, are using both electron and x-ray diffraction techniques to study the molecular structure of energetic monomers and their polymers. The electrostatic molecular potential energy contour maps provide three-dimensional quantitative estimates of the energy of attraction for a positive hydrogen cation in the proximity of the oxetane molecule. The maps make possible an estimate of the relative basicities and reactivities of the substituted oxetane rings toward cationic polymerization. The molecular structure of the newly synthesized and semicrystalline homopolymer of 3,3-bis(azidomethyl) oxetane (BAMO) will also be determined. These data are essential to estimate the potential properties of multiblock energetic azido copolymers that are current research opportunities. The polymer of BAMO is a candidate hard segment in the multiphase thermoplastic elastomers for potential use in Naval gun propellants.

Chemical Structure

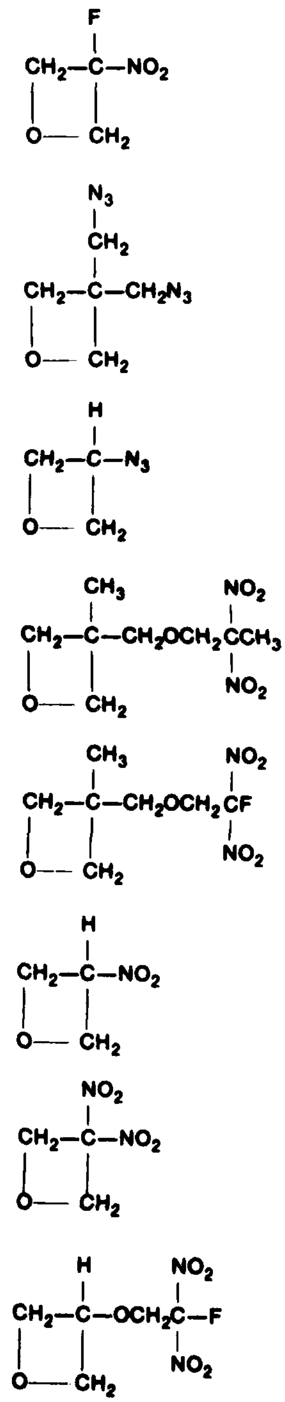

Table 3: Energetic Oxetane Monomers and Polymers

Chemical Name	Acronym	Responsible Chemist	Date	Density (g/cc)	
				Monomer	Polymer
3-fluoro-3-nitro oxetane	FNOX	Dr. Kurt Baum Fluorochem, Inc.	1978	1.47	1.59
3,3-bis(azidomethyl) oxetane	BAMO	Dr. Milton Frankel Rockwell Intl., Rocketdyne, Div.	1979	1.22	1.30
3-azidooxetane	AZOX	Dr. Kurt Baum	1979	1.17	---
3-methyl-3-(2,2-dinitropropoxy methyl) oxetane	PNOX*	Dr. Donald Ross SRI, Int.	1980	1.23	---
3-methyl-3-(2-fluoro-2,2-dinitroethoxy-methyl) oxetane	FOE	Dr. Donald Ross	1980	1.36	---
3-nitrooxetane	NIOX	Dr. Kurt Baum	1979	---	---
3,3-dinitrooxetane	DNOX	Dr. Kurt Baum	1980	1.65	---
3-(2-fluoro-2,2-di-nitroethoxy)oxetane	FNEO**	Dr. Kurt Baum	1981	---	---

**PNOX was synthesized at SRI, International under Air Force Rocket Propulsion Laboratory sponsorship*
***FNEO is a proposed monomer*
---Density has not been determined as of 25 November 1980

Summary and Future Plans

Several types of energetically substituted oxetane monomers have been produced under current ONR programs; some of these monomers have been converted to homo and copolymers using both established and new techniques. In addition, low cost oxetane substrates, 3,3-bis(chloromethyloxetane) (BCMO), and 3-hydroxyoxetane (HYOX), are available. The experimental control of the polymerization of energetically substituted oxetanes has been achieved and the theoretical development of the understanding of the polymerization of energetically substituted oxetane monomers is underway. To date, the successful polymerization of energetically substituted epoxides has not been demonstrated with respect to molecular weight control and reproducible functionality. However, isomeric oxetane monomer analogues of the desirable energetically substituted epoxides are now available or can be synthesized. A summary of energetic oxetane monomers is presented in Table 3. The densities of the monomers and polymers are presented if they have been determined.

Future work will include the synthesis of additional cyclic ether monomers, their homopolymers, selected random copolymers, and the experimental investigation of the polymerization mechanism of energetically substituted oxetanes. In addition, the scale of the energetic oxetane polymerizations will be increased to provide material for evaluation both in Navy missile propellant and explosive exploratory development programs and in Independent Research and Development Programs of missile propellant manufacturers. The properties of nitro substituted hydroxyl-terminated poly(butadiene) synthesized at the University of Massachusetts will soon be determined at the Naval Surface Weapons Center. If the thermal stability of these materials and the mechanical properties of the crosslinked elastomers made from them are acceptable, then other properties of these elastomers, such as their ability to be plasticized by energetic nitro substituted liquids (plasticizers), will be determined. The success of these evaluations may justify the synthesis of larger quantities at the Naval Ordnance Station, Indian Head, Maryland, and further evaluation of nitro substituted hydroxyl-terminated poly(butadiene) in missile propellant and explosive formulations. ■

References

1. Process for the Production of Nitrocellulose Propellants. U.S. Patent 3,378,611. April 16, 1968 (Original application filed 12 April 1945).

2. E. J. Corey and H. Estreicher, J. Am. Chem. Soc., *100*, 6294 (1978),

3. J. C. W. Chien, T. Kohara, C. P. Lillya, T. Sarubbi, B. H. Su, and R. S. Miller J. Poly. Sci. *18*, 2723, (1980).

4. J. R. Fischer, M. B. Frankel, R. D. Hamlin, J. P. Kispersky, G. B. Linden, and C. R. Vanneman, "Research in Nitropolymers and Their Application to Solid Smokeless Propellants," Report No. 1162 (Final) dtd 28 September 1956, ONR Contract N7ONR-462, DDC Locator 132723.

5. V. Grakauskas, J. Org. Chem., *35*, 3030 (1970).

6. M. J. Kamlet and H. G. Adolph, J. Org, Chem., *33*, 3080, (1968). Also V. Grakauskas and K. Baum, J.Org., Chem., *33*, 3080, (1968).

7. BAMO, 3,3-bis(azidomethyl)oxetane, was first synthesized by Dr. Wayne Carpenter at the Naval Weapons Center, China Lake, CA in 1962 and patented in 1964, (U.S. Patent 3,138,609).

Acknowledgements

The theoretical figure of merit calculations were made by Dr. Russell Reed, Jr., Naval Weapons Center, China Lake, CA., Drs. Horst Adolph and Kurt Mueller, Naval Surface Weapons Center, White Oak, MD., and Mr. John Guimont, SRI International, Menlo Park, CA.

profiles in science

George Ansell, the Robert W. Hunt Professor of Metallurgical Engineering and Dean of the School of Engineering at Rensselaer Polytechnic Institute, is widely recognized for his outstanding contributions to physical metallurgy. Professor Ansell's research has pioneered the understanding of the strengthening mechanisms of metals and alloys. He developed dislocation-particle interaction models to explain creep and yielding behavior in dispersion strengthened alloys. Of particular importance was the separation of the direct and indirect effects of the second phase on strength and the role of the particle-matrix interface strength on ductility, thermal shock properties and strength differential in dispersion strengthened alloys. Ansell recently demonstrated the importance of the coherency strain as a strengthening mechanism for nickel base super-alloys at both room and elevated temperatures.

Before joining the Rensselaer faculty, Professor Ansell was at the Naval Research Laboratory. The Office of Naval Research has supported his research throughout most of his career. Dr. Ansell has published 125 research papers and served as thesis adviser for 51 doctoral students. Professor Ansell is a Fellow of the American Society for Metals and of the Metallurgical Society of the American Institute of Mining, Metallurgical, and Petroleum Engineers. He has served on the National Materials Advisory Board and is currently Vice Chairman of the National Manufacturing Studies Board of the National Research Council. ■

Conducting Polymers

by

Kenneth J. Wynne
Office of Naval Research

G. Bryan Street
IBM Research Laboratory

Figure 1. The advantages of weight, flexibility and size of a piezoelectric transducer over conventional ceramic devices are illustrated in this photo. The polymer device weighs 0.3 milligram (without the metal lead) while the ceramic device weighs 21 grams.

Introduction

Electronic devices and electrically active materials play a vital role in the superiority of naval weapons systems, platforms and logistics. This article describes an entirely new class of electrically active materials, *conducting polymers*. The preparation, properties and potential naval applications for these interesting new materials are discussed.

Present electronic devices and electrically active materials are composed of a variety of metals, semimetals, ceramics and other inorganic substances. These materials serve as electrodes, electrical conductors and semiconductors and as transducers of electromagnetic or acoustic radiation. Systems in which these materials are found include computers, communications equipment, batteries and acoustic arrays.

Depending on the application, the utility of available electrically active materials may be limited by factors such as weight, mechanical fragility, fabrication problems, corrosion, scarcity and high cost. It was with this background in mind that in 1975 the Office of Naval Research (ONR) initiated a program with emphasis in electroactive polymers. In view of the exclusive but important role then known for polymeric materials in electrically *passive* applications such as insulators and dielectrics, the goal of the program was novel: the coupling of the desirable features of polymeric materials with electrically *active* functionality. Advantages commonly associated with polymeric materials include high strength-to-weight ratios, toughness, low cost, molecular tailoring of desired properties, and ease of processing into films, filaments and complex shapes. Thus, in addition to providing improved electronic materials, it was anticipated that the unique properties of polymers coupled with electrical functionality would provide entirely new capabilities for naval systems and subsystems utilizing electrically active materials.

In 1976, through the Avanced Polymer Program, ONR increased its funding activity in the electroactive polymer area. The Naval Research Laboratory (NRL) also recognized the potential of this research area and began a focussed effort on electroactive polymers under Dr. Luther Lockhart. Close coordination has been maintained between the ONR and NRL programs,[1] and in 1978 a joint ONR-NRL Symposium on Electroactive Polymers was held at NRL on 25 August. NRL research on electroactive polymers discussed at that Symposium may be found in Reference (1).

A previous article in Naval Research Reviews[2] has addressed research in the piezoelectric polymer area. Specifically, this research is largely centered on poly(vinylidene fluoride) (PVF_2, Figure 2) and related copolymers which are of interest (Figure 1) because of their light weight, excellent physical properties, environmental stability and high piezoelectric activity ($d_{31} = 25$ picocouloumbs/Newton). Navy research interest is currently focussed on basic research needed to provide elucidation of structure/activity correlations, and on processing studies which seek a facile route to thick film PVF_2 for underwater acoustic sensors. In addition, polymer synthesis is underway which may provide an entirely new class of piezoelectric polymers.

While this article focusses on conducting polymers, it should be pointed out immediately that this effort is far from comprehensive in scope. NRL accomplishments, presented in detail elsewhere are not included. Secondly, the research discussed below concerns polymers which, by virtue of their chemical structure, have a backbone which permits electronic conductivity. Thus "conducting polymers" such as those derived from the addition of metals or graphite particles to organic polymers are excluded from consideration.

The current resurgence of interest in the field of conducting polymers has its origins in Little's

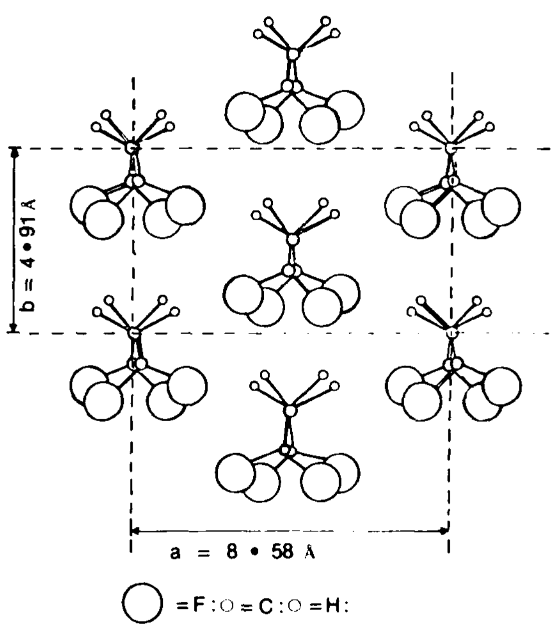

Figure 2. The planar zig-zag conformation of PVF_2 in the crystalline, highly active beta-phase (Form I).

theoretical work on room-temperature superconductors.[4] Despite the absence of the hoped-for progress in this spectacular direction, the field has maintained its impetus encouraged by systematic advances resulting from the strongly interactive efforts of chemists and physicists. These advances can be measured not only by the rapidly increasing number of widely different polymeric systems which can now be made to exhibit conductivity but also by the increasing insight into the complex mechanism of the conductivity in these novel systems. This progress has been achieved despite the difficulties of characterization of these systems whose insolubility and lack of crystallinity frequently combine to frustrate the normal characterization techniques used in polymer chemistry.

Classification of Conducting Polymers

Intrinsically Conducting Polymers. Polymers generally exhibit covalent bonding involving closed valence shells. This leads to their characteristic electrically insulating behavior. The discovery, in 1973, by Walatka, Labes and Perlstein[5] that polymeric $(SN)_x$ crystals were metallic provided the first example of an intrinsically metallic polymer. Despite extensive efforts to produce analogs, $(SN)_x$ still remains the only example of a polymer with the open-shell electronic structure necessary for metallic conductivity.[6] Thus $(SN)_x$ is presently the only member of this class of intrinsically conducting polymers.

Conducting polymers obtained by electronic modification of insulating polymers. The open-shell electronic configuration which is a prerequisite for conductivity can be achieved by oxidation or reduction of insulating polymers which contain an extended pi-bonded system. Oxidation leads to the partial emptying of previously filled bands, while reduction leads to partial filling of previously empty bands giving rise to p- and n-type conductivity, respectively.[7] Most attempts to modify sigma-bonded systems in this way have not yet been successful, perhaps because such modification of the sigma system is energetically less favorable and more disruptive to the stability of the polymer. One exception to this rule may exist. Poly(diorganosilanes) which contain a backbone comprised entirely of silicon atoms, $(R_2Si)_n$, have recently been reported to become conducting (0.5 ohm^{-1}cm^{-1}) upon treatment with AsF_5.[8] The mechanism of conductivity may involve removal of an electron from the Si-Si sigma-bonded system. In general, there are two approaches which have been used successfully for electronic modification of polymers—*direct* chemical oxidation or reduction and *electrochemical* oxidation and reduction.

Chemical Oxidation or Reduction. The first intrinsically insulating polymer converted to metallic conductivity by chemical oxidation or reduction was polyacetylene, $(CH)_x$, Figure 3b. An extensive list of the oxidizing and reducing agents effective in modifying the conductivity of $(CH)_x$ has been compiled by MacDiarmid, et al.[9] Although a wide variety of common oxidizing agents have been shown to be effective, the only reducing agents are the alkali metals. The charge transfer which takes place during a typical oxidation and reduction process for $(CH)_x$ is shown in equations (1) and (2) respectively.

$$(CH)_x + 3/2yI_2 \rightarrow (CH)_x^{y+}(I_3^-)_y \qquad 1$$

$$(CH)_x + yNa^\circ \rightarrow (CH)_x^{y-}(Na^+)_y \qquad 2$$

It is evident from these equations that the conducting derivatives of $(CH)_x$ consist of polyolefinic ions, charge-neutralized by counter ions formed from the oxidizing and reducing agents.[10] In polyacetylene these counter ions have been shown to intercalate between the planes of polyolefinic ion chains.[10,11] Although polyacetylene was the first and in many respects remains the most attractive member

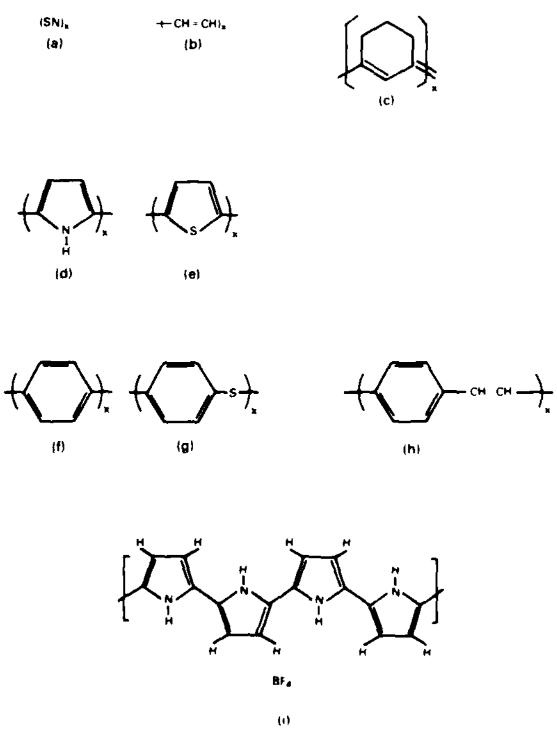

Figure 3. Conducting Polymers: (a) polysulfurnitride, (b) polyacetylene, (c) poly-1,6-heptadiyne, (d) polypyrrole, (e) polythiophene, (f) polyparaphenylene, (g) polyparaphenylenevinylene.

of this class of polymers, the class has now been extended to include many quite different polymers, which will be discussed in some detail below.

In some instances it is possible to react the monomer with oxidizing agents and simultaneously carry out polymerization and oxidation in a single step. For example, solid S_4N_4 reacts with Br_2 vapor to give brominated $(SN)_x$,[12,13] terphenyl reacts with gas to give oxidized polyphenylene,[14] and solid acetylene reacts with AsF_5 to give conducting polyacetylenes.[15]

Electrochemical Oxidation or Reduction. Polyacetylene can also be oxidized or reduced electrochemically.[16] In this case the counter ion comes from the electrolyte solution and the use of sometimes undesirable oxidizing or reducing chemicals can be avoided. Just as is the case for chemical modification, electrochemical polymerization and oxidation can be made to proceed simultaneously. This technique has been used to prepare stable, somewhat flexible films of polypyrrole by simultaneous electrochemical polymerization and oxidation of pyrrole.[17,18]

Survey of Conducting Polymers

Figure 3 shows the structural formulas of many of the conducting polymer systems currently known. The conductivities of selected doped compositions derived from these polymers and $(SN)_x$ are shown in Figure 4. The discovery that $(SN)_x$ has metallic conductivity and becomes superconducting below 0.3K led chemists to try various synthetic routes to analogous compounds.[6] Unfortunately these efforts have not yet been rewarded with success; as we have already mentioned $(SN)_x$ remains the only intrinsically metallic synthetic polymer. As can been seen from Figure 4 the room temperature conductivity of $(SN)_x$ along the chain direction is 1000 ohm^{-1} cm^{-1}, approximately three orders of magnitude less than that of copper. Reaction with halogens, particularly bromine, caused the conductivity to increase by an order of magnitude to 10^4 ohm^{-1} cm^{-1} [19,20] without destroying the superconductivity.[21,22]

$(CH)_x$ Derivatives. Oxidized polyacetylenes can be prepared with conductivities as high as 10^3 ohm^{-1} cm^{-1}. With polyacetylene the conductivity is a function of the degree of oxidation and can span the range $10^{-9} - 10^3$ ohm^{-1} cm^{-1}, which includes the semiconducting and metallic regimes.[9] Initially it was hoped that substitution of the hydrogens of polyacetylene with various functional groups would allow organic chemists to tailor an extensive family of conducting polymers whose properties could be systematically varied. Some derivatives of $(CH)_x$ have been prepared by replacing the hydrogens by methyl[23] or phenyl groups.[24,25] However, their conductivity cannot be raised to very high levels either by oxidizing or reducing agents. This failure emphasizes the importance of solid state effects in determining the electronic properties. Karasz and coworkers have shown that copolymer films of acetylene and methylacetylene can be chemically oxidized with AsF_5 to give conductivities as high as 50 ohm^{-1} cm^{-1}.[23] An interesting derivative of polyacetylene has been prepared by Gibson, *et al.*, by polymerization of 1,6-heptadiyne.[26] The proposed structure of these films is shown in Figure 3c. Oxidation of these films leads to material with a conductivity of about 10^{-1} ohm^{-1} cm^{-1}.

MacDiarmid, *et al.*, have reacted polyacetylene films with bromine to replace some of the hydrogen by bromine.[27] As with $(CH)_x$, subsequent oxidation of these brominated films with AsF_5 or I_2 leads to

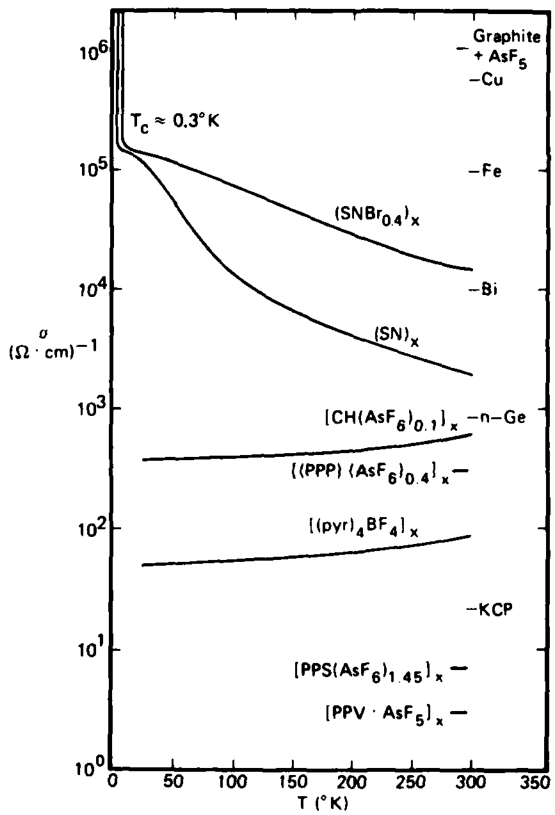

Figure 4. Room temperature conductivity for various conducting polymers, classical metals and AsF_5 intercalated graphite, and conductivity vs temperature curves for (top to bottom) brominated $(SN)_x$, $(SN)_x$, AsF_5 doped polyparaphenylene, and polypyrrole tetrafluoroborate.

material with a conductivity of 10 ohm^{-1} cm^{-1}.

Phenylene Polymers. The first demonstration that high conductivity could be achieved by oxidation or reduction of non-polyolefinic material involved poly(p-phenylene) (PPP) Figure 3f. Using AsF_5, Ivory , et al.,[28] were able to oxidize PPP increasing its conductivity from 10^{-14} ohm^{-1} cm^{-1} to 500 ohm^{-1} cm^{-1}. By using the alkali metals as reducing agents n-type PPP has also been prepared. As in the case of polyacetylene derivatives the actual conductivity of the final polymer is dependent on the degree of oxidation or reduction and both semiconducting and metallic samples can be obtained. Oligomers of poly-(p-phenylene), for example biphenyl, terphenyl and tetraphenyl, react with AsF_5 in a simultaneous oxidative polymerization leading to conducting polyphenylene.[14] Single crystal plates of terphenyl can be reacted with AsF_5 to give a polymer exhibiting strong optical and electrical anisotropy. This type of ordering has not been possible to achieve using PPP itself.[14]

Obviously, if polyacetylene and poly(p-phenylene) can each be doped to high levels of conductivity, the copolymer consisting of alternating phenylene and double bond units might have interesting properties. Wnek, et al.[29] have examined the properties of oligomers (chains of 7-9 monomer units) of poly-(p-phenylene vinylene) (PPV, Figure 3h). Pressed pellets of PPV show a conductivity 10^{-10} ohm^{-1} cm^{-1} at ambient temperature. Exposure to AsF_5 gives conductivities as high as 3 ohm^{-1} cm^{-1}.

Perhaps the most interesting of the polyphenylene derivatives investigated to date are the sulfur-linked phenylene polymer chains (Figure 3g).[30-32] Treatment of films of poly(p-phenylene sulfide) (PPS) with AsF_5 leads to conductivities of 1-10 ohm^{-1} cm^{-1}. The conductivity of AsF_5-treated PPS is somewhat surprising in view of the grossly non-planar structure of the undoped polymer.

Heterocyclic Aromatic Polymers. An extensive literature exists on powders of conducting aniline blacks[33] and pyrrole blacks[34] produced by chemical oxidation of aniline and pyrrole. Dall'Olio[35] prepared high conductivity (10 ohm^{-1} cm^{-1}) films of pyrrole polymer by stoichiometric electrochemical polymerization of pyrrole. Recent improvements on Dall'Olio's technique have given more flexible films with conductivities of 1-100 ohm^{-1} cm^{-1}.[36] These pyrrole polymers are very difficult to characterize but the pyrrole polymerization is believed to involve oxidative coupling at the alpha-position to generate the structure shown in Figure 3d. Simultaneously however the polymer is oxidized electrochemically, charge neutrality being maintained by ions derived from the electrolyte. N-substituted pyrrole polymers have also been prepared electrochemically but their conductivities were found to be much lower (10^{-3} ohm^{-1} cm^{-1}).[37] Copolymers can also be synthesized, and they show intermediate conductivities.[38]

Polythiophene (Figure 3e) has been synthesized both chemically[39] and electrochemically.[40a] As in the case of polypyrrole the electrochemically generated polymer is simultaneously oxidized. The chemically prepared polymer was subjected to subsequent oxidation by iodine. In neither case were high conductivities obtained, however. Typical values are in the range $10^{-3}-10^{-4}$ ohm^{-1} cm^{-1}. Conductivities as high as 70 ohm^{-1} cm^{-1} have been reported for halogen-doped polymers derived from polyacrylonitrile.[40b]

Bridged-Stacked Phthalocyanines. A number of bridged-stacked phthalocyanines have been prepared and have been oxidized with a variety of reagents to the metallic regime.[41] A general structure for this class of materials is shown in Figure 5. The polymeric nature of the bridged-stacked phthalocyanines arises from the presence of an $(M\text{-}X)_n$ repeat unit which "skewers" the disk-like phthalocyanine (Pc) rings. A variety of oxidants have been used to prepare conducting ($10^{-3}-1$ ohm^{-1} cm^{-1}) oxo-bridged silicon, germanium and tin phthalocyanines.[42] The conductivity decreases with increasing size of the metalloid in this series, because of increasing ring—ring separation. This and other evidence point to a conduction band resulting from pi-orbital overlap of the Pc-rings, rather than conduction along the M-X backbone.[42] Polymers with fluorine-bridged structures (PcAlF, PcGaF, PcCrF) have also been prepared and partially oxidized with iodine to give conducting compositions ($0.1-5$ ohm^{-1} cm^{-1}).[43-45] Interest in these PcMF-based materials stems from their high thermal stability, processability (they can be sublimed to form films), and potential optoelectronic properties.

Compared to the classical metals, present conducting polymers have relatively low conductivities which are at least two orders of magnitude less than copper. However, in the case of the AsF_5 graphite system the conductivity can approach that of copper. This suggests that higher conducting polymers may yet become available.

Applications of Conducting Polymers

As indicated in the previous section, polymers can be made to exhibit semiconducting, metallic, or even superconducting properties not traditionally associated with these materials. This has encouraged the belief that conducting polymers may eventually

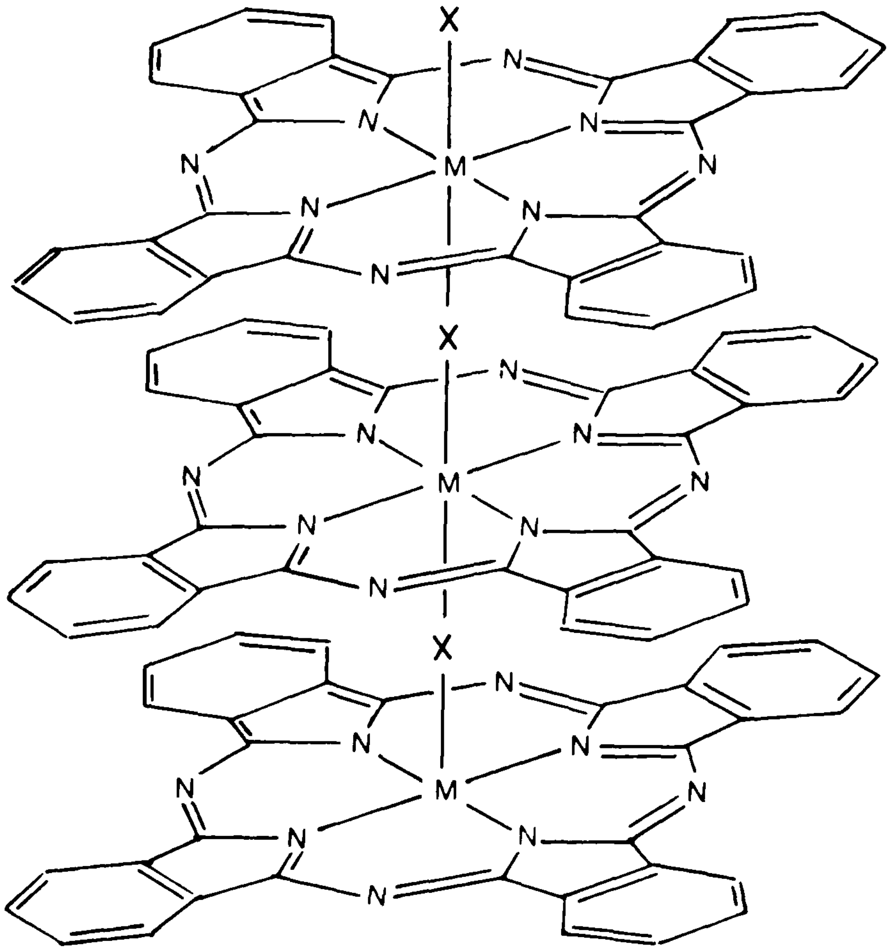

Figure 5. Schematic structure of a bridged-stacked metal phthalocyanine. Known M-X groupings include: Si-O, Ge-O, Sn-O, Al-F, Ga-F, Cr-F.

challenge the more classical materials in certain areas.

It has been suggested that conducting polymers might compete with metals forming light-weight wiring. Of the presently known systems, only AsF_5—graphite appears to have sufficiently high conductivity.[46, 47] Barrier height measurements of $(SN)_x$ films and various semiconductor substrates have shown that $(SN)_x$ has a higher work function than elemental metals.[48] Cohen and Harris[49] have taken advantage of this fact to enhance the open circuit voltage of GaAs solar cells. Polyacetylene has also been shown to form Schottky barriers[10, 11] and heterojunctions.[11] Tskukamoto, et al.,[12] have fabricated Schottky barrier type solar cells using HCl doped $(CH)_x$ as the semiconductive element. The energy efficiency is about 0.2%. Grant[13] has evaluated the metal-insulator field effects in polyacetylene. Pristine $(CH)_x$ has been used as the photoelectrode in a photochemical photovoltaic cell.[14]

In addition to their use in the role of classical semiconductors and metals, which may challenge established materials in established technologies, conducting polymers offer additional technological opportunities which take advantage of their unique properties. The electroactive properties of polypyrroles and $(CH)_x$ have been explored, and it has been shown that these materials can be repeatedly electrically switched between the metallic and the insulating states—a change which can be followed optically as well as electrically.[40] The large surface area of polyacetylene (60 m^2 g^{-1})[9a] and the fact that the

fibrils can be covered with finely divided silver metal[55] suggest possible catalytic applications. It is also possible that replacing carbon-loaded "conducting" polymers with intrinsically conducting polymers would lead to superior performance, avoiding problems with high-frequency cut off and high field breakdown associated with the carbon particles.

The metallic properties of conducting polymers permit them to be utilized as electrode materials. Nowak, *et al.*[56] have shown $(SN)_x$ has good electrode characteristics and Diaz *et al.*[40] have shown that polypyrrole tetrafluoroborate forms a stable non-porous electrode. Noufi, et al.,[57] have used polypyrrole as a passivating layer to prevent dissolution of n-GaAs photoanodes in a photochemical solar cell. Polypyrrole films also produce a dramatic improvement in the stability of n-type silicon against photooxidation in aqueous electrolyte; high photocurrents ($\sim$6mA/cm^2) are still observed after 5 days.[58] The polymer film is easy to apply and exhibits excellent adhesion.[58,59]

Conducting polymeric materials derived from $(CH)_x$ have been shown to function as cathode materials which show promise for use in lightweight high energy density rechargeable storage batteries.[60] This potential application can be illustrated by reference to the simple cell shown in Figure 6. The cell consists of $(CH)_x$ polymer film and lithium metal immersed in a $LiClO_4$ solution. Charging was accomplished in about 30 minutes using a 9-volt dry cell. Upon discharge, the cell displayed an initial open circuit voltage of 3.7 volts and a short circuit current of about 25 mA for a 0.5 cm^2 (2 mg) piece of polymer. Initial studies have shown that the cell can be charged/discharged in excess of 20 cycles. With intermittent discharge cycles a total energy density of about 80 W hr/lb is observed. Because of the small mass of films used thus far, the measured capacities have been relatively low.

It should be noted that although the energy density value cited above is interestingly large, it is not necessarily the maximum obtainable. Recent results suggest that it is possible to oxidize $(CH)_x$ to even higher levels when perchlorate is used as a counter ion; other anions may produce even higher levels of doping.

Problems and Future Opportunities in Conducting Polymers

Exciting as the above outlined prospects may be, it is important to recognize the problems that must be solved before conducting polymers can find widespread technological application.

From the discussion of the magnitude of the conductivities of presently known conducting polymers (except perhaps AsF_5-treated graphite), it is obvious that they will not displace copper or the classical metals. In most applications, if they are to become practical materials rather than laboratory curiosities, their usefulness will most probably be found in a rather unique blend of their electronic, mechanical, and processing characteristics. Indeed, conducting polymers are probably best considered not as competitors for the classical metals or semiconductors, but as materials providing new opportunities due to the incorporation into conducting materials of such attractive polymer properties as melt and solution processibilities, low density, and plasticity or elasticity. Ideally, these polymers would also satisfy a variety of increasingly important ecological considerations such as low toxicity and non-energy-intensive synthesis and processing. Preparation from non-polluting aqueous media would, of course, be desirable. Advantage could also conceivably follow from the relatively high thermal conductivities and high optical absorption coefficients of these metalic polymers.

Though some of these properties, such as low density and high optical absorption coefficient, characterize all of the existing conducting polymers, some of the other desirable properties described here are not typical of either $(SN)_x$ or the chemically (as opposed to electrochemically) modified systems. In particular, neither $(SN)_x$ nor the chemically modified conducting polymers are stable in air (particularly the alkali metal reduced n-type polymers) nor are they thermally stable much above room temperature. However, it is possible to stabilize $(CH)_x$ to atmospheric oxidation; this has been accomplished by Rohm and Haas through a proprietary coating process.[61] The majority of dopants used to impart conductivity to the polymers (e.g., AsF_5, I_2, Br_2, etc.) are highly toxic. In addition, the chemical doping process universally appears to degrade the mechanical properties of these polymers, making them brittle where previously they were flexible. In contrast to the chemically oxidized systems, electrochemically oxidized polypyrrole-BF_4, after initial air oxidation, is stable in air and shows appreciable thermal stability, though its flexibility is not yet ideal. Some of the copolymer films of acetylene and methylacetylene reported by Karasz and coworkers have exhibited elastic properties when wet with solvent.[21] When dry these films are relatively brittle but on wetting again with solvent they can be readily stretched and retain their elongation if dried under tension.

ELECTROCHEMICAL "UNDOPING"
i.e., (CH)x BATTERIES

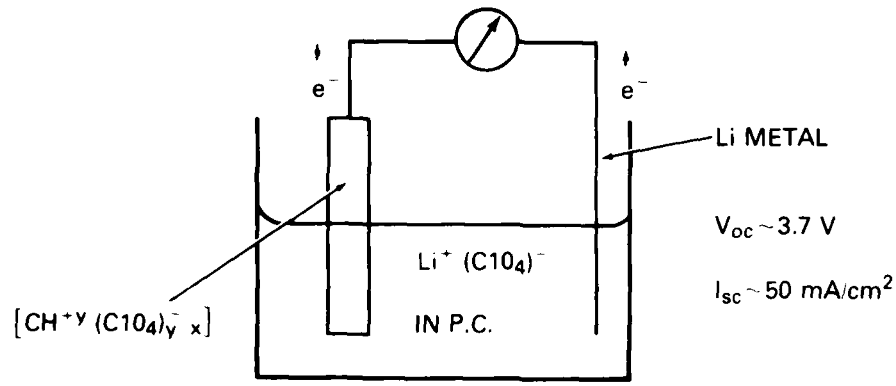

(i) $yLi \rightarrow yLi^+ + ye^-$

(ii) $(CH)_x^{+y} + y(ClO_4)^- + ye^- \rightarrow (CH)_x^0 + y(ClO_4)^-$

∴ NET DISCHARGE REACTION:

$$(CH)_x^{+y} + xy(ClO_4)^- + xyLi \rightarrow (CH)_x + xyLi^+(ClO_4^-)$$

Figure 6. Schematic illustration of a $(CH)_x$-lithium battery.

Obviously there will be certain applications such as batteries in which the conducting polymer system can be maintained in a restricted atmosphere and considerations of air stability and flexibility are perhaps not as crucial. For widespread applications, however, if full advantage is to be taken of these materials a significant amount of polymer chemistry and engineering will be necessary to stabilize them and improve their polymeric properties in the metallic and semiconducting state. The increasingly wide variety and complexity of polymers which can be made to show high conductivity bode well for the ability of scientists to incorporate these desirable properties into such materials. ■

References

1. L. B. Lockhart, NRL Memorandum Report 3960, The NRL Program on Electroactive Polymers, March, 1979.

2. P. E. Bloomfield, R. A. Ferren, P. F. Radice, H. Stefanou, and O. S. Sprout, Naval Research Reviews, *31*, 1 (1978).

3. R. B. Fox, NRL Memorandum Report 4335, The NRL Program on Electroactive Polymers, March 30, 1979.

4. W. A. Little, Phys. Rev., *134*, A1416 (1964).

5. V. V. Walatka, M. M. Labes and J. H. Perlstein, Phys. Rev. Lett., *31*, 1139 (1973).

6. G. B. Street and R. L. Greene, IBM J. of Res. and Develop., *99*, 21 (1977).

7. G. B. Street and T. C. Clarke, Adv. Chem. Ser., *186*, 177 (1980).

8. K. Stewaley, L. D. David, and R. West, unpublished data.

9. a. A. G. MacDiarmid and A. J. Heeger, Synthetic Metals, *1*, 1980.
   b. C. K. Chiang, A. J. Heeger and A. G. Mac-

Diarmid, Ber. Bunsenges. Phys., Chem., *83*, 407 (1979).

10. G. B. Street and T. C. Clarke, IBM J. of Res. and Develop. (1981).

11. S. L. Hsu, A. J. Signorelli, G. P. Pez and R. H. Baughman, J. Chem. Phys., *69*, 106 (1978).

12. G. B. Street, R. L. Bingham, J. I. Crowley and J. Kuyper, J. C. S. Chem Commun., 464 (1977).

13. M. Akhtar, C. K. Chiang, A. J. Heeger, J. Milliken and A. G. MacDiarmid, Inorg. Chem., *17*, 1539 (1978).

14. L. W. Shacklette, H. Eckhardt, R. R. Chance, G. G. Miller, D. M. Ivory, R. H. Baughman J. Chem. Phys., *73*, 4098 (1980).

15. K. Soga, Y. Kobayashi, S. Ikeda and S. Kawakari, J. C. S. Chem. Commun., 931 (1980.)

16. a. P. J. Nigrey, A. G. MacDiarmid and A. J. Heeger, J. C. S. Chem. Commun., 594 (1979).
    b. A. F. Diaz and T. Clarke, to appear in J. Electronal. Chem. (1980).

17. K. K. Kanazawa, A. F. Diaz, R. H. Geiss, W. D. Gill, J. F. Kwak J. A. Logan, J. F. Rabolt and G. B. Street J. C. S. Chem. Commun., 854 (1979).

18. K. K. Kanazawa, A. F. Diaz, G. P. Gardini, W. D. Gill, P. M. Grant, J. F. Kwak and G. B. Street, Synthetic Metals, *1*, 329 (1980).

19. W. D. Gill, W. Bludau, R. H. Giess, P. M. Grant, R. L. Greene, J. J. Mayerle and G. B. Street, Phys. Rev. Lett, 38, 1305 (1977).

20. C. K. Chaing, M. J. Cohen, D. L. Peebles, A. J. Heeger, M. Akhler, J. Kleppinger, A. G. MacDiarmid, J. Milliken and M. J. Moran, Solid State Commun., *23*, 607 (1977).

21. G. B. Street and W. D. Gill, Molecular Metals, Ed. W. E. Hatfield (Plenum Press 1979) p. 301.

22. R. H. Dee, J. F. Carolan, B. G. Turrell and R. L. Greene, Phys. Rev., B22, 174 (1980).

23. G. E. WNEK, J. C. W. Chien and F.E. Karasz, Organic Coatings and Plastic Preprints, *43*, 882 (1980).

24. I. Diaconu, S. Dumitrescu, and C., Simionescu, Eur. Polym. J., *15*, 1155 (1979).

25. G. M. Hobb and P. Ehrlich, J. Polym Sci., Polym. Phys. Ed., *15*, 627 (1977), P. Cukor, J. I. Krugler and M. F. Rubner, Polymer Preprints *21* (1), 161 (1980).

26. H. W. Gibson, F. C. Bailey, A. J. Epstein, H. Rommelmann and J. M. Pochan, J. C. S. Chem. Commun., 426 (1980).

27. M. J. Kletter, T. Woerner, A. Pron, A. G. MacDiarmid, A. J. Heeger and Y. W. Park, J. Chem. Soc. Chem. Commun., 426 (1980).

28. D. M. Ivory, G. G. Miller J. M. Sowa, L. W. Shacklette, R. R. Chance and R. H. Baughman, J. Chem. Phys., *71*, 1506 (1979).

29. G. E. Wnek, J. C. Chien, F. E. Karasz and C. P. Lillya, Polymer Communication, *20*, 1244 (1979).

30. J. F. Rabolt, T. C. Clarke, K. K. Kanazawa, J. R. Reynolds and G. B. Street, J. Chem. Soc. Chem. Commun., 347 (1980).

31. T. C. Clarke, K. K. Kanazawa, Y. Y. Lee, J. F. Rabolt, J. R. Reynolds and G. B. Street. Submitted to J. Polym. Sci., Polym. Phys. Ed.

32. R. R. Chance, L. W. Shacklette, G. G. Miller, D. M. Ivory, J. M. Sowa, R. L. Elsenbaumer and R. H. Baughman, J. Chem. Soc. Chem Commun., *348* (1980).

33. J. Bacon and R. N. Adams, J. Amer. Chem. Soc., *90*, 6596 (1968).

34. G. P. Gardini Advances in Heterocyclic Chemistry, Ed A. R. Katritzky and A. J. Boulton, Vol. 15 (1973).

35. A. Dall'Olio, Y. Dascola, V. Varacca and V. Bocchi, Compt. Rend. *C267*, 433 (1968).

36. A. F. Diaz, J. I. Castillo, J. A. Logan, W. Y. Lee, J. Amer. Chem. S c. Submitted 1980.

37. K. K. Kanazawa, A. F. Diaz, M. Krounbi and G. B. Street, J. Syn. Metals., in press.

38. T. Yamamoto, K. Sanechiuka and A. Yamamoto, J. Polym. Sci., Polym. Lett. 5d, *18*, 9 (1980).

39. A. F. Diaz, to appear in Chemical Scripta.

40. A. Brokman, M. Weger and G. Marom, Polymer, *21*, 1114 (1980)

41. K. F. Schoch, Jr., B. R. Kundalkar and T. J. Marks, J. Amer. Chem. Soc., *101*, 7071 (1979).

42. C. W. Dirk, E. A. Mintz, K. F. Schoch and T. J. Marks, J. Macromol. Science-Chemistry, in press.

43. P. M. Kuznesof, K. J. Wynne, R. S. Nohr and M. E. Kenney, J. Chem. Soc. Chem. Commun., 121, (1980).

44. R. S. Nohr, K. J. Wynne, M. E. Kenney, Abstracts Inor. 161, Second Chemical Congress of the North American Continent, Las Vegas, Nevada, August 1980.

45. R. S. Nohr, P. M. Kuznesof, K. J. Wynne and M. E. Kenney, J. Amer. Chem. Soc., in press.

46. F. L. Vogel, Synthetic Metals 1, 274 (1980).

47. L. V. Interrante, R. S. Markiewicz and D. W. McKee, Synthetic Metals, *1*, 287 (1980).

48. R. A. Scranton, J. B. Mooney, J. O. McCaldin, T. C. McGill and C. A. Mead, Appl. Phys. Lett., *29*, 47 (1976).

49. M. J. Cohen and J. S. Harris Appl. Phys. Lett., *33*, 812 (1978).

50. T. Tani, W. D. Gill, P. M. Grant, T. C. Clarke and G. B. Street, Synthetic Metals, *1*, 301 (1980). T. Tani, P. M. Grant, W. D. Grant, G. B. Street and T. C. Clarke Solid State Commun., *33*, 499 (1980).

51. M. Ozaki, D. Peebles, B. R. Weinberger, A. J. Heeger and A. G. MacDiarmid, J. App. Phys., *51*, 4252 (1980).

52. J. Tsukamoto, H. Ohigashi, K. Matsumura and A. Takahashi, Jap. Journ. Appl. Phys., *20*, 213 (1981).

53. P. M. Grant, to appear in Chemica Scripta.

54. S. N. Chen, A. J. Heeger, Z. Kiss, A. A. MacDiarmid, S. C. Gam and D. L. Peebles, Appl. Phys. Lett., *36*, 96 (1980).

55. T. C. Clarke, R. H. Geiss, J. F. Kwak and G. B. Street, J. C. S. Chem. Commun. 489 (1978).

56. R. J. Novak, H. B. Hart, A. G. MacDiarmid and D. Weber, J. C. S. Chem. Comm., 9 (1977).

57. R. Noufi, D. Tench and L. F. Warren, J. Electrochem. Soc., *127*, 2310 (1980).

58. R. Noufi, A. J. Frank and A. J. Nozik, J. Am. Chem. Soc., *103*, 1849 (1981).

59. T. Skotheim, I. Lundström and J. Prejza, J. Electrocem. Soc., in Press.

60. P. J. Nigrey, D. MacInnes, Jr., D. P. Nairns, A. G. MacDiarmid and A. J. Heeger, unpublished results.

61. W. Niederhauser, Rohm and Haas Co., private communication.

Continued from page 20

26. J. Stoop and E. A. Metzbower, "A Metallurgical Characterization of HY-130 Steel Welds", Welding J., Vol. 57, p. 346 (Nov. 1978).

27. I. J. Spalding, "High Power Lasers for Processing Materials", in *Lasers in Modern Industry*, ed. John F. Ready, Society of Manufacturing Engineers, Dearborn, Michigan, (1979).

28. F. W. Gobetz, "Feasibility of Laser Welding at NIROP" UTRC, Report R79-914782-1, (1979).

29. T. M. Trainer and R. D. Fannon, "Additional Investigations of the Feasibility of Laser Welding at NIROP", Battelle Report, Contract No. N00173-79-C-0338, (1980).

Ultrahigh Carbon Steels—Their Properties and Potential

by

Oleg D. Sherby
Stanford University

Bruce A. MacDonald
Office of Naval Research

and

Edward C. Van Reuth
Defense Advanced Research Projects Agency

The preparation, properties and potential of ultrahigh carbon steels are described in the following article. It appears that the metallurgical key to the development of fine-grained, ultrahigh carbon steels is the use of thermal mechanical processing for attainment of submicron microstructures. Such steels behave in a superplastic manner at warm temperatures and are strong and ductile at room temperature. Their similarity to the ancient Damascus steels and Japanese laminated tools is noted with the recognition that the forgotten art of making the Damascus steels may have been rediscovered in this program at Stanford University.

Research on ultrahigh carbon (UHC) steels, superplastic bonding and UHC steel laminated composites has been a major interest in materials science at Stanford University over the last few years [1-9]. This effort builds on past research supported by the Office of Naval Research and other agencies in the areas of steel metallurgy and superplastic behavior. Basic information developed on the mechanisms of strengthening of steels and effects of thermal mechanical working and heat treating has laid a foundation for understanding how such processing can be used to control the microstructure and properties of carbon steels. The Stanford program also draws upon past research on superplasticity in metals providing an improved understanding of the requirements on microstructure, temperature and strain rate to develop superplastic behavior in UHC steels. The result is a highly interesting alloy group with remarkable properties, as will be seen in the following discussion.

The iron-carbon phase diagram shown in Figure 2 illustrates the carbon range which is designated as ultrahigh carbon steel, 1% to 2.1% carbon. Below 1% carbon, are high carbon steels (0.6 – 1%C), medium carbon steels (0.25 – 0.6%C) and mild steels (<0.25%C). The cast irons are above 2.1%C since cast iron, by definition, contains carbon in excess of the maximum amount that can be dissolved in austenite[10].

Ultrahigh carbon steels can be processed to exhibit many desirable characteristics. They can be made superplastic (<1500% elongation) at warm temperatures, strong (1000 MPa yield strength) and ductile (20% elongation) at room temperature, and

Figure 1 *Damascus swords used by the Russians in the War of 1812 are illustrated. Such swords were often of carbon content in the range of 1.5%C and were extensively mechanically worked prior to heat treatment. [Swords are displayed in the Armoury Museum in Moscow]*

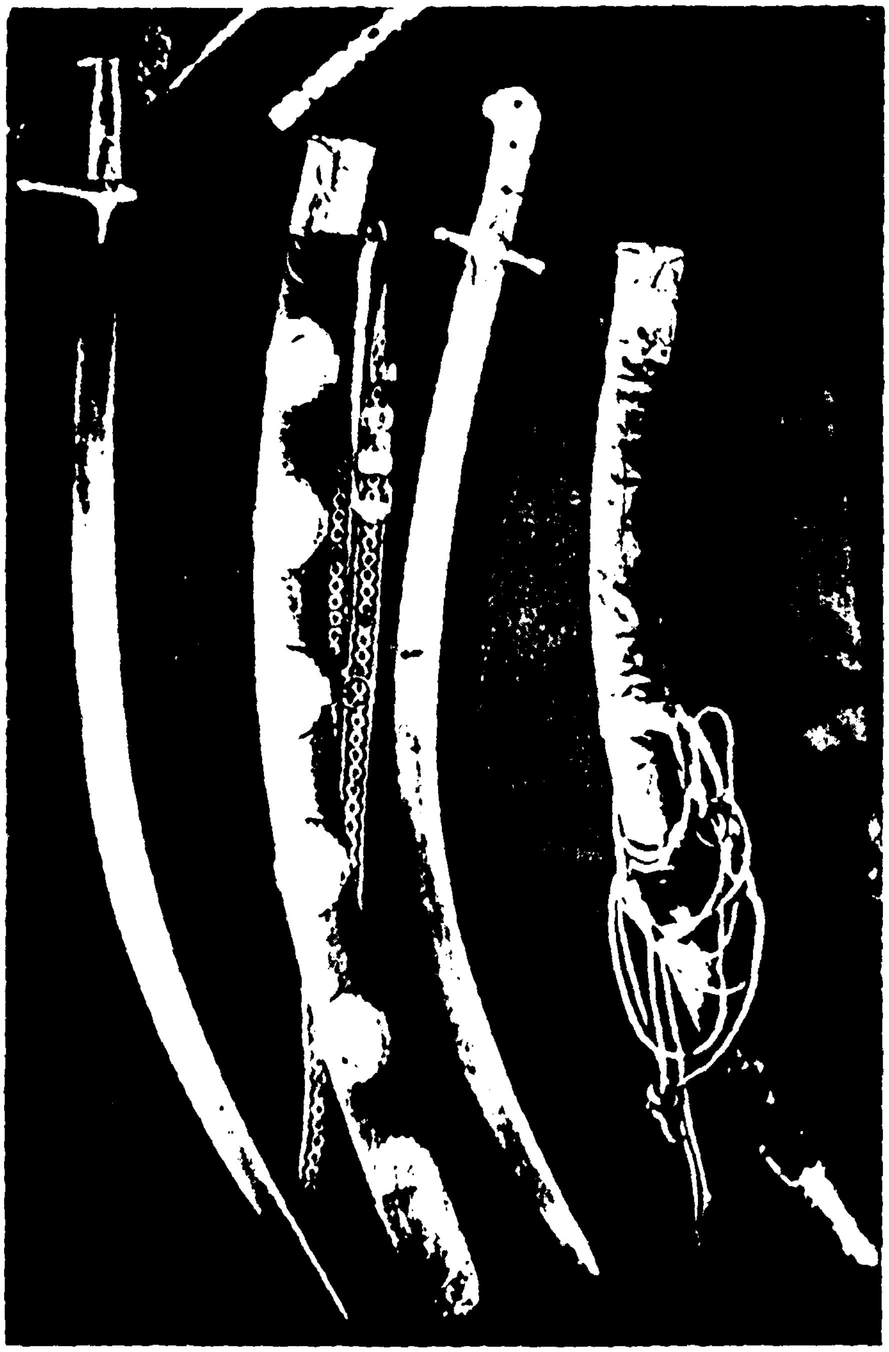

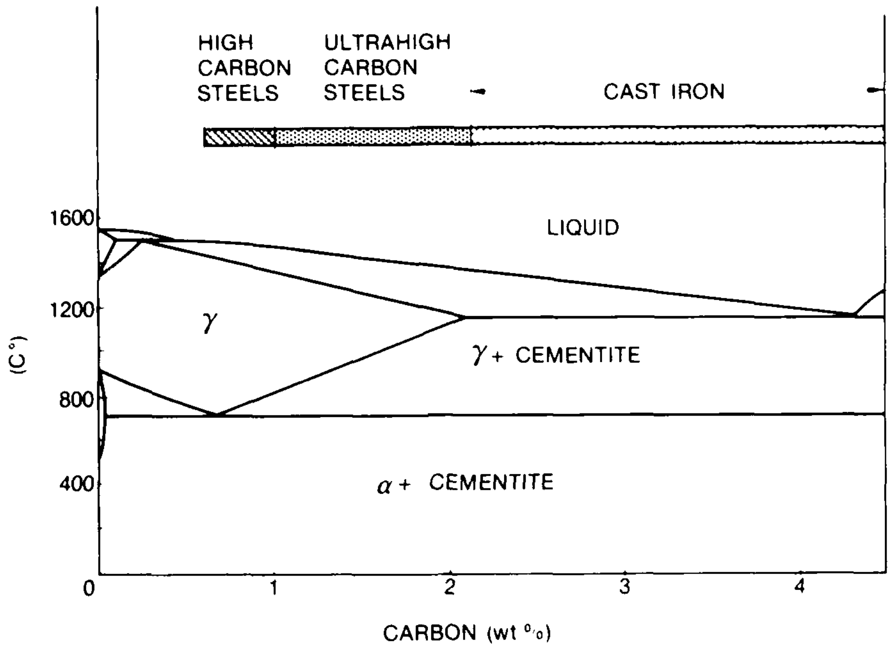

Figure 2. Ultrahigh carbon (UHC) steels are defined in this paper as steels containing 1 to 2.1%C as shown in the above iron-carbon phase diagram. Cast irons contain carbon in excess of the solubility limit of carbon in austenite (>2.1%C) and high carbon steels generally contain 0.6 to 1.0%C.

very hard ($R_c = 68$ with 4300 MPa compression fracture strength) by heat treatment. And, they can be used as a solid-state bonding agent through superplastic joining. While these properties appeared to be unique at the time of their discovery at Stanford, it now appears that the ancient and forgotten art of making Damascus steel and Japanese laminated steel composites may have been uncovered.

Damascus steel swords such as those illustrated in **Figure 1** were used by the Russians in the War of 1612. They were beautiful in design and known for their high toughness and fine cutting edge. In a review of the history of "bulat steel" (the Russian Term for Damascus steel), Belaiew [11] mentioned that such steels were in the composition range of 1.2 to 1.8% carbon and were extensively worked mechanically. Similarly, the UHC steels are worked extensively at elevated temperatures (in both the gamma and alpha phase fields) to develop fine uniform microstructures. Thus, the analogy between the UHC steels and Damascus steels is strong. (It should be noted that fine structure can be obtained by methods other than extensive working, such as by thermal cycling [12] or warm temperature consolidation of rapidly quenched fine powders[13].)

Japanese blacksmiths from ancient times worked with ultrahigh carbon steels. An example is shown in Figure 3 where "uagane" steel is solid state welded to a piece of soft iron and then processed and heat treated to make a cutting tool with a hard tip and a soft matrix. Uagane steel, a hypereutectoid* steel (typically 1.2 to 1.5%C) was prepared in at least two ways. One method was to prepare it from tamahagane, a product of a reduction process using iron, sand and charcoal. If fixed amounts of iron ore and charcoal are mixed and heated in air to 1200°C, the product is molten pig iron and slag with unmelted ultrahigh carbon steel. When the pig iron and slag are allowed to separate by pouring, the end product is lumps of ultrahigh carbon steel containing about 1.9%C (tamahagane). Such a material was then forged, folded on itself, the repeatedly forged and folded until the appropriate shape and carbon content was achieved. Forging and folding led to the exposure of much of the material to an oxidizing atmosphere allowing decarburization to occur and in this manner

*A steel with carbon concentration above 0.8 weight percent

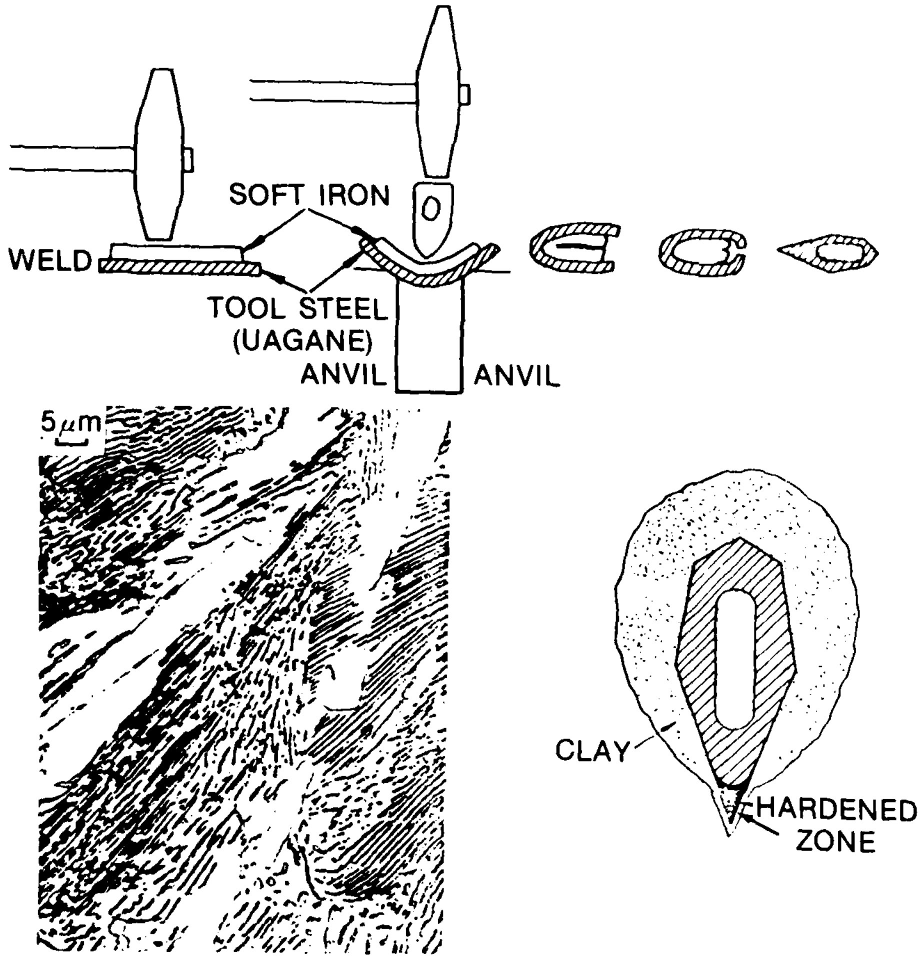

Figure 3. Japanese blacksmiths of ancient times made laminated tools by solid state bonding ultrahigh carbon (UHC) steels, known as uagane, to soft iron. After hot forging, the laminated tool was heat-treated to yield a hard cutting edge (adapted from E. C. Bain[4]).

the carbon content could be controlled and reduced from 1.9%C to 1.3%C[14]. A second method of making uagane was to add cast iron to wrought iron, and then melt the cast iron. This was followed by repeated folding, welding and forging at high temperature to obtain a steel of intermediate carbon content.

The following sections will describe some of the unique properties that are achievable with ultrahigh carbon steels.

Superplasticity in UHC Steels

When studies on UHC steels were initiated in 1973 we did not realize the parallels to ancient steel making, the metallurgy of Damascus steel, and early Japanese laminated tool fabrication. The chief interest was in developing the superplastic effect in UHC steels. This property refers to the ability of metallic alloys to elongate extensively (<400%) at warm temperatures. Considerable work in the past had clarified the superplastic characteristics of aluminum-zinc[15] and uranium-base alloys[16]. These efforts had led to an understanding of the many prerequisites needed for superplastic properties[17-18]. The major prerequisite is a fine grain size which should remain stable at superplastic-forming temperatures. While the grain boundaries should be sufficiently mobile to minimize high-stress concentrations at triple points, at the same time they should

be inhibited from rapid grain growth by the presence of fine, second-phase particles. The second phase should exhibit ductility at the superplastic-forming temperatures in order to avoid interphase boundary separation. In addition, the grains should possess high angle boundaries[11]. (The angles between the crystallographic orientations of adjoining grains should be large.)

UHC steels are made superplastic by utilizing the above principles. The basic idea is to process the steels so that the matrix consists of ultrafine ferrite grains stabilized by the presence of submicron cementite particles. The composition and temperature range where superplasticity can be expected is shown in the iron-carbon phase diagram of Figure 4. As can be seen, the temperature range of potential superplastic behavior is quite wide. For example, a UHC 1.6%C steel can be superplastic from 600 °C to 800 °C. This range permits considerable flexibility in temperature control during superplastic forming of such materials.

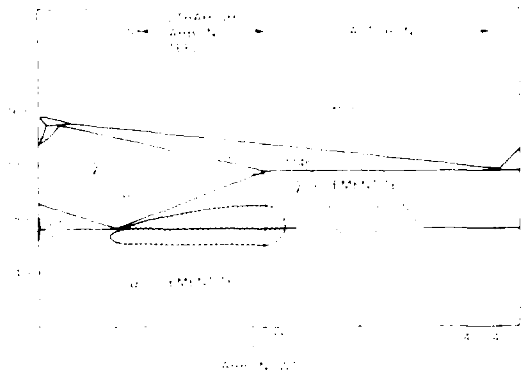

Figure 4. The above Fe-C phase diagram illustrates the range of composition and temperature where UHC steels can be superplastic if they are made sufficiently fine grained. A high carbon content is needed in order to introduce a large volume fraction of cementite particles for stabilization of the fine ferrite grains.

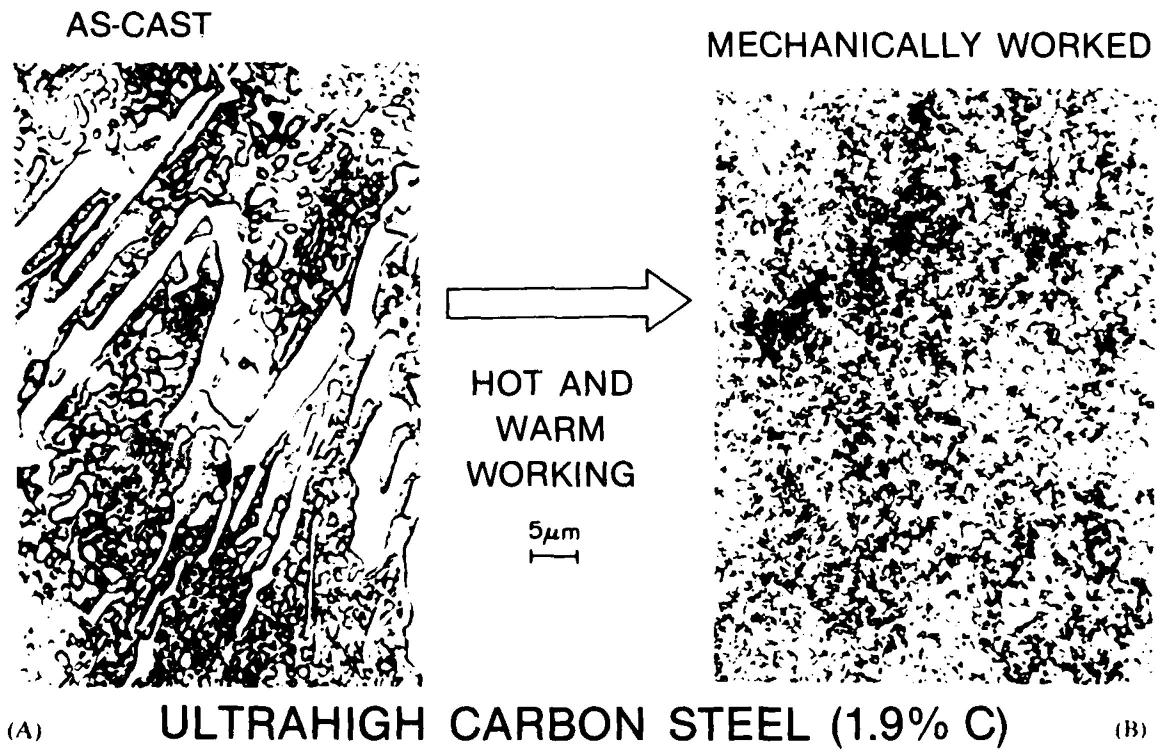

Figure 5. Optical photomicrographs of a 1.9%C steel. (A) Reveals course proeutectoid cementite particles in a matrix of ferrite and cementite in the as-cast state and (B) reveals fine equiaxed structure of ferrite grains containing submicron cementite particles after hot-and warm working.

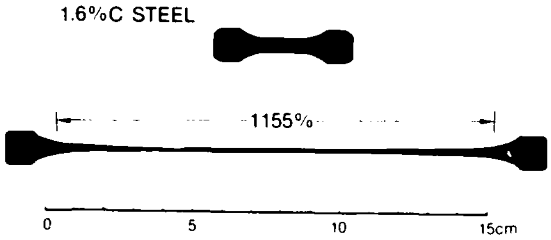

Figure 6. The above photograph illustrates a sample of a fine-grained UHC steel (1.6%C) deformed superplastically at 650°C. The initial engineering strain rate was 1% per minute.

Several methods[2] have been developed for preparing fine ferrite grains in UHC steels. The most common one is a hot-and-warm working process. In this method the UHC steel is heated into the austenite range and soaked for a sufficiently long time to dissolve all the carbides. The material is then deformed continuously as it cools through the austenite-cementite region. This leads to a refinement of the austenite grains, to subgrain formation, and to generation of randomly dispersed dislocations, allowing uniform precipitation of fine carbides at dislocations, subgrain and grain boundary sites. On continued cooling, when the A_1 temperature (727 °C) is reached, austenite of eutectoid composition (0.8 weight percent carbon) transforms to ferrite and cementite[19]. Further deformation leads to a deformed pearlite resulting in refinement of the cementite into fine spheroidized particles. Isothermal deformation at 650 °C is commonly used to refine the structure further. A typical strain during working in the austenite and austenite-plus-cementite region is 1.5 (i.e. a reduction of 4 to 1 in rolling). About the same strain is used during working in the ferrite-plus-cementite region. During isothermal rolling at 650 °C, about 5 to 10% per pass is commonly used with 5 minute reheating soaks between passes. Figure 5 reveals optical micrographs of the as-cast UHC steel and of the hot-and-warm processed UHC steel. The cast structure reveals the presence of coarse cementite particles in a matrix of ferrite and cementite. Hot-and-warm working leads to a refined structure consisting of ultrafine ferrite grains (typically one micron or smaller) with a uniform distribution of submicron cementite particles. Such a material is superplastic at warm temperatures. An example of a tensile test performed on a 1.6% steel at 650 °C at a strain rate of 1% per minute is shown in Figure 6. This material exhibits 1155% elongation prior to failure.

As can be seen in the transmission-electron microscope photomicrograph in Figure 7A, the initial ferrite grain size after hot-and-warm processing is about one-half micron, with a high concentration of dislocations within each ferrite grain. Submicron cementite particles are readily evident. After superplastic deformation, the UHC steel sample

Figure 7. Transmission electron micrographs of hot-and-warm worked 1.9%C steel. The microstructure shown in (A) is the steel in the as hot-and-warm rolled condition, revealing a submicron ferrite grain size with fine cementite particles and a high dislocation density within the ferrite grains. The microstructure shown in (B) is after 100% superplastic deformation at 650 C at 1% per minute strain rate. A dislocation-free microstructure is noted with some ferrite grain growth occurring as a result of concurrent straining.

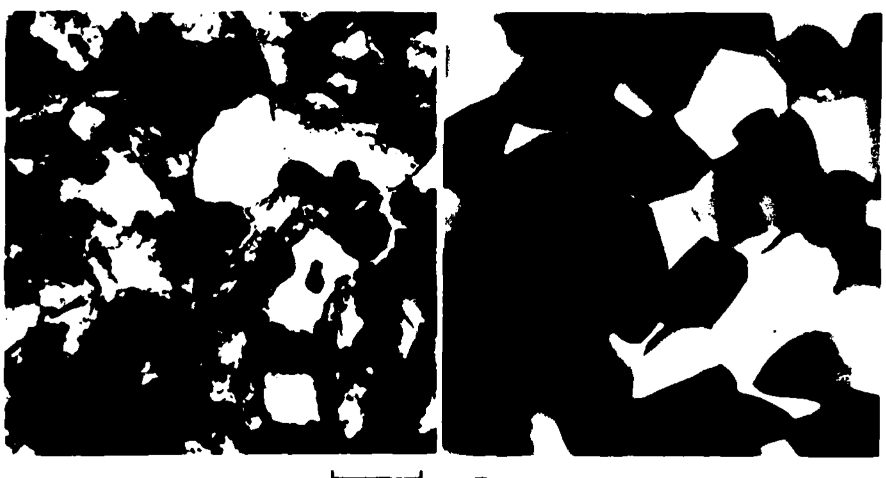

reveals dislocation—free ferrite grains, equiaxed in shape, containing cementite particles (Figure 7B). The ferrite grains are approximately one micron in size revealing that some grain growth occurred as a result of the deformation. The grip region of the superplastically deformed sample experienced little grain growth (although the high dislocation density within the ferrite grains decreased considerably) attesting to the stability of the ferrite grains due to the presence of carbide particles.

Tensile Strength and Ductility of UHC Steels at Room Temperature

The fine submicron ferrite grains created by extensive hot-and-warm working of the UHC steels suggest that high tensile strengths at room temperature may be achieved. Figure 8 reveals the stress-strain curve of a 1.3%C UHC steel in the as-processed condition and after annealing at 650°C. The yield strength of the hot-and-warm processed UHC steel is about 1400 MPa (200 ksi) with a tensile ductility of about 4% elongation. After annealing for 20 minutes at 650°C, the dislocation density is reduced, the yield strength is decreased to 1000 MPa (140 ksi), but the tensile elongation increases to about 20%. This high ductility is a surprising but pleasing result. In this condition the strengths of UHC steels are about twice those for HSLA (high strength low alloy) steels (500 MPa) with essentially the same tensile ductility. Since only sheet form (2mm thick) of the UHC steel has been prepared to date, impact characteristics and fracture toughness have not been investigated.

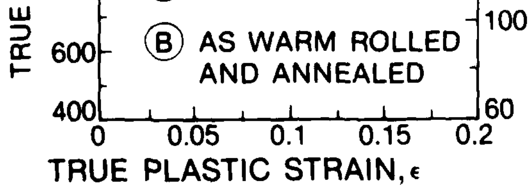

Figure 8. True stress-true strain curves for a 1.3%C steel at room temperature. Sample A was warm worked extensively at 565°C with no annealing after warm-working. Sample B was annealed for 20 min. at 650°C after warm-working at 565°C.

Heat Treatment of UHC Steels

Ultrahigh carbon steels containing fine ferrite grains with a large volume fraction of fine spheroidized carbides represent materials with unique heat treating possibilities. This is because fine ferrite grains, containing many nuclei for transformation, will transform to fine austenite grains when heated to just above the A_1 temperature (723°C). The undissolved cementite that exists (ten volume percent in a 1.6%C steel) will stabilize the austenite grains and inhibit their growth. Upon quenching, ultrafine martensite* results because the martensite that forms cannot propagate through the austenite grain boundaries. This heat-treating procedure is illustrated in Figure 9. The quenched martensite structure shown cannot be resolved optically; hence, the term "quasi-martensite" is used as a subscript underneath the photomicrograph (apparently, similar unresolvable structures called "hardenite" were noted in quenched hypereutectoid steels over fifty years ago[20]). Recently, the structure of "quasi-martensite" was revealed by transmission-electron microscopy to be submicron packets of lath martensite with a small fraction (about 20%) of ultrafine (<0.1um) twin martensite[7].

The compression properties of "quasi-martensite" are impressive, as illustrated in Figure 10. The stress-strain behavior of the quenched UHC steel is such that yielding does not begin until a yield strength of over 2300 MPa (350 ksi) is surpassed. The material then deforms plastically to a strain of about ten perecent before fracture occurs at stresses approaching 4300 MPa (650 ksi). This strength is equivalent to the compression fracture strength of tungsten carbide. Of note, however, is that, whereas tungsten carbide has virtually zero compression ductility, the UHC steel can plastically deform about ten percent prior to fracture. This quality, together with the high hardness ($R_c = 68$), suggests that such steels may be good candidates for use where resistance to wear or abrasion is important.

**Martensite is a low temperature phase transformation product which imparts high strength and hardness to steels.*

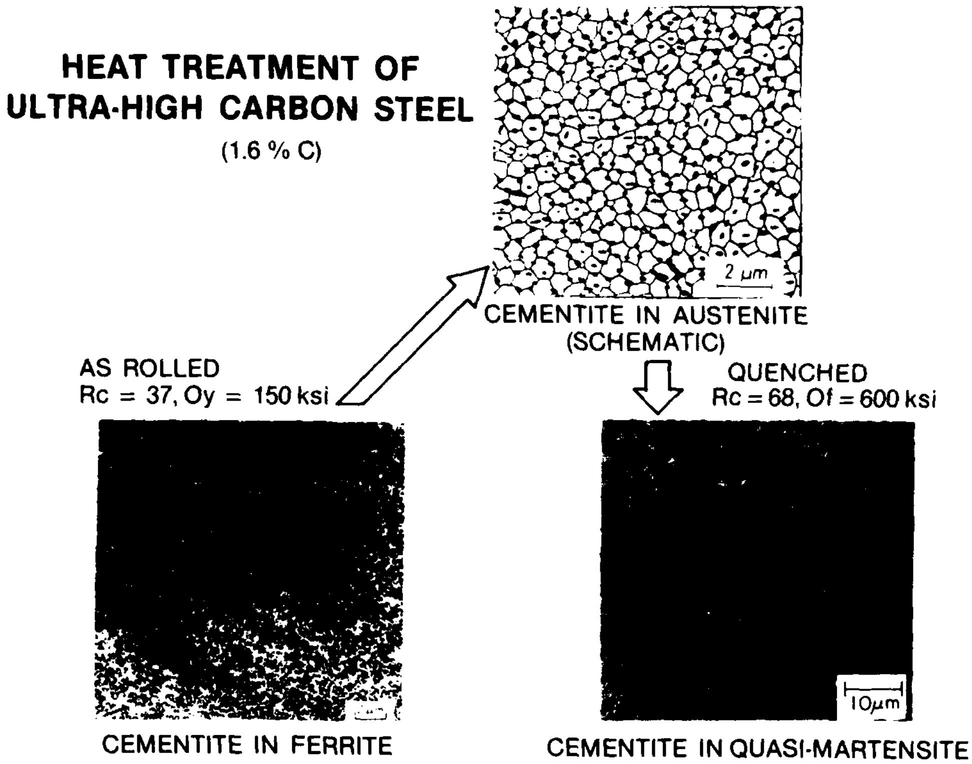

Figure 9. A partially schematic diagram illustrating the expected transformation from fine ferrite grains to fine austenite grains when heating a UHC steel to just above the critical temperature (723°C). Upon water quenching, optically unresolvable martensite is obtained. Transmission electron microscopy has revealed the presence of submicron lath and twin martensites[illegible].

Superplastic Bonding and UHC Steel Composites

The ultrafine ferrite grains produced in the hot-and-warm processed UHC steel (Figure 7A) presents a unique situation. The material contains a large fraction of grain boundaries which represent regions of high atom mobility. In fact, at 650°C, the diffusivity of iron atoms is one million times faster in the ferrite grain boundary than in the ferrite matrix[20, 21]. Such efficient paths for atom mobility suggest that UHC steel may be bonded readily in the solid state at temperatures below the A_1 temperature. This concept was verified by pressure-bonding experiments performed at 650°C[21]. Figure 11 shows

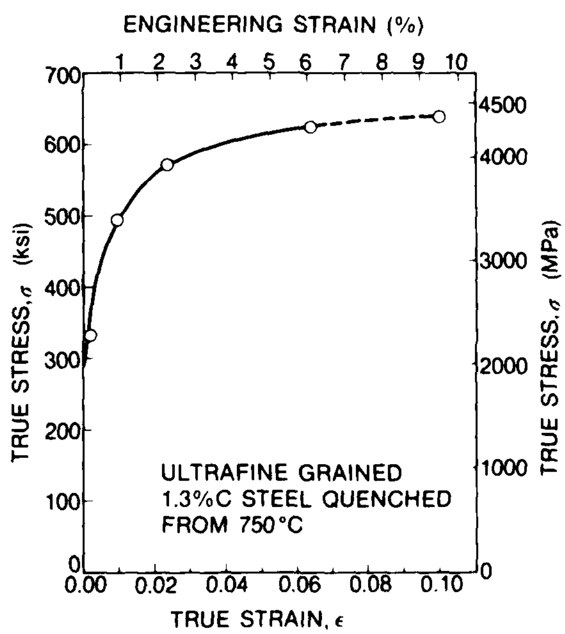

Figure 10. Room temperature compression stress-strain curve of a fine grained 1.3%C steel heat treated to 750°C and water quenched. A high compression ductility is obtained (~10%) with high compression fracture strength (~4300 MPa).

the excellent bond developed between two UHC steel plates (1.3%C) when pressure bonded. The plates were ground flat prior to pressing at 70 MPa (10 ksi) at room temperature. They were then heated under pressure in air to 650°C for two hours where solid state bonding was achieved. The line of demarcation seen in the photomicrograph is due to the flattening of the grains at the interface from deformation arising from the applied compression force. It appears that the grain boundaries act as sinks for impurity atoms on the mating surface, keeping the surfaces clean and thus allowing for bonding by inter-atom exchange across the interface. Recently, ready bonding of UHC plates was achieved by roll bonding at 650°C. In this case the ground plates were welded on the edges to minimize oxidation prior to roll bonding at temperature[24].

The success of bonding fine grain UHC steel plates led to consideration of the possibility of joining superplastic UHC steel to nonsuperplastic steels below the critical temperature of 723°C. This possibility of ready bonding seems quite reasonable if the presence of many grain boundaries leads to establishing clean surfaces at the interface of the plates. Figure 12 reveals that success was achieved when UHC steel was alternately layered with mild steel (1005) and pressure-bonded at 650°C at about 70 MPa (10 ksi). A low magnification photomicrograph of the laminated composite is shown in the lower portion of Figure 12 and high magnification photomicrograph of one of the interfaces is shown in the upper portion of the figure. The bond appears metallurgically perfect. The ferrite in the mild steel appears to be in intimate contact with the ferrite in the UHC steel. No major interdiffusion due to chemical gradients has occurred because the carbon content in solution in both steels is the same (.01 carbon) and lattice diffusion of substitutional atoms is very slow at 650°C ($D = 10^{-15}$ cm^2 sec) [20]. Laminated composites of the type shown in Figure 12 have also been prepared by the roll-bonding technique described earlier.

Three predictions can be made with respect to the laminated composite depicted in Figure 12. The first relates to an applied mechanics argument regarding the possibility of making the laminated composite superplastic at warm temperature. The argument goes as follows: if the UHC steel is superplastic, but stronger than mild steel at warm temperatures, it should control the plastic flow behavior of the composite when tested in the layered direction. Thus, the composite, as a whole, will behave superplastically barring unexpected effects arising at the interface of the dissimilar steels. Sec-

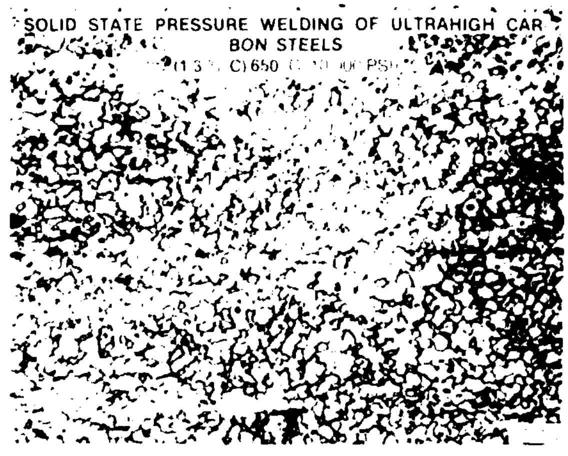

Figure 11. The above photomicrograph illustrates that superplastic UHC steel plates (1.3%C) can be readily solid-state diffusion bonded in air at relatively low temperature (0.51 T_m) and low pressure (69 MPa). A line of demarcation can be seen at the bond interface because the cementite particles and ferrite grains are flattened at the interface, leading to flat ferrite grain and interphase boundaries.

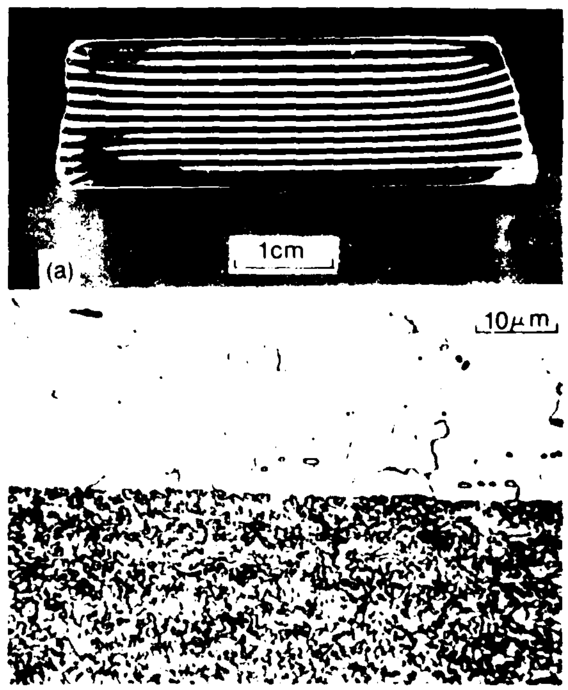

Figure 12. A twenty-five layer laminated composite of UHC steel—1005 steel is shown after pressure bonding (69 MPa) at 650°C. A high magnification optical photomicrograph of the interface between a UHC steel—1005 steel layer, shown above the laminated composite, indicates that a good metallurgical bond is present.

ond, the laminated composite should not experience delamination since a true metallurgical bond is developed involving an indistinguishable and continuous ferrite phase. Third, the laminated composite is capable of "selective heat treatment". For example, when the laminated composite is heated just above the A_1 temperature, the UHC steel will transform to austenite-plus-cementite whereas the mild steel will remain untransformed. Upon quenching, the UHC steel will become martensite of Rockwell "C" 68 perfectly bonded to the unaffected mild steel. The result should be a strong fracture tough material. The next three figures illustrate the possible validity of the above three predictions.

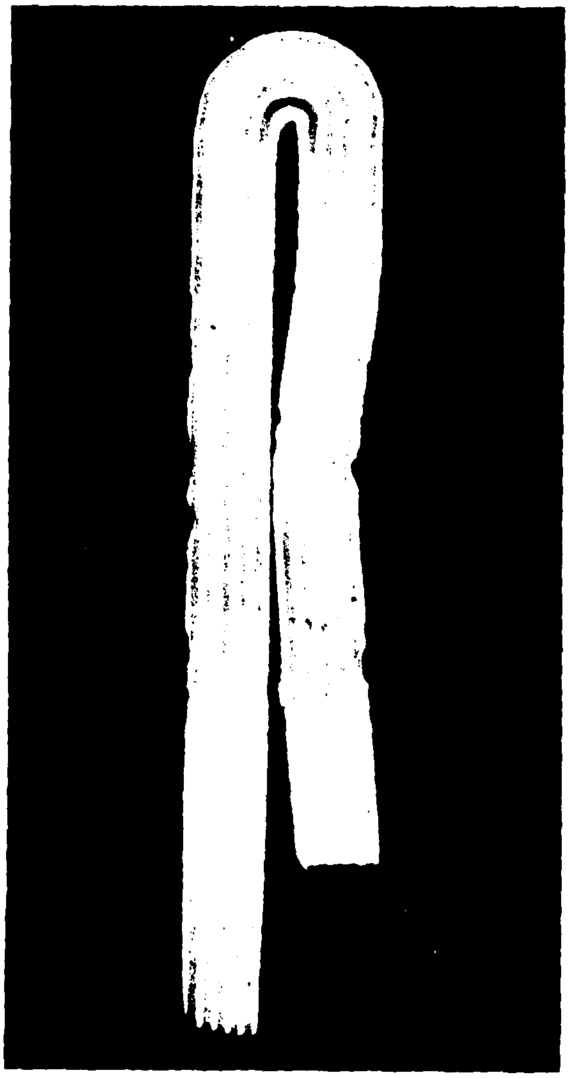

Figure 13. A zero T bend is readily achieved in an eleven layer laminated composite of a 1.6%C UHC steel/1005 steel at warm temperature (600°C). The uniform deformation of each layer, with no evidence of fracture, attests to the possible superplastic nature of the laminated composite. The thickness of the composite is 2.5 mm.

Figure 13 shows the possible superplastic tendency in the laminated UHC steel/mild steel composite. This eleven-layer laminated composite was heated to 600°C and then bent with pliers to a zero T bend. The uniform deformation of each layer and the total absence of any tendency to crack suggest that the laminated composite is superplastic.

Figure 14 shows a severe bend performed at room temperature on a two-layer UHC steel composite in the as-pressed condition. A photomicrograph of the interface at the most severely deformed region indicates no sign of delamination. Another sample was bent at right angles to that shown in Figure 14 and again no sign of delamination was observed. Both observations attest to the integrity of the metallurgical bond between the UHC steel/mild steel plates.

Figure 15 illustrates in a more dramatic way the integrity of the bond between a UHC steel/mild composite prepared by warm pressing. In this case, the two-layer composite, after warm pressing at 650°C, was selectively heat treated. It was heated to 770°C for 20 minutes and then water quenched. The sample was then bent at room temperature until cracks were visually observed in the martensite portion of the composite, as shown in the low magnification photograph (Figure 15). At high magnification one specific large crack is shown. The crack is arrested just as it enters the mild steel region. A fine crack propagates transversely from the main crack. This crack propagates only in the martensite region. No delamination is evident at the original interface of the two-layer composite or in the narrow interdiffusion zone that formed during heat treating at 770°C (the carbon gradient in the austenite that forms at the interface is the driving force for interdiffusion). This example attests to the potential of optimizing strength and toughness of UHC steel composites through selective heat treatment.

Lamination of steels by solid state bonding is not a new process. Reference was made to Japanese cutting tools (Figure 3) that were prepared in this manner. Bonding appeared to have been made invariably at temperatures much above the A_1 where considerable interdiffusion occurs. The Stanford studies indicate that bonding is relatively easy to achieve below the A_1 temperature if one of the steels is superplastic. This concept and practice seems novel in the history of contemporary metallurgy. There is

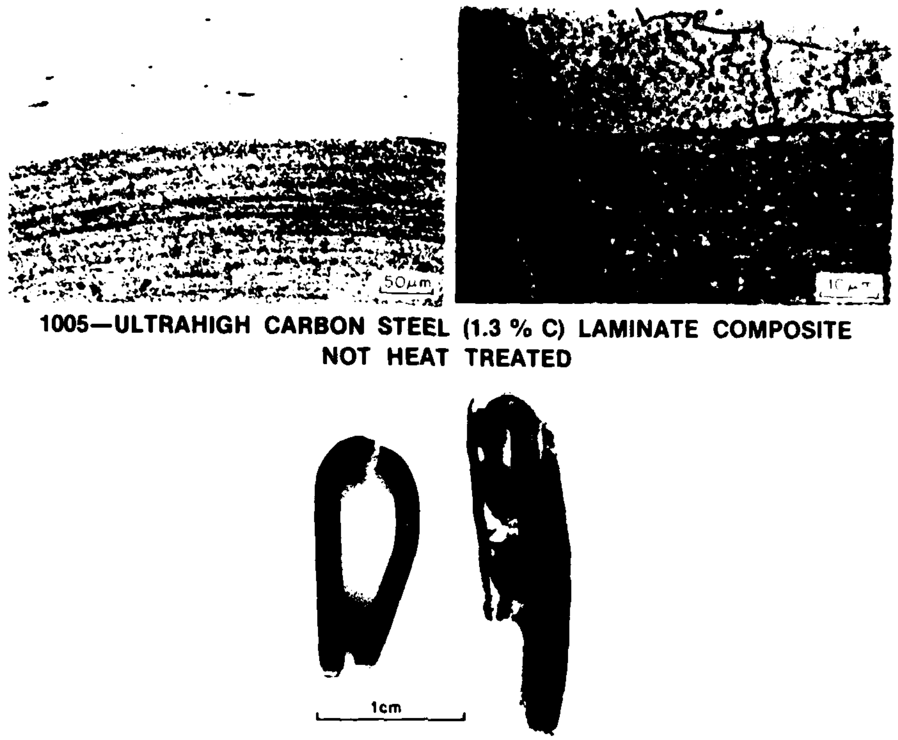

Figure 14. A warm-pressed two-layer laminated composite of a 1.3%C UHC steel/mild steel is bent at room temperature. Photomicrographs of the interface at the bent region reveal no sign of delamination attesting to the sound metallurgical bond in the laminate.

evidence, however, that over 2000 years ago, the ancient blacksmiths of Asia Minor performed similar processing treatments[25]. Figure 16 illustrates the magnified region of an interface in an Adze blade dated 400 BC found on the coast of Turkey. The dissimilar carbon-content steels appear to be metallurgically bonded, and the possible absence of an interdiffusion zone suggests that the two dissimilar steels making up the bonded blade may have been hammered at temperature below the A_1 temperature. The dark regions near the interface may be graphitized regions due to extensive mechanical working if graphitizing elements such as silicon or nickel were present in the high carbon steel. The similarity between the Adze blade and the UHC steel composite (bottom of Figure 16) shown at the same magnification is striking.

Superplastic bonding of steels may prove a useful method of welding without the deleterious features of heat-affected zones that occur in conventional, liquid-phase welding. Figure 17 illustrates two 4140 steel couplings joined at 700 °C by pressure bonding with a UHC steel wafer. The tensile strength of the bond was evaluated by mating two solid cylinders of 4140, square in cross-section, with a UHC steel superplastic wafer. After appropriate pressure bonding at 650 °C, samples were machined for tensile testing at room temperature. Figure 18 shows three tensile samples. The left specimen is as-machined, and the middle specimen is a similar one but etched to show the position of the UHC steel wafer. The specimen on the right was tensile deformed to failure. Failure occurred outside of the UHC steel—4140 region indicating the high integrity of the bond (the yield strength of the sample was 400 MPa).

Summary and Conclusions

Recent research work at Stanford University has led to the development of submicron ferrite grains containing very fine cementite particles in ultrahigh carbon (UHC) steels. Much of the work is centered on plain carbon steels containing 1 to 2.3% carbon (fifteen to thirty-five volume percent cementite, respectively). These UHC steels have been shown to

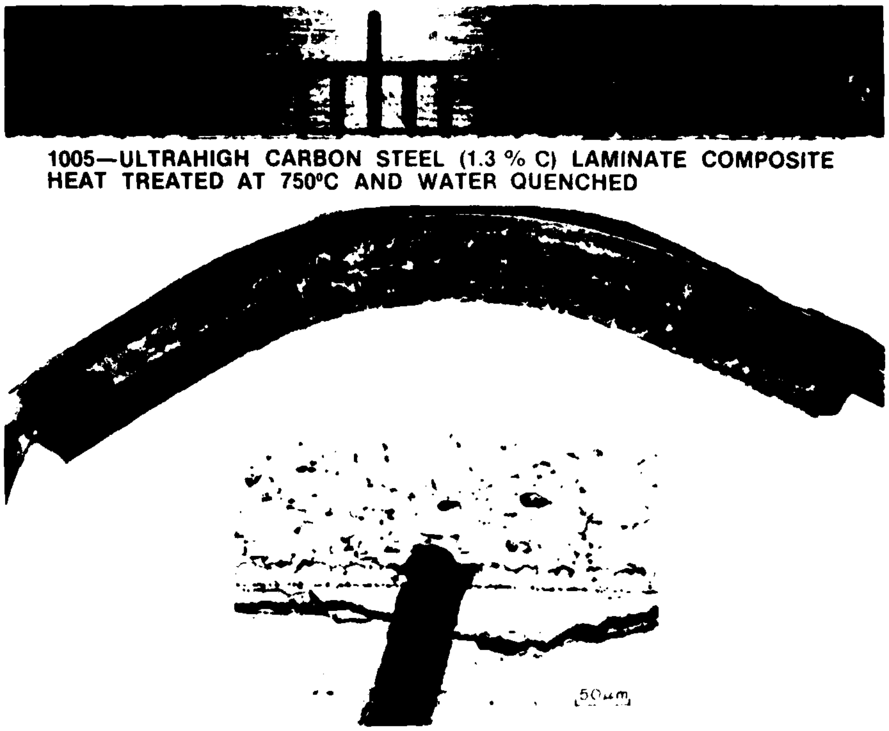

Figure 15. A 1.3% UHC steel/mild steel composite after "selective-heat-treatment" (770°C for 20 minutes then water quenched) is bent until cracks in the martensite portion of the composite become visible. The photo-micrograph shown above illustrates that the crack in the martensite region is arrested in the mild steel region. No delamination is noted in the interface region indicating that a good metallurgical bond is present in the laminated composite.

exhibit at least four unusual and desirable characteristics:

(1) they are superplastic at warm temperatures (elongations exceeding 1500% have been achieved),

(2) they are both strong and ductile at room temperature after appropriate thermomechanical treatment (1000 MPa yield strength with 10-20% ductility are readily achievable),

Figure 16. Photomicrograph of the interface of a laminated Adze Blade (dated 400 BC; attests to the metallurgical skill of the blacksmiths of ancient time (a). The bond is compared with the UHC steel/mild steel composite press bonded at Stanford (b). The authors thank Dr. Robert Maddin for permission to publish the photograph.

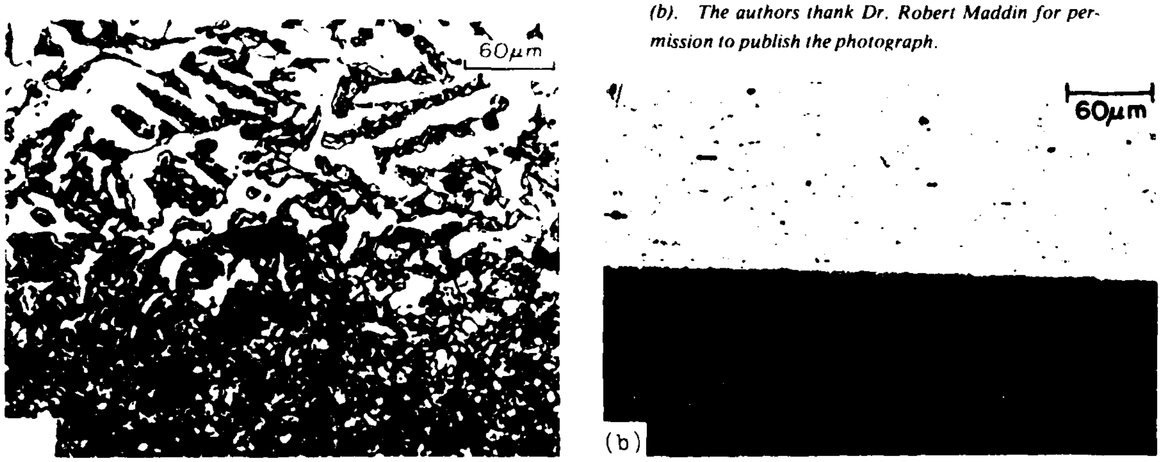

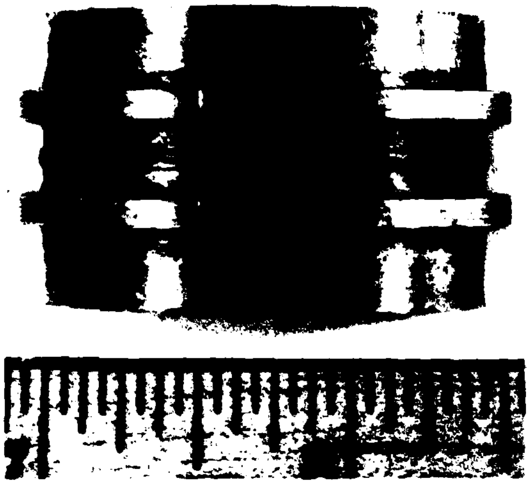

Figure 17. Two 4140 steel couplings are joined by pressure bonding with a 1.6%C UHC steel at 700°C (courtesy of E. Slaughter, Pratt and Whitney Corporation, West Palm Beach, Florida).

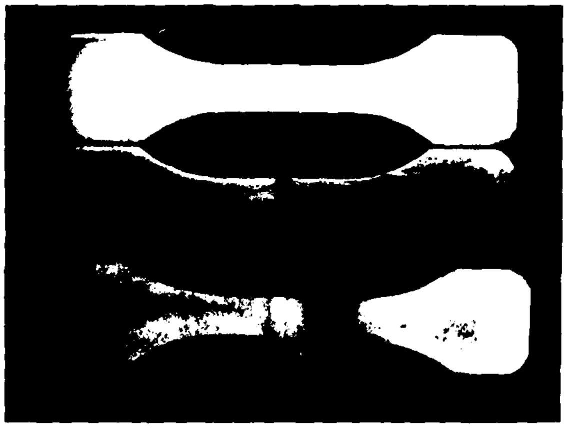

Figure 18. Tensile test samples of 4140 steel solid state bonded with a 1.6%C UHC steel. The two samples on the top are illustrated in the as-machined condition, unetched and etched respectively. The sample on the bottom is shown after testing at room temperature. The sample failed in a region away from the welded zone attesting to the soundness of the UHC steel—4140 steel interface.

(3) they can be made exceptionally hard ($R_c = 68$) by appropriate heat treatment with high compression fracture strength (4300 MPa) and good compression ductility (7-10%), and

(4) they can be bonded superplastically to other ferritic steels at temperatures below the lower critical temperature (< 723 °C). Laminated composites made by such bonding techniques exhibit metallurgically sound bonds, are superplastic at warm temperature, and can be selectively heat treated to result in strong and tough material.

Many of the features of the ultrahigh carbon steels described herein appear to be similar to those attributed to the legendary Damascus steels and to ancient Japanese laminated tools. The blacksmiths of centuries ago were known to work with ultrahigh carbon steels and the thermal mechanical processing techniques that they used could well have been similar to those utilized in present studies.

Acknowledgements

The authors are indebted to many colleagues for the results described in this paper. Dr. Conrad Young and Professor Sherby jointly conceived in 1973 the idea that steels could be made superplastic when the carbon content was in the range 1 to 2% carbon. Mr. Eldon Cady and Dr. Bruno Walser were instrumental in the early work that led to the successful development of these superplastic steels. Dr. Sabri Kayali helped establish the importance of obtaining high-angle grain boundaries as a prerequisite for superplasticity and Professor H. Sunada determined the unique properties of heat treated UHC steels. Dr. Robert Caligiuri, Mr. Robert Whalen and Mr. Barry Snyder did the early tests on superplastic bonding and ultrahigh carbon steel composites. Dr. Jeffrey Wadsworth has worked on all phases of the UHC steel program since 1976 and has contributed extensively to the ideas presented in this paper. The research work was sponsored by the Defense Advanced Research Projects Agency and by the Office of Naval Research, and special thanks are extended to Dr. Arden Bement for his helpful guidance and support. ■

References

1. O. D. Sherby, B. Walser, C. M. Young and E. M. Cady, Scripta Met., *9*, (1975), 569.

2. U.S. Patent #3,951,697, April 20, 1976, titled "Superplastic Ultrahigh Carbon Steels", O. D. Sherby, C. M. Young, B. Walser and E. M. Cady.

3. B. Walser, S. Kayali and O. D. Sherby, Fourth International Conference on the Strength of Metals and Alloys, Nancy, France, *1*, 1976, 456.

4. J. Wadsworth and O. D. Sherby, Jnl. of Mechanical Working Tech., *2*, 1978, 53.

5. J. Wadsworth and O. D. Sherby, Jnl. Mat. Sci., *13*, 1978, 2645.

6. B. Walser and O. D. Sherby, Metallurgical Transactions, in press, 1979.

7. H. Sunada, J. L. Lin, J. Wadsworth and O. D. Sherby, Int. Jnl. of Mats., Sci. and Engr., in press, 1979.

8. T. Oyama, J. Wadsworth, M. Korchynsky and O. D. Sherby, Fifth International Conference on the Strength of Metals and Alloys, Aachen, Germany, September 1979.

9. J. Wadsworth and O. D. Sherby, Foundry Management and Technology, *106*, 1978, 59.

10. Metals Handbook, vol. 8, 1973, American Society for Metals, Metals Park, Ohio.

11. N. Belaiew, J. Iron and Steel Institute, *97*, 1918, 417.

12. S. Kayali, H. Sunada, T. Oyama, J. Wadsworth and O. D. Sherby, submitted for publication.

13. L. E. Eiselstein, Ph.D. Thesis, Department of Materials Science and Engineering, Stanford University, Stanford, California, 94305, 1979.

14. E. C. Bain, J. Iron and Steel Institute, *200*, 1962, 265.

15. Charles M. Packer and O. D. Sherby, Trans. ASM, *60*, 1967, 21.

16. O. D. Sherby, D. L. Bly and D. H. Wood, *Physical Metallurgy of Uranium Alloys*, 1976, J. J. Burke, D. A. Colling, A. E. Gorum and J. Greenspan (editors), Brook Hill Publishing Company, Chestnut Hill, Mass.

17. O. D. Sherby, Science Journal, *6*, 1969, 75.

18. O. D. Sherby, R. D. Caligiuri, E. S. Kayali and R. A. White, Proceedings of the Twenty-Fifth Sagamore Conference, August 1978, in press.

19. J. H. Lin, J. Wadsworth and O. D. Sherby, submitted for publication.

20. S. L. Hoyt, Metallography, Part II, McGraw-Hill Book Company, Inc. 1921, 167.

21. F. S. Buffington, K. Hirano and M. Cohen, Acta Met., *9*, 1961, 434.

22. D. W. James and G. M. Leak, Phil. Mag., *12*, 1965, 491.

23. R. Caligiuri, Ph.D. Thesis, Department of Materials Science and Engineering, Stanford University, Stanford, California 94305, August 1977.

24. J. Wadsworth, R. Caligiuri, R. Whalen, L. E. Eiselstein, B. C. Snyder, and O. D. Sherby, presented at annual AIME meeting, New Orleans, La., February 20-22, 1979.

25. Robert Maddin, James D. Muhly and Tamara S. Wheeler, Scientific American, *237*, 1977, 122.

research notes

Progress in Piezoelectric Polymers

Certain polymers have been found to exhibit piezoelectric (and pyroelectric) activity and have the advantage that they can be formed into films and other shapes which are impractical for ceramic piezoelectrics. It is the goal of research in this area to understand the piezoelectric phenomenon in polymers and to find the means for making practicable their use in naval acoustic sensors and detectors. Dr. Martin Broadhurst at the National Bureau of Standards has made significant progress in understanding piezoelectric behavior in polymers. Some recent research highlights from his group are outlined below.

A suitable model for piezoelectricity in polymers has been developed. The mechanism for piezoelectric and pyroelectric response in amorphous and crystalline polymers is similar. It is the change in polarization (dipole moment per unit volume) due primarily to the thermally or mechanically induced volume changes of the sample (secondary piezoelectricity and pyroelectricity) rather than dipole moment changes which are commonly responsible for piezo- and pyroelectric response in ceramics. In semi-crystalline polymers such as poly(vinylidene)fluoride, PVDF, dipole alignment is established by electric field induced rotation of molecules in individual crystals with stabilization by crystal packing energy. A cooperative six-site model has been developed for beta-phase PVDF which accounts for this ferroelectric behavior. Results from the model mimic the essential features of polarization, infrared and x-ray hysteresis data. Refinements of the model are still needed to explain the observation that removal of the poling electric field results in some loss in crystal alignment.

The gamma-phase of PVDF has been prepared by depositing an additive (2% siloxane-oxyalkylene copolymer, L-520) from ethanol onto alpha-phase PVDF powder and heating (1 °C/min) to 176° C. Films without the additive melt and recrystallize in the alpha-phase when cooled. Films of alpha and gamma phases were subjected to the same poling conditions and the piezoelectric and pyroelectric responses were measured. The much larger response from gamma phase for all electric fields less than 1.25 MV/cm confirms that this is a polar crystal phase. The value of 1.3 nC/cm^2K for pyroelectric coefficient after poling for 10^3 seconds at 80° C and 1 MV/cm is almost the same as that reported for unoriented beta phase obtained by pressure quenching and poled at the same field for one hour at 23 °C. For values of electric field 750 kV/cm and greater, the alpha phase undergoes the electric field induced phase transition to a polar form so that at 1.25 MV/cm the responses from alpha and gamma phase films are comparable. Because of the field-induced phase transition of alpha phase, there seems to be no practical advantage for promoting the formation of gamma phase unless one must be confined to low poling fields.

An interesting feature related to the poling process concerns the effect of orientation on polymer conductivity. It is not generally possible to pole PVDF at fields higher than 1.25 MV/cm because of electrical breakdown. In the course of this investigation it was discovered that simply orienting the polymer film reduces electrical conductivity by more than a factor of 100. An improvement in electrical breakdown strength is indicated but not fully quantified at this time. This phenomenon is being examined more fully at the present time. Another area of emphasis will be the development and application of a digitalized thermal pulse technique which will yield information on the polarization distribution in the polymer films. Resolution of these data to about one-tenth film thickness has recently been demonstrated. This amount of detail in the charge and/or polarization distribution is expected to be of great value in directing the development of models for non-uniform field distribution during the early stages of poling. ■

(Kenneth J. Wynne, ONR)

Novel Rust Removal Technique

The Naval Research Laboratory has devised an economical and nontoxic method for cleaning rusty metal surfaces. The method calls for a mixture of a water soluble polymer, preferably polyvinylpyrrolidone (PVP), and a chelating agent, which can be applied to a rusty metal surface as a thick paste. The outer surface of the paste gradually hardens into an encapsulating film; entrapping the cleaning agents inside. After cleaning, the tape-like coating can be easily peeled from the cleaned surface and disposed of as a solid waste.

One particular advantage of the new system would be its use to clean irregular surfaces found on ships, such as high-temperature valves and pipes. The only cleaning method presently feasible in many areas aboard ship is the lengthy and tiresome process of wire brushing the surfaces and then applying a solution of a wetting agent mixed with a cleaning agent. Such techniques suffer from the difficulty of keeping the cleaning agent in contact with the surface, such as an overhead object, as well as the subsequent disposal of liquid waste. ■

(David L. Venezky, NRL)

Molecular Dynamics, Spectra and Neighbor Effects

Neighbor effects, i.e., the influence of surrounding molecules on molecular properties, are key to understanding: (1) the different properties of different phases (e.g., gas, liquid, solid); (2) phase changes (e.g., nucleation which produces fog, rain, snow); (3) solvation; (4) why chemical reactions proceed differently in differing solvents; (5) interface phenomena; and (6) catalysis (e.g, enzyme action). One aspect of neighbor effects is how the atomic mo tions or the trajectories of atoms in a molecule are changed by the presence of surrounding molecules.

Dr. Kent Wilson, University of California, San Diego has recently demonstrated that infrared and Raman band contours are essentially a classical phenomena for translation, rotation, and vibration. To do this, we have linked classical molecular dynamics, linear response, and ensemble averaging and used simple quantum corrections where necessary. Since we now know from computing the spectra of single systems and comparing the results to accurate quantum calculations, and to experiment, that our essentially classical "Newtonian" approach gives quantitatively accurate spectra, we can look at the dynamics and spectra of molecules surrounded by neighbors. We have done this accurately for CO in Ar (infrared spectra) and N_2 in Ar (Raman spectra) as a function of Ar pressure. We thus observe theoretically and experimentally the effect on the diatomic motions of the homogeneous phase transition from the gas to liquid state as we raise the pressure. We have also made a preliminary study of the heterogeneous phase transition, through nucleation, of water vapor to liquid by looking at larger and larger clusters of water molecules and computing the atomic motions and spectra.

(George Neece, ONR)

Holographic Study of Solid Propellant Combustion

Professor David Netzer at the Naval Postgraduate School is making a high-resolution holographic study of Al/Al_2O_3 agglomerates in the propellant grain of a two-dimensional solid rock motor. Other techniques, including high-speed photography, light-scattering measurements, and post-fire scanning electron microscopy will also be studied. This fundamental study may well result in an increase in combustion efficiency of solid rocket motors since coating of the Al by Al_2O_3 essentially makes the Al unavailable for combustion (and energy release).

The work should provide fundamental information concerning combustion mechanism of solid propellants. The use of several diagnostic techniques is an excellent idea. Often, current researchers use only one technique and then make an unjustified conclusion based on insufficient data. ■

(William M. Tolles, Naval Postgraduate School)

S_2 As a Blue-Green Laser System

The sulfur dimer laser S_2 has many features which recommend it for a Blue-Green Laser system: there is a large Franck-Condon shift between the X (lower) and B (upper) states; the upper (B) state is imbedded within the dissociation level and, hence,

should be efficiently excited by electron collisions; S_2 is non-toxic and chemically inert and possesses adequate vapor pressure at low temperatures. However, sulfur does not exist as a simple dimer (S_2), but as S_n (where $2 \leq n \leq 10$) at $T > 400°C$. The conventional solution has been to utilize a two-temperature oven to dissociate these large chain molecules into S_2. This requires an ambient temperature of greater than 600°C. Drs. J. T. Verdeyen and J. Gary Eden, University of Illinois, have shown that this same effect can be accomplished by an rf simmer discharge. For instance, a characteristic absorption peak at 396 nm, associated with the higher sulfur polymers, can be eliminated by the use of an rf discharge. We have also demonstrated an S_2 laser pumped by an XeCl laser where the ambient temperature is as low as 320°C; however, the environment is created by a weak rf discharge (≈ 1 watt/cm^3). ■

(Matthew White, ONR EAST)

Potential In Situ Resin Cure Monitor

The development of a transistor that can monitor the cure of an epoxy resin raises the possibility of incorporating these small elements into large composite structures to monitor the state of cure during processing and the general "State of Health" of the composite during service. The ability to measure the "State of Health" is important because the service life of polymers and polymer-based composites is based on a different type of degradation than that which occurs in metals. In polymers, aging and environmental sorption and desorption of vapors slowly change the properties where metals are subjected to slow precipitation reactions and corrosion.

The new small transistor components appear to be roughly the same size as existing defects, delaminations, etc., that currently exist in large composite structures, hence the addition of an electrical monitoring device should have a negligible effect on the overall properties of the structure. ■

(Leighton H. Peebles, ONR EAST)

Photochemical Dynamics of Small Molecules

A unique facility is being developed by Dr. William Jackson, Howard University, to study the dynamics of photodissociation of small molecules. A tunable VUV spectrometer is being built as a photochemical source for dissociating these molecules. The photofragments will be detected by laser-induced fluorescence. This detection technique has a great deal of sensitivity and specificity. Densities as low as 10^5 cm^{-3} in a given rotational level can be determined. By scanning the laser as a function of wavelength, the quantum state distribution of the fragments may be characterized. Tuning the VUV spectrometer permits one to determine the dynamics as a function of wavelength.

The facility will incorporate several design innovations for the VUV flash lamp. A capillary flash lamp will be employed so that gases other than the rare gases may be used. This should permit us to tailor the output of the flash lamp for the particular molecules under study.

The experimental chamber will be designed so that a pulsed molecular beam may be used to lower the internal excitation of the molecule under investigation. Rotational excitation of the fragments appears to be due to geometric changes that occur when the molecule is electrically excited. These changes are due to either differences in the structure of the ground and excited states or to excitation of the bending modes of the ground state. Cooling the molecule will reduce the population of the latter rather than the former. This should be reflected in the rotational excitation of the fragment. ■

(George Neece, ONR)

Harvesting a group of Ammonium Dehydrogen Phosphate (ADP) single crystals grown from solution. Photograph taken in 1946 at the Naval Research Laboratory.